E L E C T R O N M I C R O S C O P E S T U D I E S

O F S U R F A C E S T R U C T U R E

by

Ian Y. R. Adamson

Department of Chemistry, University of Glasgow.

The Radiolytic Oxidation of Graphite by Carbon Dioxide.

Thesis submitted for the degree of

Doctor of Philosophy,

July, 1966.

ProQuest LLC.
789 East Eisenhower Parkway
P.O. Box 1346
Ann Arbor, MI 48106 – 1346

A C K N O W L E D G E M E N T S

This work was carried out in the Physical Chemistry Department which is under the direction of Professor J. M. Robertson.

I would like to express my gratitude to Dr. I. M. Dawson for his guidance and supervision of this work. Thanks are also due to the U.K.A.E.A. for financial support and to some members of staff at Harwell, namely J. Wright and F. S. Feates for discussion, and J. R. Fryer, A. G. Poole and R. S. Sach for their assistance with the irradiation work.

Finally, I would also like to thank the technical staff of the electron microscopy unit.

I. Y. R. A.

GENERAL CONTENTS

INTRODUCTION

Contents

1. Graphite Structure

(a) Ideal Lattice

Investigations into the crystal structure of graphite were begun by Ewald (1914) using x-ray analysis. The accepted structure was first proposed by Bernal (1924) and subsequent investigations have produced more accurate cell dimensions.

Graphite was shown to have a layer structure composed of flat sheets of fused, six membered carbon rings. The distance between these layers was found to be 3.3538Å (Franklin 1951a) and other similar values have been obtained by Franklin (1951b) and Bacon (1951, 1958a and b). The carbon-carbon distance in the hexagonal rings was found by Trezbiatowski (1937) to be 1.413Å and slight variations of this have also been found by Franklin and Bacon. The hexagonal networks are arranged so that an atom in one layer is situated either directly over an atom of the underlying layer or over the central point of a hexagonal ring below. This is the normal abab stacking and is illustrated in Figures 1(A) and (B). Figure 1(A) shows three successive layer planes and the darker lines outline the unit cell containing four atoms. The cell dimensions are $\underline{c}$ = 6.7079Å and $\underline{a}$ = 2.4612Å (Nightingale 1962) so the $\underline{c}$ spacing is therefore twice the interlayer spacing. Figure 1(B) illustrates a basal plane projection of this structure.

The appearance of anomalous lines in the x-ray diffraction pattern of graphite was noted by Laidler and Taylor (1940) and Lipson and Stokes (1942a,b). This was taken as evidence for another graphite

F I G U R E 1 A

Diagram showing the layer structure of graphite and illustrating the unit cell.

F I G U R E 1 B

A basal plane projection of the above structure.

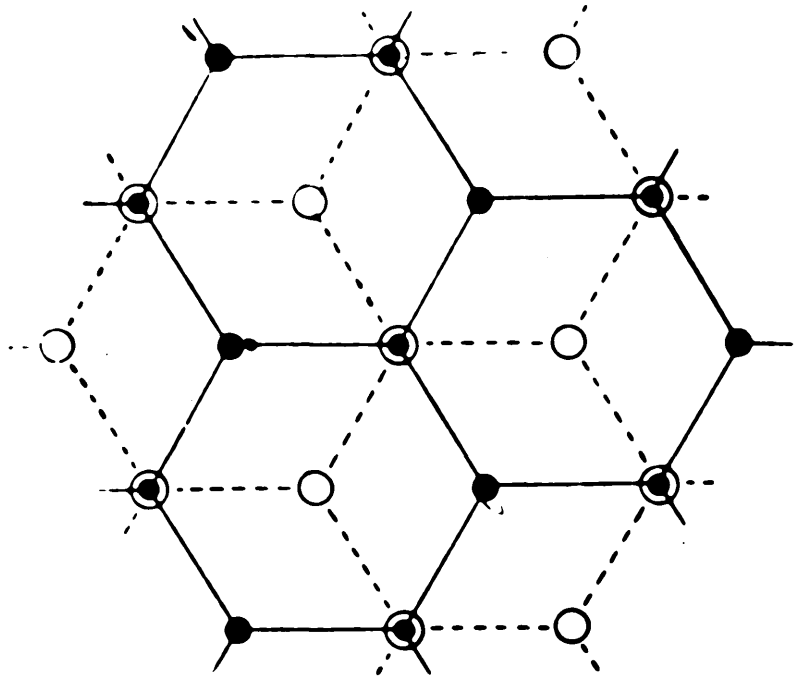

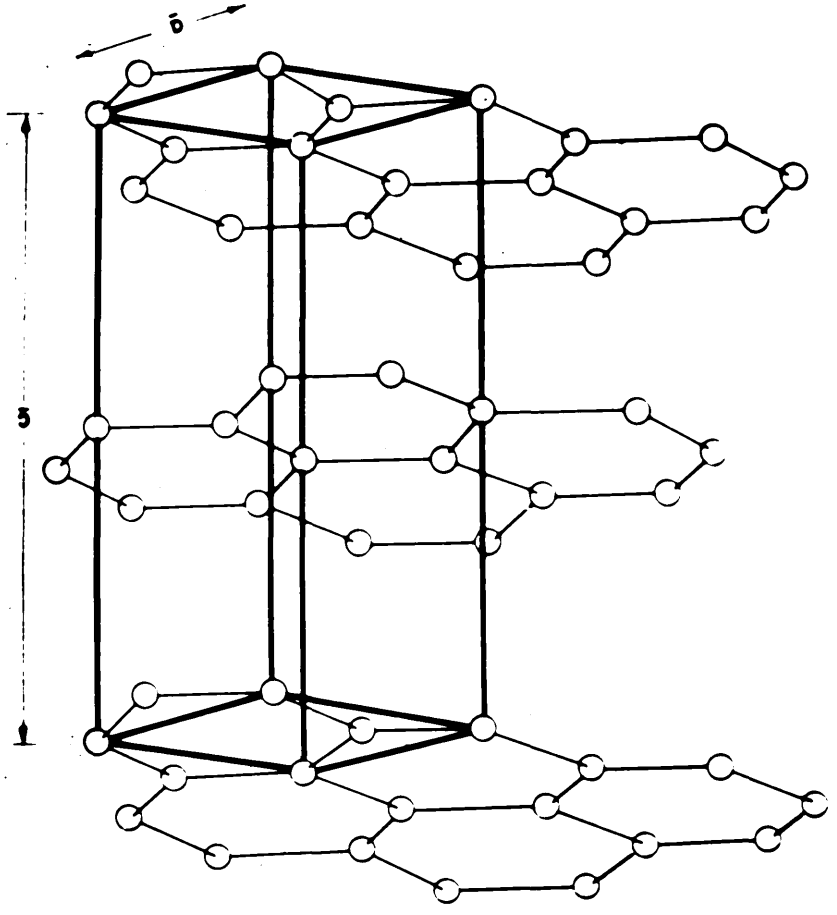
b
5

stacking arrangement. It was termed the rhombohedral form and involved abcabc stacking, in which the third layer bears the same relation to the second as the second does to the first. Both of these structures are known to exist in natural graphite and they have been interconverted by physical and chemical treatments.

The above data refers to natural graphite and although this is found in various locations, there is little difference among the structures of each type. This is not true for synthetic graphite due to the variation in preparation materials and conditions for different grades. Synthetic graphite is prepared from a disordered carbon, e.g. petroleum coke, by baking it with a 'binder', e.g. pitch, at a temperature of around 3000°C. for a few days. These conditions cause the transformation of the disordered mass into an ordered graphitic carbon. The transformation and degree of order can be followed by x-ray diffraction at different stages (Franklin 1951). As graphitization increases, the interlayer spacing decreases as it approaches 3.35Å. Variation from this value gives a measure of disorientated material present (Bacon 1958). Also the sharpness of each diffraction ring increases as the order of the material increases. Due to the graphitization process, crystallites of synthetic graphite are up to a hundred times smaller than those of natural graphite. Dawson and Follett (1959) examined the areas of nuclear grade graphite crystallites and found a mean value of $0.11\mu^2$ whereas natural graphite crystals can have diameters of up to 20μ.

(b) Pore Structure

The existence of pores in synthetic graphite is a feature of the random orientation and packing of crystallites during graphitization. Dresel and Roberts (1953) used organic liquid and helium gas displacement to prove that 20% of the total pore volume is inaccessible so they classified pores as 'open' and 'closed'. This leads to the grading of pores by size into macropores and micropores.

Macropores are believed to lie between the original coke particles and investigations by Loch, Austin, Harrison and Duckworth (1958) and Walker and Rusinko (1958) gave pore diameters between 10,000 and 100,000Å. Dawson and Follett (1959) showed, by electron microscopy, that British nuclear graphite contained pores 400 - 800Å wide at the junctions of three or more crystallites.

Loch et al. confirmed that there are always pores inaccessible to helium even after powdering the graphite, and Loch and Austin (1956) showed that the highest closed pore volume occurred in the smallest crystallites. It was then suggested that the micropores, which accounted for the closed pore volume, resulted from small separations between the adjoining crystallites or grains. The diameter of these was found to be 3 - 8Å so therefore probably inaccessible to gas or liquid. A considerable quantity of 'closed' pores can be opened by partial oxidation of the carbon. Walker and Rusinko (1958) found that closed pore volume in a sample decreased from 20% to 9.5% by oxidation at 900°C. Roberts, Harper and Small (1958) showed that there was

12 - 22% inaccessible pores in nuclear graphite but after 6% burn off all became accessible. Ashton and Winton (1961), using the same graphite, showed that 19.8% of all pores was open pore volume and as graphite was oxidised, other pores opened. This was shown by an increase in surface area.

Recent investigations by Standring and Ashton (1965) into the radiolytic attack on graphite by carbon dioxide showed that 40% close pore volume became accessible after a 2% weight loss and the remaining porosity was opened in proportion to graphite oxidised, probably at the cleavage cracks. It was suggested that the macropores were formed by plugging during the impregnation stage of manufacture and were covered by a thin layer of graphite which was removed in initial burn off. The micropores were probably formed by shrinkage during graphitization.

(c) Band Theory of Graphite

It is obvious in the graphite structure that there are strong chemical bonds between atoms in a layer plane and weak forces between the layer planes. The graphite structure is due to the combination of atomic orbitals in sp^2 hybridisation, whose lowest energy level consists of three equivalent bond orbitals directed in a plane at angles of 120°. This leaves a third p orbital which forms a π bond perpendicular to this planar system of sp^2 bonds. This means that the electrons of the π bonds are mobile in any layer plane thus giving graphite its metallic character. The π band has one electron

available for each atom and this constitutes a half filled band which is symmetrical and falls to zero in the centre. According to Coulson (1947) and Wallace (1947), there is a zero energy gap between full and empty sections of this band and the promotion of electrons is readily accomplished (Coulson and Taylor 1952). At all temperatures above $0^{\circ}K$, promotion from the valence band to the conductance band is important and this is used to explain why graphite is an intrinsic semi-conductor. Its physical properties have also been explained by this theory by many authors, and a good treatment of the present state of thought is given by Mrozowski (1950a,b, 1952a,b).

Because the bonding electrons are all used to form carbon-carbon bonds within the carbon layers, these layers are only held together by weak Van der Waals forces. Nightingale (1962) quoted a value of 150 k.cal./gram atom for the layer carbon-carbon bond strength but only 1.3 k.cal./gram atom for the interlayer binding energy. This low value accounts for the compressability and ease of separation of the sheets by interstitial atoms or compounds. This is the cause of the considerable anisotropy of graphite properties. It is well known that its physical properties are entirely different depending on whether the direction of measurement is parallel or perpendicular to the basal plane and there is much literature evidence to prove this. The reactivity in different directions will be discussed later.

The band theory works for perfect or near perfect crystals but in grossly defective samples, this theory will only be approximate since the fusion of the discrete electron levels into a continuous band will be grossly perturbed at major defects and crystallite boundaries (Ubbelohde and Lewis 1960). Long and Sykes (1950) also proposed that the increased oxidation by catalysis is due to the impurity influencing energy levels by interacting with the electrons of graphite, thus changing the bond order and facilitating reaction at these sites.

(d) Defects

The graphite lattice is subject to a variety of imperfections or defects which have been separated by Ubbelohde and Lewis (1960) into two types, namely those involving (i) interlayer disorder and (ii) actual bond network defects.

(i) Interlayer Disorder

When the deviation from the periodic arrangement extends throughout the lattice, it can be a line or plane defect. Line defects are divided into two classes: a) an edge dislocation, where a row of atoms marking the edge of a crystallographic plane extends only partly into a crystal, and b) a screw dislocation, in which there is a row of atoms about which a normal crystallographic plane appears to spiral. This dislocation can be described by a closed loop round the dislocation line. The loop is formed by proceeding through the undisturbed region

in steps which are multiples of a lattice translation. If the loop does not close, the separating distance is the Burgers Vector. The plane containing the dislocation line is the slip plane. When the Burgers Vector is perpendicular to the dislocation line, it is called as edge dislocation and when it is parallel, it forms a screw dislocation. An edge dislocation can move only in its slip plane but a screw dislocation can move in any plane parallel to itself. Horn (1952), using the electron microscope, found spiral growth steps on some natural graphites and this was taken as evidence that graphite may grow from screw dislocations. This was confirmed by Hennig (1961b) who showed that screw dislocations start and terminate within a given crystal and that their density increases near the surface.

Plane defects are also common. One type is formed at the boundary between grains where the structure and orientation of the adjoining grains is different and so there is a discontinuity in the periodicity of the lattice. In a polycrystalline solid such as graphite, the growth of the grains tends to expel all foreign and interstitial atoms and other defects, which collect at the grain boundaries which will therefore contain a variety of imperfections. When adjacent grains are misorientated a few degrees, this is termed a small angle boundary and this results in a series of parallel edge dislocations along the boundary and when the boundary intersects the surface, the edge dislocations will produce, on etching, a series of small pits at the sites of emergence of the dislocations. The motion of such

dislocations has been studied by Grenall (1958), and Grenall and Sosin (1960). By using a cine camera in conjunction with an electron microscope, they showed that dislocations are mobile and can re-arrange during their motion and sometimes disappear. Also dislocations can be slowed down or pinned by obstacles in the lattice. Speed of movement depends on whether the dislocation is 'gliding' or 'climbing', crossing a defect free area or a grain boundary. This motion can be brought about by any applied energy including the heat of the microscope beam.

Another plane defect, due to stacking faults, was deduced from anomalies in the x-ray diffraction photographs by Warren (1934), Franklin (1951) and Bacon (1951), who found that interlayer spacing depends on degree of stacking disorder. The probability, p, of a stacking error has been investigated by Bacon (1950, 1951, 1952, 1958). Amelinckx and Delavignette (1963) class stacking faults into three groups: a) when part of a c plane is removed from the stacking sequence as in the case of vacancy loops, shown in Figure 2(A); b) when the dissociation of a dislocation proceeds and partials are formed, then the area between them is a stacking fault. These partials can interact to give a triangular fault region containing nodes where they cross; c) when an extra plane is inserted as in the case of interstitial loops, shown in Figure 2(B).

Both kinds of loops have been seen by electron microscopy by

F I G U R E 2 A

Layer structure which produces a vacancy loop.

F I G U R E 2 B

Layer structure which produces an interstitial loop.

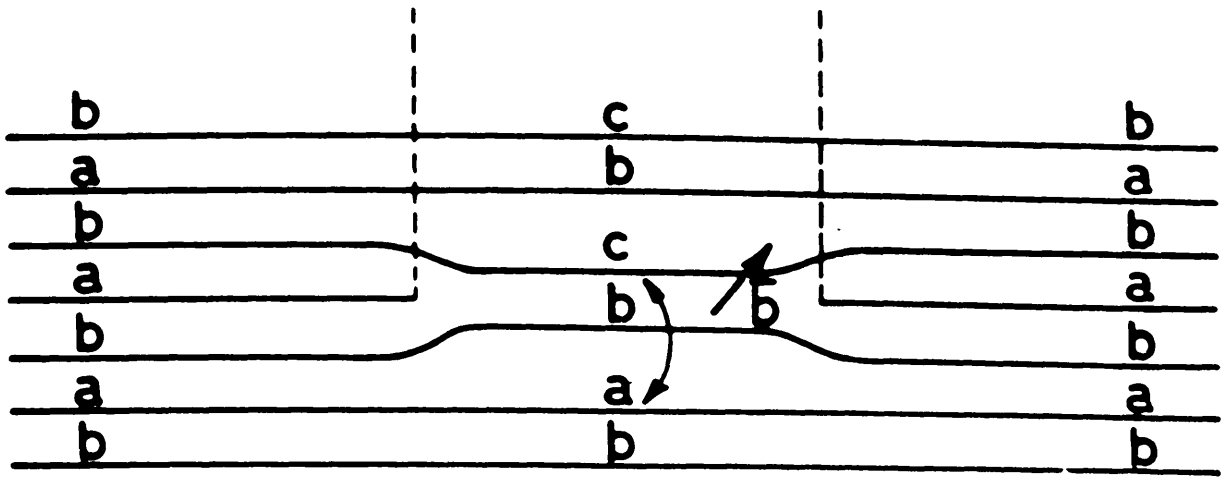

(a)

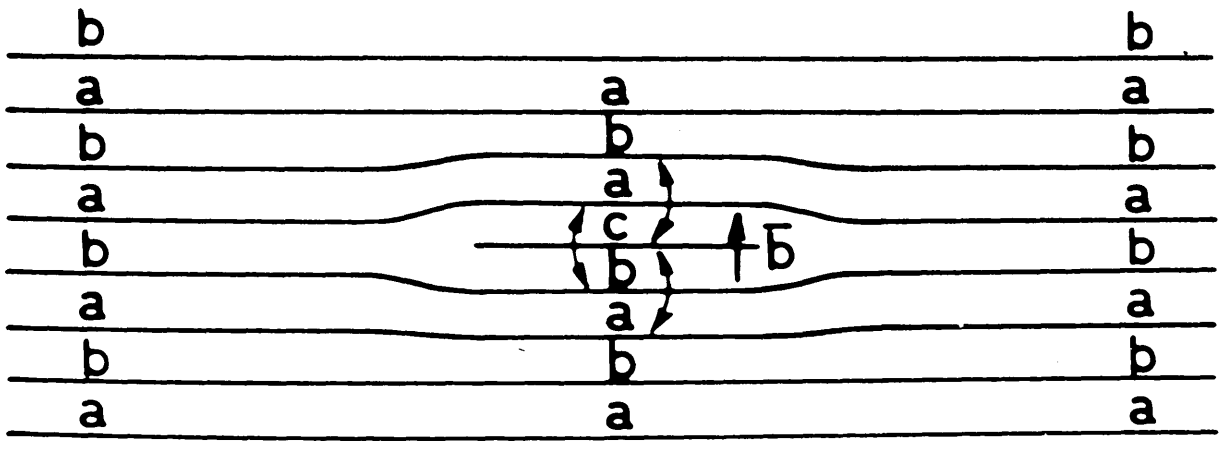

(b)

Williamson (1961), Reynolds, Thrower and Sheldon (1961), Reynolds and Thrower (1964) and Bollmann and Hennig (1964). The best way to produce these is by irradiation which produces vacancies and interstitial atoms. This has been done by Bollmann (1960, 1961 a,b,c). The appearance of dislocations in the electron microscope depends on the diffraction effects from the interaction of the beam with the strain fields of the displaced atoms. This technique has been developed by Hirsch, Horne and Whelan (1956) for metallic films and many papers have been published by these authors. The theory has been reviewed by Howie (1961) and Howie and Whelan (1961).

There are many articles on the study of dislocations including those by Amelinckx (1956, 1963), Amelinckx and Delavignette (1960a, b,c, 1961, 1963), Delavignette and Amelinckx (1960, 1961), Bollmann (1962) and Williamson and Baker (1958, 1960a,b, 1961b). The interaction between dislocations and crystal step edges and impurities was discussed by Bacon and Sprague (1961), and Siems, Delavignette and Amelinckx (1962).

(ii) Bond Network Defects

Defects in the actual carbon network are caused by the alteration of the regular hexagonal pattern. One possible cause of this could be an impurity atom. When this has a different valency from carbon, the bonding characteristics of the neighbouring carbon atoms can change. Another defect is the vacancy. This can be caused by

high energy particle bombardment which displaces carbon atoms from their original positions. Ubbelohde and Lewis (1960) also regard the pores of synthetic graphite as layer defects. Another defect, formed by tilting the layer planes during growth, is the twin plane where alternate four atom and eight atom rings are formed across the twin line. Recent investigation of these has been carried out by Thomas, Hughes and Williams (1963) and Baker, Gillin and Kelly (1965).

The principle layer defect occurs at the plane edge. Atoms at an edge are less strongly bonded and so are expected to be more reactive. Because of the incomplete use of their bonding electrons, these sites are susceptible to the adsorption of other atoms, or molecules, in particular -H, -OH, = O, -O -, and foreign atoms which can influence the properties. This is also true of hole defects as described by Ubbelohde (1957).

A consequence of the edge defects is the anisotropic behaviour of graphite. Long and Sykes (1948) showed that edge carbons had a double bond attached while basal plane carbon atoms had only single bonds, and so the edge atoms, with the available orbital for bonding to attacking species, were attacked much faster. Smith and Polley (1956) confirmed this by proving that reactivity was at a minimum when the surface of a graphitized carbon black contained the maximum number of crystallites with their basal planes parallel to the surface. This was shown to apply to natural graphite by Hennig, Dienes and

Kosiba (1958), and Grisdale (1953) showed that oxidation was seventeen times faster parallel to the basal plane than perpendicular to it.

(e) Diffraction of Graphite

The electron diffraction of a single crystal of graphite consists of a hexagonal spot pattern when the electron beam is perpendicular to the graphite layers. This was found by Finch and Wilman (1936). In polycrystalline graphite, the pattern shows a series of concentric rings (Dawson and Follett, 1959). In both cases, the strongest reflections are the $10\bar{1}0$ and the $11\bar{2}0$.

This method of indexing is generally used for hexagonal networks, such as graphite. Three of the axes are at 120° to each other and the fourth is perpendicular to the layers. The normal Miller indices h,k,l, can be used, as the extra index i can be defined from the other three by the equation $h + k + i = 0$ and so $i = \overline{h + k}$ and the graphite planes can be represented as $(h,k, \overline{h + k}, l)$. Some typical planes are illustrated in Figure 3 (from Nightingale 1962). The spacings where $l = 0$ are parallel to the c axis and give various C - C spacings while the planes 0001 give the d, or interlayer, spacings. This is not often found in graphite due to the fact that the beam is perpendicular to the layers and so parallel to c axis. However the d spacing can be readily obtained from x-ray diffraction (Bacon 1958b).

(f) Double Diffraction and Moiré Patterns

Interference fringes were first observed on graphite by

FIGURE 3

Diagram of graphite layers illustrating the indexing of some planes.

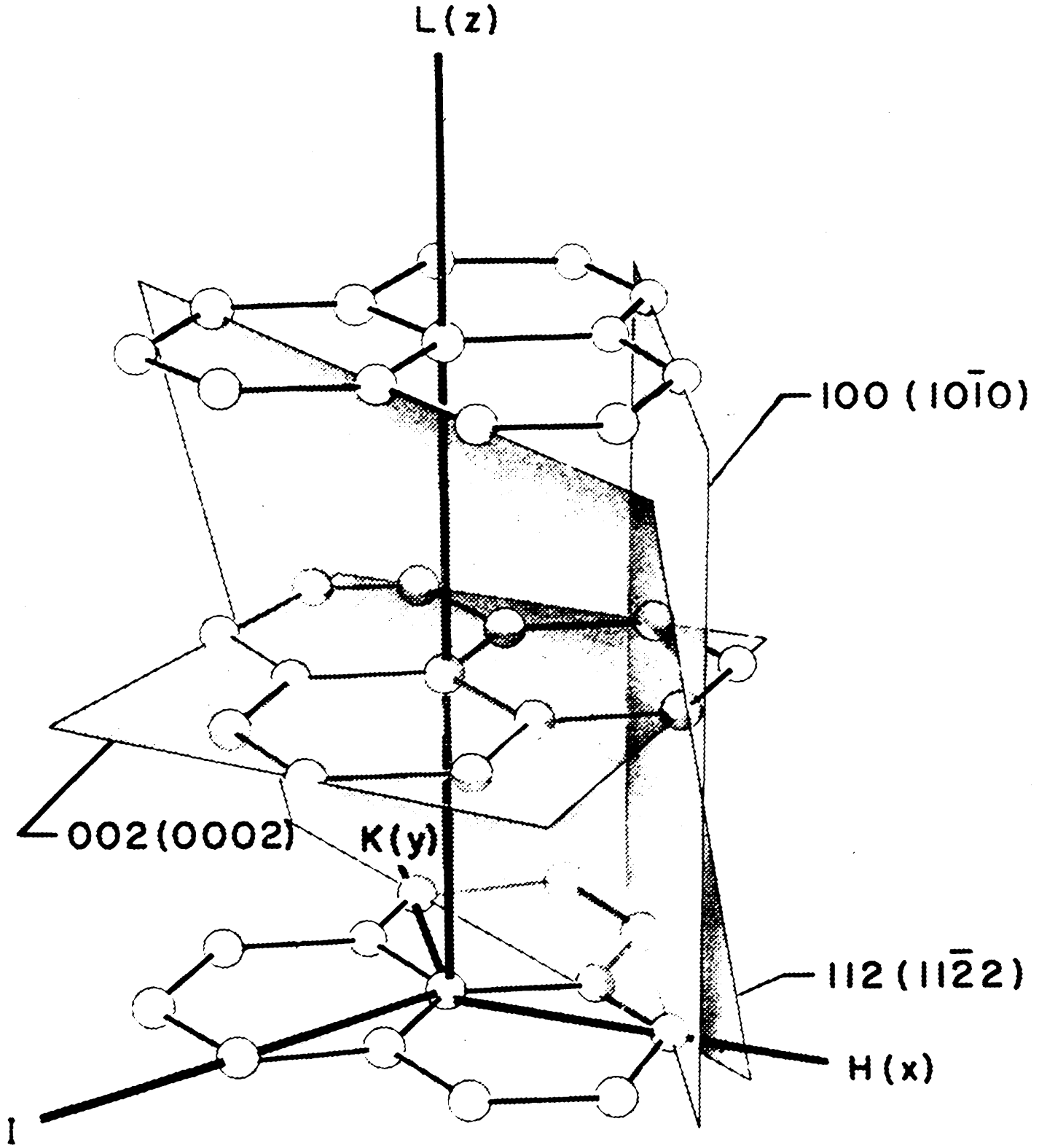
L(z)
100 (10$\bar{1}$0)
002(0002)
K(y)
112 (11$\bar{2}$2)
H(x)
I

Mitsuishi, Nagasaki and Uyeda (1951). They were also observed later by a number of workers studying different materials. Hillier (1954), examining iron oxide, believed the fringes to be moiré patterns arising from the periodic match and mismatch of projected planes of atoms in overlapping crystals. Dowell, Farrant and Rees (1958), examining molybdenum oxide, stated that this was partly true, but in addition, fringes arose from interference with the non-diffracted beam. To explain the formation of moiré patterns, consider the effect of two superposed crystals. When a beam passes through one crystal, it produces a diffracted beam which then can be diffracted by the second crystal. The result is that the diffraction pattern is made up of the two individual patterns plus reflections produced by this double diffraction. If this gives rise to a beam closely parallel to the incident beam, then a moiré pattern is formed by their recombination. Bassett, Menter and Pashley (1958) gave theories for two types of moiré pattern formation. Firstly, when two lattices overlap with an angle of rotation α, it was found that the moiré pattern spacing is d/α where d is the lattice spacing. Secondly parallel moiré patterns can be produced by the superposition of two lattices of different spacings d_1 and d_2 and this gives a pattern spacing of $\frac{d_1 \cdot d_2}{d_2 - d_1}$. In this case, two sets of spots are seen to correspond to the two lattices, but an additional set of spots are found very close to the undeviated beam. These are due to double diffraction taking place

in the opposite sense so giving spots close to the undeviated beam. Interference from these gives a moiré pattern associated with the two spacings. Dowell et al. showed that the insertion of a small apperture to cut out these extra spots had the effect of removing the pattern. Bassett et al. showed that a similar process applied to a spot moiré pattern where the pattern is related to the positions of the atoms in the lattice.

Examination of graphite moiré patterns, which was begun by Mitsuishi et al. was continued by Grenall (1958) and Dawson and Follett (1959), who found extra half-lines in the pattern and related this to the presence of a dislocation in the lattice, supporting the conclusions of Hashimoto and Uyeda (1957) from investigations of cupric sulphide. This was rejected by Williamson and Baker (1960b). By examining dislocation arrangements in graphite, they concluded that the only dislocations present are those in the layer planes.

More recent evidence, the latest being from Roscoe and Thomas (1966), illustrates the presence of both edge and screw non-basal dislocations in natural graphite.

2 (a) Radiation Effects on Graphite

Graphite has two main properties which make it suitable as a moderator in nuclear reactors. Firstly, it can slow down the fast neutrons to thermal energies by energy transfer in the collision between the neutrons and the graphite atoms. Secondly, it has the desirable property of having a small cross section for neutron absorption, since

any neutrons absorbed by the graphite would be lost to the system. Since impurities have high capture rates, the purer the graphite, the more efficient a moderator it will be. The widespread use of graphite has lead to a great number of papers on radiation damage.

Proton and neutron bombardment have been shown to produce similar changes in the physical properties of graphite (Nightingale 1962). Radiation damage can be due to the displacement of atoms or the excitation of electrons into higher levels. In graphite, the conduction electrons are mobile so they are not permanently displaced and damage is therefore due to displaced atoms. Fast neutrons can transfer momentum by elastic collisions and displace an atom which then has sufficient energy to act as a bombarding particle. If a charged species is used to bombard the graphite, electron excitation is produced and this can result in the breaking of chemical bonds with re-arrangement of atoms. Goland (1962) stated that this damage is equivalent to neutron damage from a low dose where the disordered regions are widely separated.

Single displaced atoms or interstitials and the holes or vacancies they leave are the initial products of radiation, but they may then agglomerate into clusters, depending on the irradiation temperature and dose. Another result could be a dislocation loop. This can be caused by the successive removal of neighbouring atoms leaving a high density shell round a low density core and this leads to the collapse of the lattice at that point giving a dislocation loop and a mismatch

region, in addition to the defect clusters. These loops were seen by Amelinckx and Delavignette (1960a).

An important effect of irradiation is the resultant lattice dimension changes. This was first reported by Woods, Bupp and Fletcher (1956) who showed that the interlayer spacing was considerably increased while the a spacing decreased slightly. Baker and Kelly (1962) showed that the c spacing increase equalled about ten times the a spacing decrease. Recent lattice investigations have been carried out by Kelly (1965). The effect of radiation damage on graphite properties has been studied by many workers, including Reynolds and Simmons (1961).

As the irradiation dose increases, so does the damage and the concentration of interstitials which can migrate along layer planes and combine with others. It was suggested by Bacon and Warren that these groups caused the increased c spacing, while a contraction was thought to be due to the distortion of layer planes. Kelly (1965) attributed a contraction to bond length changes due to π electron re-arrangement. Also clustering of vacancies could produce basal plane loops and, by collapsing, this could give a reduced a value.

It is possible, however, that vacancies and interstitials can combine and return that part of the lattice to normal. This self-annealing effect increases with temperature due to the mobility of the interstitials and usually all defects have been annealed at 2000°C. Vacancies do not become mobile until 1200°C (Dienes and Vineyard, 1957). Interstitial clusters are also known to be trapped and nucleate

at dislocation areas, (Kelly, 1964).

Electron microscope investigations of damaged graphite were begun by Bollmann (1960) who used dark field illumination and found black and white dots as well as loops. The dots were not found in unirradiated graphite and were supposed to be vacancy and interstitial clusters. The dose used was $10^{20} n/cm^2$. Further studies have been made by Bollmann (1961a,b,c), Williamson and Baker (1961a), Williamson (1961), Baker (1962), and Amelinckx and Delavignette (1960c).

These studies involve radiation doses in excess of $10^{20} n/cm^2$ at various temperatures up to 3000°C., conditions more extreme than those used in the work to be described. Typical results were obtained by Reynolds and Thrower who have reported investigations in 1962, 1963, 1964 and 1965 with Simmons. It was shown that loop size increased and loop density decreased as the irradiation temperature increased. They found loops 40Å in diameter, 350Å apart at 200°C., but at 650°C. they were 200Å wide and 10,000Å apart. In 1965 they showed that the main loops were interstitial, about 1000Å wide surrounded by vacancy loops about 25Å wide in natural graphite, but in polycrystalline material, defects were smaller and denser. Interstitials can nucleate at impurity and other defect sites and vacancies can disappear at edge dislocations.

These radiation effects are known to influence the rate of graphite

attack. Kosiba and Dienes (1957) found the increase in oxidation rate to be six times after pre-irradiation of the graphite in a neutron flux. They found only a small increase after irradiation in a gamma flux. This was attributed to the fact that gamma rays have no permanent effect on the properties of graphite and the enhancement was probably due to ionisation of the reactant gas molecules. Weber (1956) showed that possible gamma flux damage could arise from the dissociation of ionic or covalent bonds by the highly ionising radiation and this could cause fragmentation or re-combination. He also proposed that high temperature damage depends on the mobility of any displaced lattice atoms. Hennig and Kanter (1960) showed how radiation defects could be studied by oxidation which resulted in the production of pits. This has subsequently been the subject of much more investigation.

2 (b) Radiation Effects on Gases Used

i) Proton, Neutron and Gamma Fluxes

The action of radiation on carbon dioxide was first studied in 1908 by Cameron and Ramsay using α radiation and they found that free carbon was deposited. This was later shown to be due to impurity and the gas was found to be stable to ionising radiation by Wourtzel (1919), and Lind and Bardwell (1925). Later work by Harteck and Dondes (1955, 1957) showed that temperature did not affect the carbon dioxide radiolysis which was only slight due to the rapid reverse reaction.

$$CO_2 \rightleftharpoons CO + O$$

This was found for α and neutron irradiation. When the reverse reaction was inhibited, usually by nitric oxide or a substance capable of removing oxygen atoms, the products found were carbon monoxide, oxygen, carbon, and carbon suboxide. The mechanism proposed was

$$CO_2 \longrightarrow CO + O \longrightarrow C + O + O$$

$$CO + C + M = C_2O + M$$

$$C_2O + CO + M = C_3O_2 + M$$

$$O_2 + O + M = O_3 + M$$

$$C_3O_2 + O_3 = CO_2 + O_2 + C_2O$$

$$C_3O_2 + O = CO_2 + C_2O$$

$$CO + O + M = CO_2 + M$$

Woodley (1954), and Hurst and Wright (1955) found similar results by using gamma irradiation but this time the suboxide was believed to be C_4O_3 from the reaction

$$5\ CO = CO_2 + C_4O_3$$

This is in contrast to α irradiation which was represented as

$$6\ CO = 2CO_2 + C + C_3O_2$$

The relative stability of carbon dioxide under prolonged radiation was confirmed in nuclear reactors by Davidge and Marsh (1955) and Anderson, Best and Dominey (1962).

It is also known that certain ions were present in the system and those of carbon dioxide, carbon monoxide, oxygen and carbon have been identified by mass spectrometry by Smyth (1931), but they were proved to be ineffective for subsequent reaction by Hirschfelder and

Taylor (1938), who found that the ions were subsequently neutralised. This was also shown by Harteck and Dondes, and Claxton (1962) who used electronically excited carbon dioxide to show that the primary radiolysis product (oxygen atoms) was responsible for later reactions.

Since the passage of high energy radiation through a chemical system causes ionisation and electronic excitation, the fate of the ion will be to decompose to a smaller ion plus a neutral fragment or to be neutralised by an electron to form an excited molecule, and in this case the effect is the same as excitation. This particularly applies to proton bombardment where the production of ions is significant. The excited species are then believed to decompose to atoms and free radicals which are the principal agents of reaction.

Dominey and Palmer (1963) investigated the radiolysis of carbon dioxide by using tracers and they concluded that both ions and excited states were produced. They propose the scheme below

$$CO_2 \nearrow CO_2^* \longrightarrow CO + O$$

$$CO_2 \searrow CO_2^+ + e^- \longrightarrow (CO_2^*) \longrightarrow CO + O$$

$$O + O + M = O_2 + M$$

The radiolysis of methane has mainly been carried out using an α source. Lind and Bardwell (1925) found hydrogen and ethane products and the results led to the postulation of either an ion-molecule intermediate $CH_4{}^+CH_4$ or a free radical CH_3. It is then possible to build up larger molecules by chain reactions although these products will have a progressively smaller yield as the chance of neutralisation

and deactivation increases.

Lampe (1957), using 1.7 Mev electrons, obtained hydrogen, ethane, propane, butane and a liquid $(CH_2)_n$ which he believed to be due to the ion-molecule reaction. This liquid was also found by Sieck (1963). Wexler and Jesse (1962), using positive ion irradiation followed by spectrometry, detected CH_5^+ and $C_2H_5^+$ ions which they then postulated were neutralised and formed CH_3 and CH_2 radicals which could then form polymeric chains by insertion reactions. This was contradicted by Munson, Field, and Franklin (1965), who found no trace of such ions. Work by Hummel (1963) using 4 Mev electrons suggested that ethylene and acetylene were formed in larger amounts, than previously reported and the reaction proceeded through CH_2 radicals to give excited C_2H_6 molecules which could be deactivated to C_2H_4 or C_2H_2.

ii) Vacuum Ultra Violet Photolysis

This method of radiolysis of carbon dioxide was first investigated by Groth (1937) who found that the products were carbon monoxide and an oxygen atom. Inn, Watanabe and Zelikoff (1953) found that the decomposition gave carbon monoxide in the ground state plus an excited oxygen atom in either the 1s or 1d states. This was confirmed by Mahan (1960) after Jucker and Rideal (1957) gave a reaction product as molecular oxygen. This was proved to be the case after collision of the oxygen atoms, probably at a vessel wall. In this way ozone could also be produced. Warneck (1964a,b) also proposed that CO_3 molecule was a reaction product.

Feates and Sach (1965) drew up a table of inert gas discharge wavelengths and the corresponding energetically possible states of carbon monoxide and atomic oxygen. By this method of irradiating carbon dioxide, insufficient energy was obtained to produce ions, so any reactions with carbon must have been due to the excited species.

On this basis it was hoped to discover the species responsible for attack in all irradiation systems used, by comparing the results with those of this system where a known active species was present.

Mention must also be made of the photolysis of the other gases used in these experiments. Photolysis of carbon monoxide has been studied by Groth, Passara and Rommel (1962). They stated that the high bond strength would require high energy for decomposition and they explained the production of carbon dioxide and a carbon suboxide polymer (C_3O_2) by a mechanism involving excited carbon monoxide molecules. The secondary photolysis of carbon monoxide was also found by Feates and Sach who noticed dark deposits on the transmission window after a long experimental run in carbon dioxide.

Photolysis of methane has been investigated by many authors including Leighton and Steiner (1936), Mains and Newton (1961), Mahan and Mandal (1962), and Magee (1963). The reaction products varied greatly and included hydrogen as well as many saturated and unsaturated hydrocarbons higher than methane. It has been established that the build up process is one of radical insertion which probably commenced with the detachment of hydrogen to form a methylene radical which could

then insert in a fresh methane molecule. Mechanisms through the ethylidene radical (CH_3CH) have also been proposed and molecular detachment processes have also been found by Sauer and Dorfman (1961) and Okabe and McNesby (1961).

Ketene photolysis has been investigated by Vanpee and Grard (1951) and Strachan and Noyes (1954) who found products of the general formula C_nH_{2n} as well as carbon monoxide. These were proved to arise from a radical insertion process giving $(CH_2)_nCO$ before decomposition. Kistiakowsky and Rosenberg (1950) showed that ethylene formation resulted from this process and not by direct radical combination.

3. Oxidation

(a) Graphite - Carbon Dioxide Thermal Reaction

This thermal reaction was first studied by Boudouard (1901) who found the equilibrium

$$C + CO_2 = 2CO$$

This was found to be inadequate to explain later results by workers including Langmuir (1915), Broom and Travers (1932) and Gadsky et al. (1948). These authors proposed the existence of a chemisorbed species on the carbon surface. This could either be (CO) or (O). The review by Walker, Rusinko and Austin (1959) amply covers the relevant work in this field and they summarised the possible mechanisms into two simple classes, one involving carbon monoxide adsorption, the other involving oxygen atom adsorption.

Support for carbon monoxide being the chemisorbed species came

mainly from Gadsby while work by Reif (1952), Ergun (1956) and Strickland - Constable (1947,1950) supported oxygen chemisorption. This was confirmed by radioactive tracer studies by Bonner and Turkevich (1951) and Brown (1952). Later results from Harker, Marsh and Wynne - Jones (1958), and Vastola and Walker (1961) showed that some adsorption of carbon monoxide must take place and as a result some retardation of oxidation rate must occur since the fraction of surface covered by oxygen atoms would be reduced.

Once the active sites on the graphite have been covered, Blackwood (1954) stated that the rate determining step for the gasification reaction is the decomposition of the oxide to gaseous carbon monoxide. Copestake, Davidson and Tonge (1959) showed that this reaction only becomes appreciable above 625°C. This carbon monoxide can also retard the reaction by recombining with an oxygen atom to regenerate carbon dioxide. Board (1965) added carbon monoxide to the system and reduced the gasification of nuclear grade graphite by a factor of 4.

Most of the above results were obtained using different types of carbon and conclusions have been drawn for the general case. However, carbon type must be important since Laine, Vastola and Walker (1963) showed that surface area affected the reaction rate, and Butcher and Grove (1961) showed that pore volume affected the reaction, particularly in the early stages when closed pores were opened. Crystallite orientation also plays an important role in oxidation. Grisdale (1953) showed that carbon crystallites react 17 times faster in the direction

parallel to their basal planes than perpendicular to them. Board and Squires (1965) showed that larger specimens oxidise slower than thinner ones, with fine grain material being preferentially oxidised.

An important factor in discussing reaction rates is the effect of graphite impurity content. Rate enhancement due to this has been found by Blackwood (1954), Lang and Magnier (1961), Rakszawski, Rusinko and Walker (1961), and Jacquet and Guerin (1962). Gulbransen and Andrew (1952) gave a rate increase of 530 times for the oxidation of spectroscopic pure graphite with iron impurity, while Sykes and Thomas (1961) quoted an increase of 324 times for the same reaction. Gallagher and Harker (1964) attributed catalysis to the liberation of free metal whose atoms can become incorporated into the carbon structure to produce a complex of higher reactivity. This metal could bond at dislocation and vacancy sites.

Another method of increasing graphite reactivity is by pre-irradiation. It is known that this treatment will introduce defects into the graphite, and Ragone and Zumwalt (1961) stated that these can act as active sites and so increase the dissociation of surface complexes. Watt and Franklin (1957,1958) showed that the most defective regions of graphite were preferentially oxidised. This was proved by an x-ray technique.

(b) Graphite-Carbon Dioxide Radiolytic Reaction

Since the development of nuclear reactors using graphite as a moderator and carbon dioxide as a coolant gas, the investigation

of the oxidative corrosion of graphite has become important. Although the thermal reaction does not become prominent till 625°C., the radiation induced reaction has been shown to proceed rapidly at 350°C. (Davidge and Marsh, 1955) where the reaction was followed by analysis for carbon monoxide. Methods also used have included graphite weight loss, the use of tracers and even strength changes.

The first review of the reaction including a possible mechanism was reported by Anderson and co-workers (1958). They considered that the primary reaction is the absorption of radiation energy in the gas which results in the formation of an active species which can migrate to a surface and attack the graphite. They considered the active species to be the oxygen atom produced by

$$CO_2 \longrightarrow CO + O \quad \text{and then} \quad O + C \longrightarrow CO$$

This represents the reaction in its simplest form. To explain results, they also concluded that the reverse reaction must be enhanced by irradiation. They found deposited material presumed to be from carbon monoxide radiolysis, and when some of this gas was added to the system, it reduced the carbon removal either by adsorption or, in some cases, deposition of the suboxide polymer which was found at irregularities in the graphite blocks, but the bulk weight loss was not offset by the deposition reaction.

Due to the variability of the reaction, no definite mechanism has so far been proposed. Nightingale (1962) suggested that any mechanism must include the primary dissociations of carbon dioxide and carbon

monoxide, whose products may produce a number of secondary reactions, for example, the formation of carbon and carbon suboxide polymer deposits and their reactions with oxygen atoms or ozone to regenerate carbon dioxide; the reactions of oxygen atoms at surfaces to produce oxygen or ozone; the reactions of oxygen atoms with deposited carbon to give carbon monoxide and with this, to form carbon dioxide; heterogeneous oxidation of graphite by oxygen atoms. The relation between carbon dioxide pressure and radiation induced reaction is complex and depends on conditions of flow and geometry of the system. The rate in a flowing system can be considered as the product of a) the rate of formation of active species, b) the fraction of them arriving at a graphite surface and c) the fraction which react after arrival.

Temperature does not play an important role in gasification. The reaction rate was shown to be independent of temperature in the range 25 - 350°C. by Anderson et al. (1958) and up to 500°C. by Gow and Marsh (1958). This means that the rate of carbon monoxide production reaches a constant value and the only change is brought about by increasing the number of surface atoms available as sites for surface oxide (Gow and Marsh, 1960). This was also stated by Sach (1961) who showed that initial production of carbon monoxide was affected by the number of unoccupied free sites and some gas could be lost by radiolysis. Dominey (1961a) showed by tracer experiments that carbon monoxide production and carbon transport to the gas phase decreases as the dose increases, proving that there is either inhibition due to the reverse reaction

$CO + O \longrightarrow CO_2$ or deposition by CO radiolysis. He supported the first conclusion. He also heated samples in pure carbon dioxide after irradiation and the gases obtained were due to the decomposition of a surface oxide layer.

Since most of the work on this reaction has been carried out on nuclear grade synthetic graphite, its pore structure has been shown to be important in the reaction. Tomlinson and Walker (1961) showed that, within a factor of two, there was no significant difference in the type of carbon used and impurities did not catalyse the reaction as was found in thermal reactions. They also showed that reaction took place in the pores, and despite the proximity of the graphite surface, recombination reactions could also take place. Hutcheon, Cowen and Godwin (1962) showed that reaction took place internally as well as externally on graphite blocks due to the radiolysis of gas within the pores and rates were found for materials of different porosities.

The effect of pores is usually seen in the initial stages of a reaction when the first few per cent burn off usually opens some of the closed pores so increasing the surface area and therefore the available reaction sites. For this reason most rate measurements are made once a steady state has been reached, usually after a few per cent burn off.

Lind and Wright (1963) stated that the rate of carbon gasification is proportional to a) the open pore volume, since most gas radiolysed external to pores will be deactivated before reaching the surface,

most reaction will then arise from gas inside the pores, b) the density of carbon dioxide within the pores and c) the irradiation dose rate. These authors also believed that excited states of carbon dioxide as well as oxygen atoms are involved in the reaction mechanism which can be written in simplest form

$$CO_2 \longrightarrow CO + O$$

$$O + C \longrightarrow CO$$

$$CO_2 \longrightarrow CO_2^*$$

$$CO_2^* + C \longrightarrow 2CO$$

The active species may be destroyed before reaching a graphite surface by

$$O + CO \longrightarrow CO_2$$

$$CO_2^* + CO_2 \longrightarrow 2CO_2$$

These reactions were proposed for neutron irradiated systems. Claxton (1962) studied the oxidation of carbon by electronically excited carbon dioxide using low voltage electrons to limit the number of excited species and his results suggest that attack was due to a neutral species probably atomic oxygen. He found carbon removal plus deposition.

Gasification of carbon by the products of the vacuum ultra violet photolysis of carbon dioxide has been found by Feates and Sach (1965). They attributed the reaction to oxygen atoms but no stoichiometric relationship was deduced. They found that surface oxide was essential to the gasification reaction.

(c) Inhibition of Graphite Gasification

Due to the high rate of carbon gasification in nuclear reactors, there is a great need for a method of curtailing this loss. Since the radiation induced reaction proceeds mainly at pores, a new type of closed pore graphite has been produced. By using impregnants and regraphitization techniques the rate was reduced by a factor of three (Lind and Wright, 1963).

Another method is the use of gaseous additives to inhibit the gasification. The addition of carbon monoxide has been widely studied. The work by Anderson et al. (1958) has already been mentioned. They found that the weights of graphite samples increased due to reduced carbon gasification and deposition of carbon suboxide polymers. These could also be destroyed to give

$$C_3O_2 \longrightarrow C_2O + CO \qquad C_2O \longrightarrow CO + C$$

Dominey (1961b) found that carbon monoxide was a better inhibitor at external graphite surfaces than at internal pores. Copestake and Feates (1962) used C^{14} tracer experiments to show that carbon monoxide inhibited gasification more readily at geometric surfaces than within the pores and that there was also some irreversible carbon monoxide adsorption. It was reported that the maximum inhibition was obtained at low carbon monoxide concentrations and Feates, Sach, and Walker (1964) found that 1 - 7% CO gave an inhibitory factor of 3 times. Early results indicated a reduction of as much as 10 times for 7% carbon monoxide addition, but this was found to be due to impure carbon

monoxide. The nature of the impurity was found to be methane and will be discussed below.

Lind and Wright (1963) listed the possible processes occurring to give a rate reduction: - 1) interception of the active species in the gas phase (considered unlikely); 2) the modification of attack by forming an adsorbed phase on the surfaces; 3) deposition of carbonaceous solids by radiolysis so compensating for some carbon removal and 4) deposition of such a layer which could act sacrificially to prevent attack on underlying graphite. These authors considered that carbonaceous deposits did not appear to accumulate continuously within the pore structure around 300°C. for the pure carbon dioxide reaction, but when carbon monoxide was added, deposits were formed and in addition some deposit was carried by the gas stream to the surfaces out of pile. Ashton, Labaton, and Wilson (1965) observed a negligible increase in surface area after an initial 2% burn off, and with the dioxide-monoxide gas mixture, they found a negligible amount of deposit and so concluded that the reduction in weight loss was due to a lower attack rate, i.e. explanation (2) of Lind and Wright.

Cluley and Corney (1962) also found deposit in reactions of carbon monoxide-dioxide mixtures in a neutron flux but they found barely detectable deposition and carbon monoxide formation in a gamma flux from experiments using C^{14} active gases.

The addition of .1% methane to carbon dioxide has been shown by Feates and Parry (1964) to reduce gasification by a further factor

of three and this is supported by Dominey and Morley (1964) who used a mixture of 1% carbon monoxide, .1% methane in carbon dioxide. The inhibiting gases caused an exponential fall of reactivity but, on their removal, the reactivity recovered much slower showing that the inhibition effect had taken place at a graphite surface. Dominey and Morley considered that graphite protection was due to a short lived product of the radiolysis which interfered with the normal processes at the graphite surface. These results held for both neutron and gamma irradiation experiments and there was no deposit in gamma reactions probably due to the lower dose rate.

Tomlinson and Wright (1965) also investigated this inhibition and found that pure carbon monoxide was not very effective but compounds such as sulphur dioxide, chlorine or iodine reduced gasification by up to fifteen times. This was also true of compounds which could decompose to give these substances, hydrogen or the above mentioned carbon monoxide-methane mixture.

(d) Microscopy of Graphite Oxidation

Light microscopy observations into the attack on graphite by molecular oxygen were carried out by Greer and Topley (1932) who found that attack was localised at certain regions which appeared as hexagonal holes. They suggested that this was due to catalysis by impurities. This type of attack pattern has been found frequently since that time but in addition there was also found the more basic edge attack.

Edge sites normally have valencies which are not taken up in the network system and these can be satisfied by bonding to a foreign atom, e.g. an oxygen atom, and subsequent removal of carbon monoxide will leave fresh sites for adsorption and reaction. By studying the oxidation of graphite single crystals, Hennig (1959) showed that edge atoms exhibit much greater reactivity than those within the layer planes. This confirmed earlier physical results of Smith and Polley (1956), and Walker, Rusinko, Rakszawski and Liggett (1959), and later by Lang, Magnier, Sella and Trillat (1962).

The production of pits on the graphite surface has been widely reported and discussed. The results of Earp and Hill (1958), Duval (1961), and Jacquet and Guerin (1962) suggested that impurity catalysed the carbon oxidation and this reaction was studied by Presland and Hedley (1962,1963). They found the basic edge attack plus catalytic attack which resulted in the formation of channels with a catalyst particle at the head of each one. These channels were parallel to the basal plane, tapered and usually started at steps and crystallite edges. Using platinum catalyst, attack was examined after reaction with oxygen and carbon dioxide. The latter gave no channel widening and there was random removal of graphite at points round the basal plane edges together with some hexagonal pitting, sometimes associated with terminating surface steps, as described by Hennig (1961a). Hexagonal attack in air was also found by Hennig and Kanter (1960), Hughes and Thomas (1962), and Trillat, Sella and Miloche (1962) who also showed that

carbon dioxide attack was slower than air but gave the same geometric hexagonal attack, and so they concluded that the same mechanism applied. They found the strongest evidence of oxidation at the convergence or intersection of dislocations and also their emergence at grain boundaries. They found that only surface dislocations played an active role. Lang, Magnier, Sella and Trillat (1962) found that the number of pits was proportional to the number of dislocations. This is counter to the conclusions of Presland and Hedley who stated that crystal defects had no effect on the oxidation. Support for an impurity catalysed oxidation was given by Dawson and Follett (1963) who studied the air oxidation of polycrystalline synthetic graphite. These authors showed that attack occurred around the edges of the microcrystals of which the crystal was composed and also at the pores. This was really edge attack catalysed by impurity at these sites. Lang and Magnier, (1963) showed that the oxidation rate with carbon dioxide increased as the number of micropores increased.

Evidence has been produced by Hennig (1959, 1960, 1962a and b) and Hennig and Kanter (1960) to suggest that catalyst alone is not enough to promote attack, but that catalyst particles are believed to act in conjunction with defects. In 1962, he showed that crystals free of defects were attacked parallel to the cleavage surface, but those crystals containing defects or impurities were attacked perpendicular to the plane and pits were produced.

In order to study the effect of defects on oxidation, certain

workers reacted pre-irradiated graphite with oxygen or carbon dioxide. The reaction has been shown to be catalysed. Dawson and Follett (1963) showed that the basal plane was covered by shallow pits after reaction and these pits were often associated with dark impurity particles. Follett (1964) showed, by adding impurity, that unirradiated graphite showed only edge attack catalysed by the impurity, whereas pre-irradiated graphite exhibited deep surface pits produced by catalytic oxidation. This suggests that the increased reactivity was due to the active sites produced by irradiation acting in conjunction with the impurity catalyst.

However, pits have been produced in graphite after the removal of all impurity. Lang et al. (1962) purified pyrolytic graphite above 3000°C. and, on subsequent oxidation, hexagonal pits were found. This was also found by Presland and Hedley (1963) for purified natural graphite. Papers by the group of workers, Hughes and Thomas (1962), Hughes, Williams and Thomas (1962), Thomas, Hughes and Williams (1963), Hughes and Thomas (1964), showed that graphite with impurity content less than 20 p.p.m. will always give etch pits which must therefore be an intrinsic feature of chemical attack. They showed that reaction above 700°C. in oxygen produced concentric hexagonal pits, with two of the pit sides parallel to twin bands, in addition to edge attack. They found that carbon gasification occurred faster along the $10\bar{1}\ell$ planes than the $11\bar{2}\ell$.

Hennig (1959) suggested that terraced etch pits were due to a

variation in oxidation rate amongst the terminating edges of the basal planes, but the above authors suggest that etch pit formation is due to two species, one etching and the other inhibiting. The extra species in the graphite-oxygen cycle could be surface oxide, since high temperature produces less well defined pits which could be explained by the instability of surface oxide so giving less inhibition. Thomas et al. suggested that pits can be nucleated at screw dislocations and point defects but they found difficulty in distinguishing this from catalytic attack since impurity particles are almost invariably found at defect centres. They also found, using carbon dioxide at 900°C. for five hours, that no pits or other attack perpendicular to the basal plane was produced in their pure graphite.

The most recent paper by Hughes, Thomas, Marsh and Reed (1964) suggests that the most important defects in pit formation are line dislocations (edge and screw), condensed point defects, impurities, or any combination of these. They also showed that condensed vacancy loops and c-axis screws can stimulate pit formation. Thomas and Walker (1965) also showed that non-basal line dislocations were responsible for some basal plane etch pits.

The oxidation of graphite by atomic oxygen was shown to have a completely different mechanism (Marsh, O'Hair and Reed, 1965). During this reaction, the effects of anisotropy were largely absent and reactions parallel and perpendicular to the basal plane were equal.

Atomic oxygen is capable of removing carbon from basal plane positions. This could have been due to surface oxide formation protecting edge positions on which atoms can be more readily adsorbed. The oxidation resulted in a general background of conical pits as well as the usual etch pits associated with defect structures. In this case, iron impurity promoted the recombination of atomic oxygen and so decreased the oxidation rate, and also produced hexagonal hillocks around which normal graphite removal had taken place.

4. Decoration

This is the name given to the phenomena produced when certain metals are evaporated onto some surfaces and, after heating and viewing directly, the metal particles are noticed to vary from random distribution and 'decorate' the surface.

The technique was instigated by Bassett (1958,1960) and Bassett, Menter and Pashley (1959) who studied the decoration of rocksalt by silver and gold particles. Bassett (1960) observed silver deposition of particles 70 - 100Å in diameter. On subsequent heating of the sample, movement of metal was produced and on cooling, the particles became immobile. Sears and Hudson (1963) suggested that the silver crystallites could be nucleated on an adsorbed surface layer of gas and produce slight interaction between the particle and the substrate. The particles then moved by Brownian motion until they reached a section where true contact took place between the particle and the substrate. Thomas and Walker (1964) investigated the motion of different metals

over graphite in different atmospheres. They found that silver moved by a rotary motion about an axis perpendicular to the graphite surface and also some translatory motion was noticed. Particles of iron, cobalt, nickel were immobile. They found that various gases altered the mobility so chemical factors must influence mobility, possibly the formation of certain metal oxides. These authors consider the chemistry of particle and substrate important to this study, in particular the behaviour of the chemisorbed layer over which they believe motion will take place. The motion of gold particles over alkali halide crystal faces has been the subject of papers by Hucher and Oberlin (1961) and Sella, Conjeaud, and Trillat (1959). They observed gold particles at steps, dislocations and other defects. Gold mobility was attributed to a charge effect and particles could be held at negatively charged sites by Van der Waals forces. In this way the more polar the adsorbed molecule, the easier it could be held, and when suitable sites had been filled, no more decoration could take place.

Observations have been made by Hennig (1964) on the decoration of graphite samples by gold which he found to aggregate at surface irregularities such as steps, dislocations, impurity and point defects. This resulted in these areas being made visible in the electron microscope. At a decoration temperature of 250°C. he found 10^9 particles per sq. cm. but at 900°C. this was reduced to 2×10^8 per sq. cm. Irradiated samples increased this number to 2.2×10^{10} at

10^{18} n/cm^2 and 1.4 x 10^{11} at 10^{20} n/cm^2. Plates showed single metal crystals at point defects and broken lines to show the presence of dislocations. From the irradiation experiments, it can be seen that the number of particles increases with the dose so the technique can give a quantitative estimation of vacancy cluster concentration. Hennig proposed that 10^{18} n/cm^2 displaced 2.5 x 10^{12} atoms/cm^2 in clusters of several hundred, and if each cluster caused the nucleation of one particle, 10^{10} would be produced and this figure agreed with his experiments. Also Hennig (1965) used controlled cleavage and etching to convert defects to surface depressions which could be made visible by decoration and this was used to estimate the number of active lattice sites. He noted that any surface complex present not only inhibited reaction but reduced particle numbers by blocking sites.

5. Aim of the Present Work

The studies to be described were undertaken in order to examine the oxidation of graphite by carbon dioxide in the presence of radiation. The electron microscope investigations can be divided into four main aims: -

(a) To study the graphite oxidation under different types of irradiation, i.e. proton beam, neutron flux, gamma rays and vacuum ultra violet radiation.

(b) To compare the reaction effects on natural and synthetic graphite with a view to relating oxidation features to graphite structure.

(c) To try to identify the active species responsible for reaction. This could be done since the vacuum ultra violet radiation, produced by an inert gas discharge, has a known wave length and the possible energetic states of the reactant gas could be found. If the reactant species for this reaction was known, it was hoped that comparison of results would lead to a similar identification for the other radiation systems.

(d) To try to find materials capable of effective inhibition of the oxidation, without complicating the system by side effects.

EXPERIMENTAL

Contents

1. Materials

(a) Graphite

Three types of graphite were used in this work. One type was pile grade A polycrystalline synthetic graphite which is the grade used in British Nuclear Reactors. Also used was spectroscopically pure natural graphite (SP1). This is a purified graphite from Ceylon or Madagascar and a table is shown overleaf of the impurity contents of these two graphites (Labaton 1965). The natural graphite, in addition to its greater purity, also has a greater crystallite size and lower defect content.

Another specimen of natural graphite was extracted from American dolomite rock. This consisted mainly of calcium carbonate which was dissolved in dilute hydrochloric acid. After washing with distilled water and ammonia, whose chloride was removed by dialysis, a clean specimen of this graphite was obtained. This specimen, after a few initial experiments, was found to behave identically to the purified material and further experiments were concentrated on that material in addition to the synthetic grade. Similarity of natural graphite material under oxidation was also reported by Carr (1965) for chemical oxidation.

(b) Gases

Carbon dioxide was purified before use by passing over copper oxide at 800°C. to oxidise any hydrocarbons, and by cooling to -78°C. to remove water vapour. It was finally purified by repeated vacuum

Typical Analysis for Impurity (p.p.m.)

	SP1 Maximum	P.G.A. Range
Ash	-	.005 - .025
Aluminium	.015	.25 - 2.5
Barium	.015	.3 - 15
Beryllium	.015	.02 - .03
Bismuth	.06	.06 - .15
Boron	.02	.03 - .16
Calcium	.15	7 - 60
Chromium	.015	.1 - .7
Cobalt	.015	.01 - .03
Copper	.04	.01 - .5
Hydrogen	-	15 - 40
Indium	.04	.04 - .08
Iron	.05	2 - 16
Lead	.025	.04 - 2.5
Lithium	.005	.04 - .15
Magnesium	.025	.03 - 1.5
Manganese	.015	.01 - .06
Nickel	.025	.03 - 8
Phosphorus	-	.1 - .2
Silicon	.15	15 - 60
Sodium	.1	1 - 2
Tungsten	.08	.08 - 2
Vanadium	.02	.4 - 30
Zinc	.08	.08 - .2
Others	.045	.1 - 1.64

sublimation. Passing the gas over B.T.S. catalyst (reduced copper oxide) removed any oxygen which might be present. Methane was also obtained in cylinder form in which the impurity was a small concentration of higher saturated hydrocarbons. Carbon monoxide was prepared by the reaction of sodium formate with concentrated sulphuris acid, and it was purified by vacuum distillation at the temperature of solid nitrogen. Ketene was prepared by refluxing acetone in the presence of a red hot nichrome wire. The resulting gas was purified by boiling off from a liquid pentane trap ($-120^{\circ}C.$) which retained any acetone which could have been present.

2. Specimen Preparation

(a) Mounts

The normal copper grids of diameter 3.05 mm. were not used in this work. It was found that seven holed platinum - iridium mounts covered by silicon monoxide films were most suitable. These films were prepared by firstly covering the mounts with a formvar film, floated off a glass slide in water, and, after drying, a silicon monoxide film was evaporated onto them. This was done by the method of Bradley (1954) by evaporating a silicon - silicon dioxide mixture from a molybdenum boat under a vacuum around 10^{-4}mm. Hg. using a 10v.60 amp. transformer. The formvar could then be removed either by holding the mounts in the vapour of refluxing ethylene dichloride or better still, firing in a porcelain crucible to a dull red heat.

This type of platinum - iridium mount was suitable for all

experiments except those in the nuclear reactor, where the neutron flux could activate the metals considerably and leave them too active to handle. For this reason, first aluminium mounts and later zircalloy mounts were used in these experiments. These mounts were specially cut to the same specifications as normal mounts i.e. 2.30 mm. diameter with seven 70μ holes. The aluminium mounts were found to be too susceptible to slight acid attack from the formvar solution in ethylene dichloride and the zircalloy mounts were almost exclusively used. Since both these materials are also subject to oxidation at moderate temperatures, no great heating can be used to remove the formvar films. Zircalloy consists of zirconium plus 1.2 - 1.7% tin as the main ingredients but some metal impurities (total .2%) of iron, aluminium, chromium, magnesium and nickel can be present.

(b) Graphite

The purified natural graphite SP1 was obtained as a powder and by placing a small amount in a test tube with distilled water and repeatedly centrifuging and withdrawing the supernatent liquid, a clean sample was obtained. This material was suspended in distilled water and subjected to ultrasonic disintegration for less than one minute. This was sufficient to produce a suspension of thin flakes suitable for microscopy.

The other natural material could be prepared similarly after removing the larger graphite sections which could be ground down to

a more convenient size.

The nuclear grade material was received as large blocks and the usual preparative method was to scrape gently along any surface with a razor blade. This produced a fine powder which could be ultrasonically disintegrated into small flakes, usually after a longer treatment than for natural material.

After sonic treatment, the largest particles of graphite were allowed to settle out and a drop of the fine suspension was removed and dropped onto a mount with supporting film. This was then dried in a cool oven and so was ready for microscopy.

Apart from the increased stability of mounts to reaction conditions, they are useful in the attempts to relocate specific areas after reaction. By marking and numbering a mount and its holder for microscopy before reaction, and by drawing out maps of the graphite distribution on particular mount holes photographed, it was possible to return to that same area after reaction and so obtain a visual comparison of it before and after reaction.

In order to examine the influence, if any, of the preparation conditions on the reactions, some samples were prepared using the graphite powder without wetting or utrasonic treatment. This was done by drawing a mount over an area of graphite powder. Not very much adhered but there was usually enough to study the reaction effects.

(c) Shadowing

This technique can be used to give some information on the

surface of a material. By using the conditions described for film preparation, a metal shadow, particularly nickel - palladium evaporated from a tungsten filament, or a finer platinum - carbon shadow, from a carbon rod with a platinum centre, can be produced by having the specimen holder tilted at any angle to the evaporation point. Usually angles of 15° - 20° are wanted with the specimens being at least 10 cms. from the source. Any raised surface areas will appear dark where the metal strikes and the shadow will be light due to the absence of metal, and shadow length will therefore give information on the height of that area.

(d) Decoration

A known weight of gold or silver was evaporated from a tungsten filament which was held a known distance above the specimens to be decorated. The normal evaporation conditions were used. From Kay (1965) an expression for the thickness of metal on the specimen, t, was derived.

$$t = \frac{m}{4\pi r^2 \rho}$$

where ρ = metal density

r = distance from source to specimen.

The specimens were heated to give mobility of the metal over the graphite surface. This was done by supporting the specimens for decoration on a flat surface of a carbon rod connected between two terminals, and a thermocouple was placed at the centre of the rod to give an accurate temperature reading for the specimens. In this

way the specimen temperature could be held at any value during decoration. Most evaporations were carried out using .004 g. of metal wire from a tungsten filament held at a distance of 10 cms. from the mounts, giving a metal thickness of around 30Å. Specimens were usually heated to 300°C. before evaporation and held at that value for a few minutes afterwards to ensure mobility.

3. Reaction Apparatus

(a) Proton Irradiation

These experiments were carried out in a proton Van de Graaff generator. The principle of this apparatus is that a high constant potential is generated electrostatically and is distributed along an evacuated tube for the acceleration of charged particles. A fast moving belt, conveying an electric charge, developes high voltage and protons can be produced from a source at the terminal end of the acceleration tube. The protons are accelerated to high energy and the beam can be collimated.

The experiments to be described were carried out in a generator at A.E.R.E., Harwell. In that apparatus, the beam passes through a thin aluminium foil window into the reaction chamber containing the graphite specimens and the reactant gas. The window had the effect of reducing the beam energy from 1.77 Mev to 1.5 Mev. A view of the reaction vessel is seen in Figure 4. The beam produces luminescence in the irradiated carbon dioxide gas and this is the only source of illumination for the photograph. In the path of this illuminated

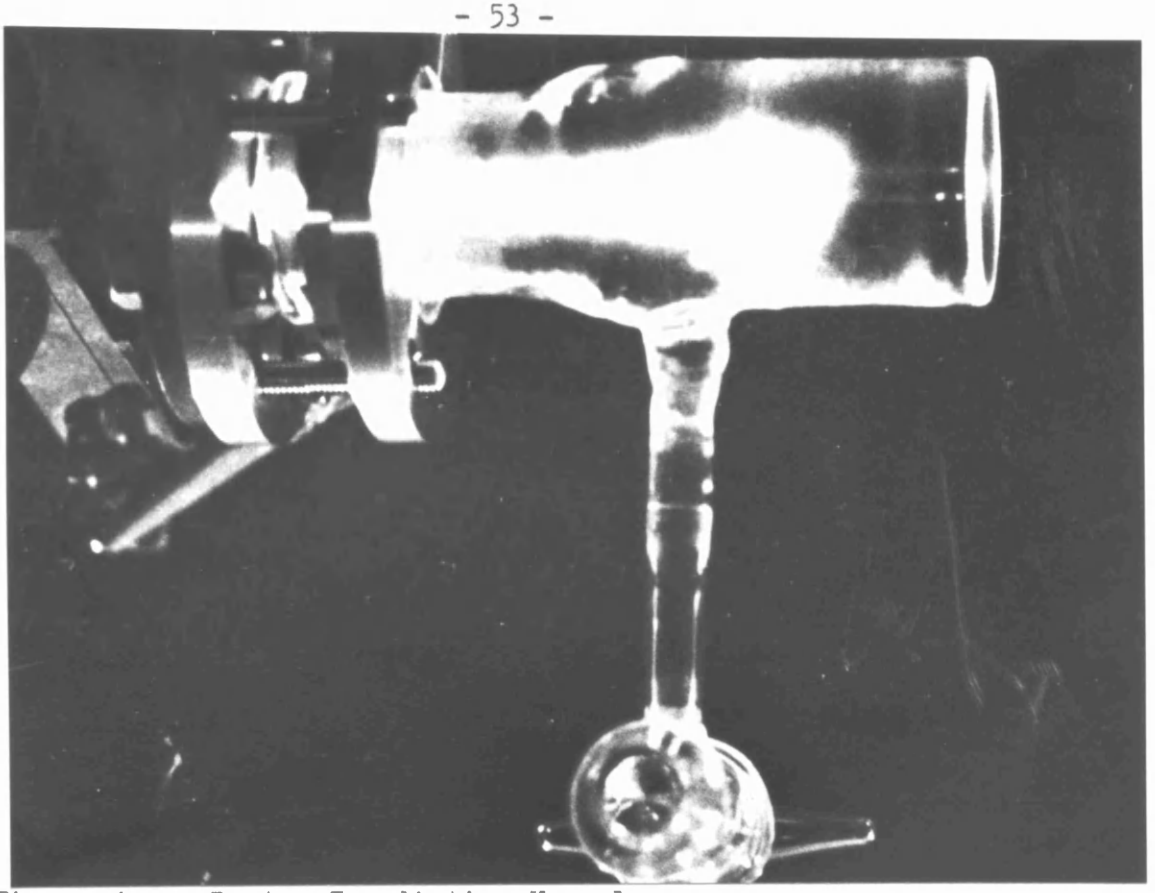

Figure 4 Proton Irradiation Vessel

- - - - - - - -

beam, all the protons are lost through excitation and ionisation of any substance directly in this beam. In this way only when graphite samples are in the beam will they be damaged, and otherwise the irradiation will only affect the gas molecules.

Platinum - iridium mounts with silicon monoxide films were used to support the graphite samples. Specimens of the three graphite types mentioned before were used. The mounts were placed on a tray which was fixed to the tungsten collector, which protruded into the vessel to measure energy. The height of the tray could be varied so that the mounts could be placed either in or out of beam. The photo-

graph of Figure 4 illustrates a static system but a flowing system was constructed by the inclusion of a gas outlet through which the gas was pumped to keep up a flow of 100 c.c. per minute at 30 cms. pressure. The experiments were carried out in pure carbon dioxide at 25°C. for times varying between one and six hours for out of beam experiments, and between half a minute and one hour for in beam experiments.

(b) Neutron Irradiation

The first experiments using this type of radiation were carried out in the reactor DIDO at A.E.R.E., Harwell. This gave a dose of greater than 10^{20} n/cm^2 and produced too much reaction. The reactor BEPO was used subsequently. This is an air cooled, graphite moderated experimental reactor. A rig was assembled in the form of an aluminium can. Graphite samples were prepared on zircalloy mounts and these were supported in an aluminium holder near the foot of the can. A heater coil was also built in to the mount support, and inlet and outlet tubes at the top and bottom of the can allowed the reactant gas to flow, if required. After insertion of the samples, an air tight lid was sealed on and the rig could be lowered into a hole in the reactor. The dose rate received by this set up was around 10^{12} n/cm^2/sec. i.e. a dose of 10^{18} n/cm^2 in two weeks. The ambient temperature of the reactor was around 80°C. so no runs could be carried out at 25°C. A temperature of 350°C. was used invariably since this was known to be high enough for reasonable attack but not too high to oxidise the aluminium can or zircalloy mounts. Pure carbon dioxide was first used but later

the gas mixtures 1% carbon monoxide/.1% methane in carbon dioxide and .3% ketene in carbon dioxide were used in attempts to inhibit gasification. Most series of experiments were carried out in a flowing system where gas at 1 atmosphers pressure was allowed to flow over samples at a rate of 10 c.c./min. A few experiments were carried out in a static system at a gas pressure just above 1 atmosphere. The reaction time was limited to multiples of two weeks which was the normal reactor running time between successive shut-downs.

(c) Vacuum Ultra Violet Irradiation

The irradiation work was again carried out at A.E.R.E., Harwell. A few experimental runs were done using a xenon gas lamp which gives absorption at 1470Å and 1295Å but the vast majority of experiments were performed using a krypton lamp which gives absorption at 1236Å and 1165Å.

For both gases, the experimental arrangement was identical. Gas at 110 mm. pressure was sealed off in a glass discharge tube excited by a microwave cavity provided by radiation from a 200W 2450 Mcsec^{-1} microwave generator which provided continuous wave output. A zirconium-alluminium getter was fixed at the end of the discharge tube where the gas entered and by keeping its temperature at 400°C., impurities were removed from the filling gas and also any gas desorbed from the tube walls. At the other end of the tube, a small thin walled silver tube was sealed between the glass and a lithium fluoride window. This was cut approximately 1.4 cm. diameter and .5 mm. thick. This window

transmitted the ultra violet light into a specimen chamber as shown in Figure 5. The disc-like holder was specially constructed to hold four specimen mounts, which were invariably platinum - iridium mounts two of which supported purified natural graphite and the other two held nuclear grade material. The gas to be used in each experimental run continually flowed over the specimens at approximately 3 c.c. per minute and was kept at a pressure of 30 cms. Hg.

The time of each experimental run cannot be taken as a guide for comparing results since the conditions are known to vary. The principle cause of this is the lithium fluoride window, which must either be cleaned or replaced for every new experiment. The conditions are therefore variable due to its thickness, the production of colour centres which can stop emission in the required ultra violet region, and the deposition of silver on this window. For these reasons, the energy output of the system at the start and finish of each run was measured by the estimation of the quantity of ozone produced from oxygen in a known time of passage through the system. A quantum yield of two was taken for ozone production and this was estimated by passing it into 5% potassium iodide and by titrating the liberated iodine against .01 N sodium thiosulphate. From this, the total quanta passed was calculated. Experimental runs varied from two to five hours and gave quanta emitted of from 1×10^{19} to 4×10^{19}.

The graphite samples were irradiated in pure carbon dioxide and

F I G U R E 5

Vacuum ultra violet irradiation apparatus.

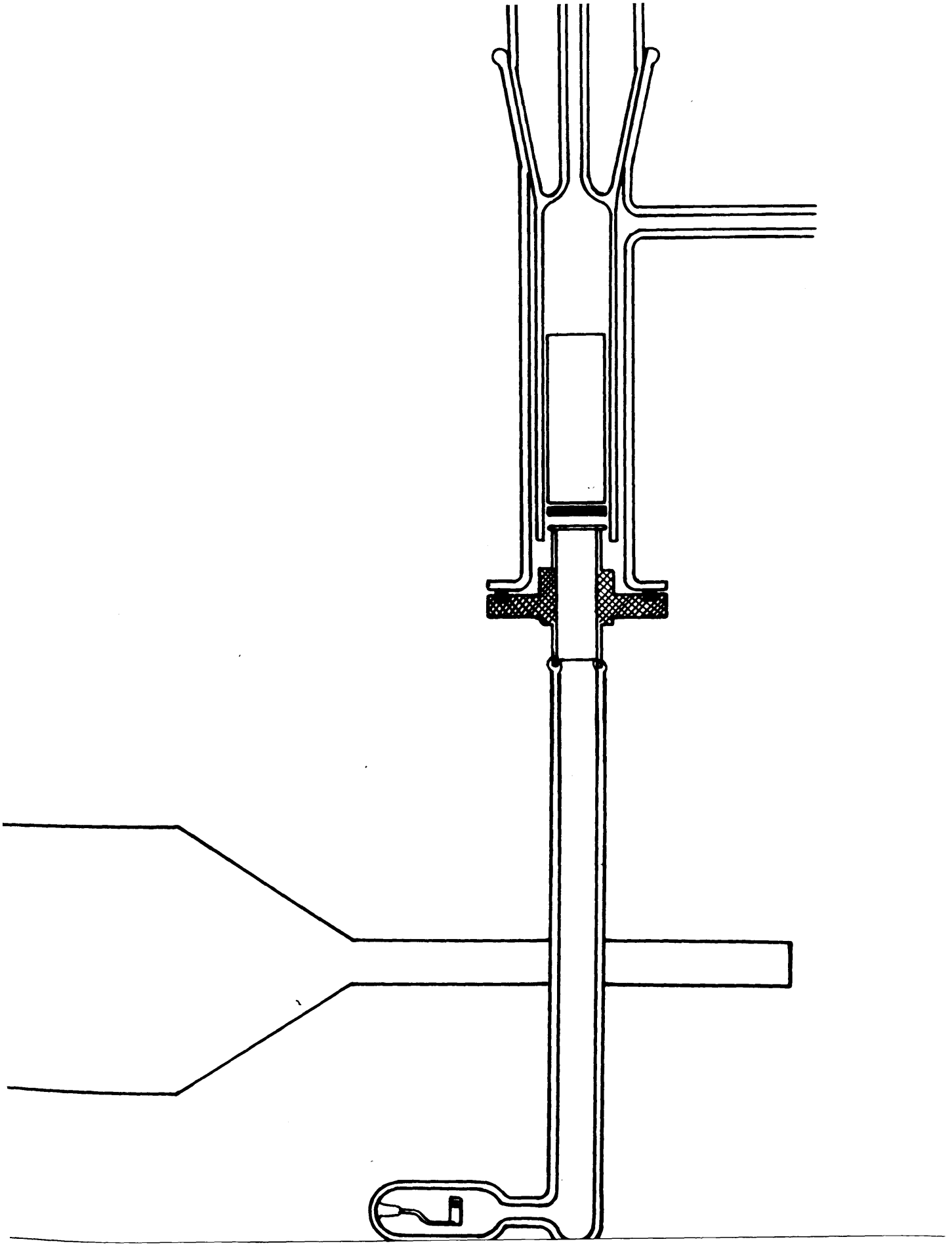

in carbon dioxide with small quantities of other gases added. These were .1% methane and 1% carbon monoxide, .1% methane, 1% carbon monoxide, 1% ketene, all in pure carbon dioxide. Most experiments were performed at room temperature (25°C.) but some using pure carbon dioxide and the methane, carbon monoxide, carbon dioxide mixture were carried out at 350°C. For this purpose the specimen chamber illustrated was heated by an electric muffle furnace wrapped around it.

As usual, suitable graphite areas were photographed before and after reaction and some samples were reacted without prior examination to ensure that the examination did not affect the subsequent reaction process. Some samples were also mounted dry to ensure that normal specimen preparation did not affect the results. Also some samples, after initial reaction, were re-irradiated to study the effect on the initial oxidation features.

(d) Gamma Irradiation

These experiments were carried out in the T.I.G. pond at A.E.R.E., Harwell. Radioactive cobalt rods are arranged in a circle at the foot of a water filled, steel pond. A rig, similar to that used in BEPO, was lowered into the centre of the circle and so received the gamma irradiation. The only extra equipment used was a waterproof casing for the gas and heater leads. This system gave a dose of approximately 10^6 rad/hour. Any desired dose could be calculated as a function of time and reaction could be stopped merely by raising the rig out of the radiation zone. Platinum - iridium mounts could be used in these

experiments.

4. Electron Microscopy

(a) Introduction

The electron microscope used for this work was the Siemens Elmiskop 1 which can give magnifications varying from 200 to 160,000 by means of a projector lens with four different pole pieces. The instrument also has magnetic lenses and a double condenser illumination system and can operate at 40, 60, 80 or 100 kV. This section will deal mainly with the operation and techniques used during microscopy and detailed theoretical considerations of design and uses have been summarised by Cosslett (1951), Hall (1953) and Kay (1965).

(b) Resolving Power

The performance of any microscope is usually judged by its resolving power which has been defined as the distance between separate points in the final image. This value can be influenced by a number of factors, and Abbé deduced the resolution limit, d, to be given by the formula,

$$d = \frac{k\lambda}{n \sin\alpha}$$

where k is a constant usually taken as unity, n is the refractive index of the object space, normally unity, α is the angle subtended by the lens aperture and λ is the wave length of the illuminating source. From the equation, it can be seen that the resolution is best when $\sin\alpha$ is high, i.e. when a large angular aperture is used. Also the reduction in wave length considerably increases the resol-

ution. This is the reason why the electron microscope has a better resolving power than any light microscope. The wave length of electrons varies from 3.7Å to 6.1Å depending on the operating conditions of the instrument, and these figures will represent the best possible resolution.

Factors influencing resolving power are astigmatism, chromatic and spherical aberration. Aberration from the objective lens can have a great affect since imperfections in its image are magnified by the intermediate and projector lenses. Chromatic aberration arises when electrons produced with differing velocity and wave length, are focussed at different points. Spherical aberration arises when parts of the lens farthest from the axis have different refractive powers. These faults are overcome in the instrument design by high tension and lens current stability.

Astigmatism can occur in the whole system and the objective lens in particular. This is caused by electrons not converging to a focal point but forming images on either side of focus so deforming the focal field. This can often be caused by dirt in the system, particularly on apertures. If, however, cleaning does not rectify the fault, a stigmator control on the instrument can be used. This consists of a small moveable part of the lens which can be shifted until its own elliptical field corrects the fault.

(c) Specimen Contrast

Contrast in an electron microscope image arises from the differ-

ential scattering by the specimen. This means that a dense area will scatter more electrons out of the beam than will the lighter parts so the corresponding part of the image will receive fewer electrons and will appear darker than thin specimen areas. By decreasing the aperture diameter, lens scattered electrons will take part in image formation and so the contrast will increase. The limiting size occurs when the aperture is so small that diffraction effects predominate.

It has been shown that there is a small increase in resolving power with higher beam voltage due to electrons of lower wave length being produced, but this is offset by the greater velocity of these electrons which therefore interact less with the matter through which they pass. This leads to diminished contrast. The recommended voltage to compromise these two effects is 80 kV.

(d) Condenser System

When the single condenser illuminating system is in operation, and the beam is focussed on to the plane of the object, an area of 40 - 50μ in diameter is illuminated. Focussing above or below this plane increases the area of illumination and consequently decreases the intensity. A ray diagram of this system is seen in Figure 6(a), where the single condenser system uses the second condenser which is fairly weak.

For high resolution work, a double condenser system is used with projector pole piece 3. The first condenser is a very strong lens which can form an image of the electron source demagnified fifty

times. The second condenser projects this beam into the specimen where the object area illuminated can be 2μ but the brightness is sufficient for viewing at the higher magnification required. A ray diagram of this system is shown in Figure 6(b). An effect of this reduction in specimen area examined is that this area becomes damaged quite rapidly and there is a greatly increased contamination build up, as much as 1Å per second under optimum conditions.

Because the experiments were carried out in order to compare areas before and after reaction, it was thought unwise to expose sample areas to these conditions. Also, at the magnification desired, satisfactory conditions were obtained using single condenser illumination using projector pole piece 2.

(e) Diffraction

The wave theories for electron diffraction have been discussed by Thomson and Cochrane (1939) and Pinsker (1953). When an incident wave strikes a row of opaque objects, it will mainly pass through along the axis and be focussed into a final image, but some of the wave will be diffracted. These rays will interact in the back focal plane of the objective lens and give a diffraction pattern which will then be magnified as usual.

It is often desirable to have a comparison between a normal image and the diffraction of that particular specimen area and so the technique of selected area diffraction has been developed. Single condenser illumination and projector pole piece 3 are used in this

F I G U R E 6

Ray diagrams of Siemens microscope single and double condenser systems.

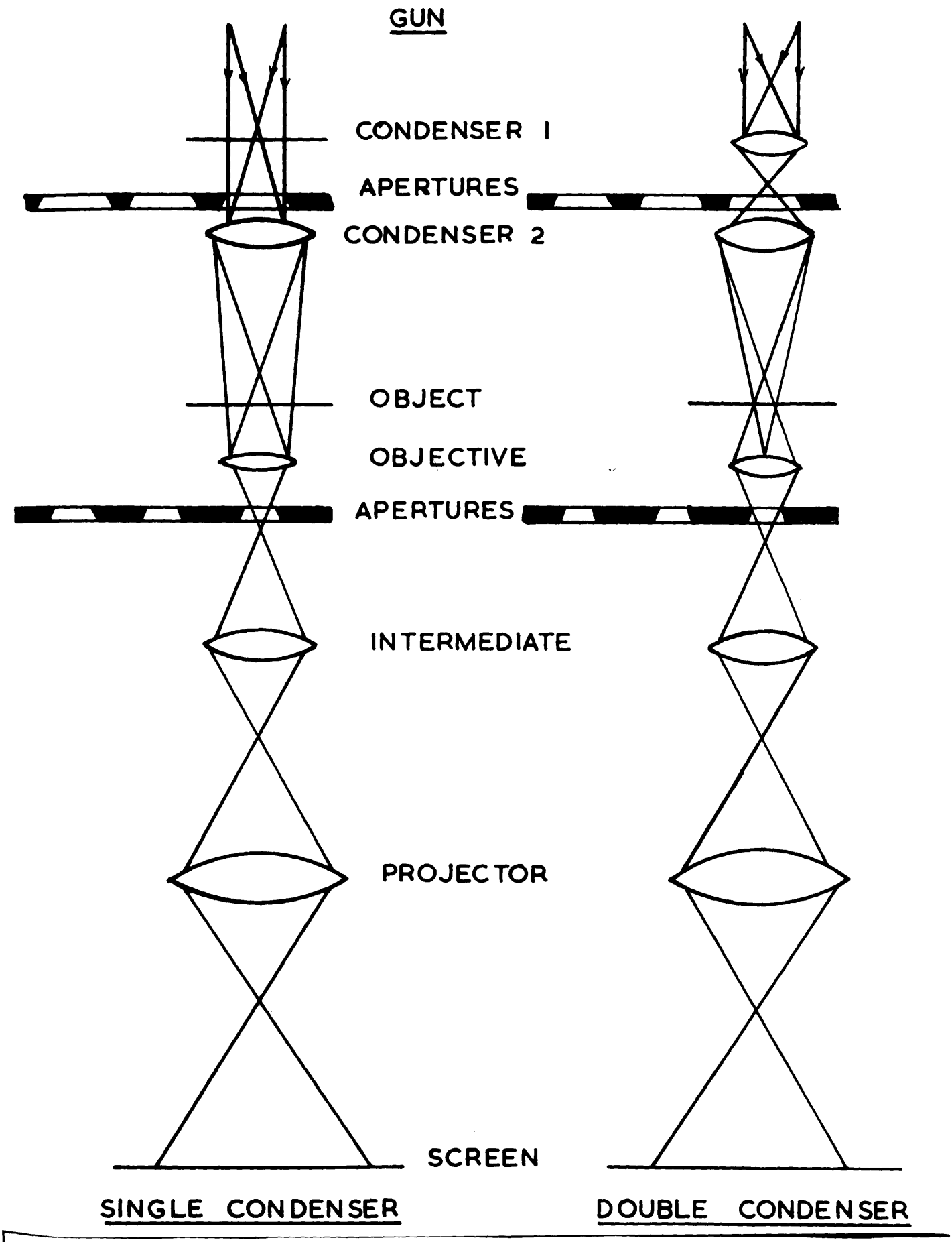
GUN
CONDENSER 1
APERTURES
CONDENSER 2
OBJECT
OBJECTIVE
APERTURES
INTERMEDIATE
PROJECTOR
SCREEN
SINGLE CONDENSER
DOUBLE CONDENSER

technique. The area of the specimen whose diffraction pattern is wanted, is defined by a selector or intermediate aperture in the plane of the objective lens. The intermediate lens is adjusted until the selector aperture is in focus on the final screen then the objective lens is adjusted until the specimen is in focus. The specimen and aperture are now in focus in the same plane. The intermediate lens is then weakened until the zero order maximum of the final image i.e. the centre spot of the diffraction pattern is as small as possible. By removing the objective aperture, the whole of the pattern is seen. The image of the area forming this pattern can be obtained by reversing this process to the point where the aperture and specimen are both in focus.

A plate is taken of a standard substance usually thallous chloride, soon after under identical conditions. Since the pattern ring spacings of this material are known, those for the specimen can be calculated. This can be done more accurately by simultaneous comparative diffraction where the two samples can be mounted side by side and therefore the camera constant used in the calculation can be more accurately determined.

(f) Dark Field

An image in dark field illumination can readily be obtained by displacing the object aperture so that the central undeflected beam of electrons is stopped and electrons forming the image are those

scattered by the object through such an angle that they pass through the aperture. This technique was used in conjunction with selected area diffraction. By centering the objective aperture on a diffraction spot or ring arc, this could be used instead of the central beam for illumination. By reversing the diffraction procedure, this time only the areas which diffract electrons from the planes corresponding to the spot or arc chosen will show up as bright areas.

RESULTS

Contents

1. Experiments Using Proton Irradiation

As mentioned in the experimental section, samples of three different graphites were irradiated in pure carbon dioxide at 25°C. in a flowing gas system (100 c.c./min.) at 25 cm.Hg. pressure.

The actual dose rate for this system was 640 milliwatts received by 4 milligrams of carbon dioxide and this can be converted to more standard units of 7.3×10^{-2} ev./mol./sec. The dose is therefore proportional to the time of irradiation and this proportionality can be used to evaluate the relative doses in different experimental runs. Moreover, some comparison can be obtained from the number of coulombs passed through the system from a current of .5 microamps, but this is also a function of reaction time.

Attempts to find reaction conditions for in-beam experiments were unsuccessful. For a few minutes exposure to radiation, no reaction was found whereas for longer periods, e.g. 30 minutes, no trace of graphite or background film remained. No intermediate satisfactory period could be established. The unsatisfactory results were probably due to the radiation damage to the graphite and film, caused by the position of the mounts in the beam of radiation.

The majority of experiments were done with the specimens outwith the proton beam. In general, since direct beam irradiation causes specimen damage, the geometry of the reaction system must be important since the proximity of out-of-beam specimens to the beam could give effects similar to those obtained for in-beam conditions. Also highly

activated gas species have more chance of deactivation by collision than in the case of specimens further from the beam.

The first observable results were obtained after 100 minutes reaction on the purified natural graphite held out of the beam. A typical area is illustrated by Plates 1A and B which show the same area before and after reaction. This demonstrates that the flake edges have been attacked, particularly at the stepped layers, where approximately twenty layer edges have been etched back to a thicker edge. These thin edge regions have been attacked faster than the thicker edges seen elsewhere on the same micrograph. Edge reaction has also taken place at the edges of the small rectangular flake lying on the graphite surface. After attack a long white line has become more obvious and since it has dark boundaries on either side, it is likely to be a fold in the graphite which has been viewed perpendicularly. Another feature of attack is the appearance of some dark particulate material which occurs on the graphite only, and not on the supporting film. Although this could be a reaction product which was deposited on the graphite, the original area shows some similar material and no definite conclusion can be reached from this evidence.

Plates 2A and B, however, give a much clearer picture. The original flake shows a clean area of the purified natural graphite which, after the same conditions as the above case, shows some edge attack plus dark particulate material deposited solely on the graphite, preferentially at the attacked regions. Edge attack was not so

pronounced probably due to the thickness of the edge. No particles were seen on the background film and since a flowing system was used, the deposit must have been bonded to the graphite during the formation process.

Results obtained after increased reaction times showed more advanced attack at the same sites. Edge attack was more pronounced and was noticeable even at the thickest edges. In general, however, six hours reaction did not produce the equivalent increase in attack over that seen on the previously illustrated samples. The Plates 3A and B illustrate the effect of six hours reaction under the same conditions on the sample of natural graphite extracted from dolomite. Attack was identical to that found in the case of purified natural material and was confined to the flake edges, particularly step edges and the area where two grain boundaries emerged at the edge of the flake. This is still edge attack and these sites show enhanced reactivity since they embrace two edges. There is again evidence for some surface deposition particularly at areas where the graphite was attacked.

This work confirms that the samples of different natural graphites behave similarly, and later experiments were carried out using the purified material as representative of natural graphite.

The interaction of nuclear graphite and carbon dioxide was first investigated after a 1 hour exposure but no reaction had taken place. Experiments using 2 hour irradiations were successful and an area of

this graphite after reaction is illustrated by Plate 4. Edge reaction was found to be prominent but in addition surface pitting appeared and a dark particulate material was found extensively on the graphite surface. Distribution counts of these particles showed that there were 3.2×10^{11} per sq.cm. and the mean size was 58.3 ± 7Å.

When the nuclear graphite was subjected to 4 hours irradiation, the reactivity was not greatly increased. Plates 5A and B illustrate an area before and after this treatment. There has been gasification at the flake edges particularly at points marked 'A' where grain boundaries emerge, and at small flakes marked 'X' along the edge which have been completely removed. Some parts of the graphite surface give increased transmission after reaction and are therefore shallower than before, and occasionally pits have been produced. Again a deposited material covered the surface. Particles seen on the background were found to have been present originally.

From these experiments, it can be concluded that nuclear graphite shows more features of attack than natural graphite under similar conditions. Also it has been shown that deposition occurs predominately near regions of attack, i.e. the deposit on natural graphite occurs mainly at the edges, but in addition nuclear graphite shows evidence of surface deposition. These two observations must be related to the structure of the graphites in question and in particular, to their impurity and defect content. These sites would be the preferred regions of attack.

When samples which exhibited attack were re-irradiated under the same conditions, very little change took place. This was probably due to deposited material or a contamination layer which prevented gasification. The second alternative is more likely since any specimen would have been examined under the microscope three times, had two irradiation treatments as well as increased handling and transportation. All of these tend to produce a contamination layer.

The dose rate quoted earlier for these experiments was 7.3×10^{-2} ev/mol/sec. received by the carbon dioxide. Taking an average reaction time of 4 hours, this will give a dose of approximately 1×10^{3} ev/mol. of gas, which produces appreciable attack.

Due to the uncertain geometry of this Van de Graff system, this figure is not too reliable, and attention was switched to the same reaction with neutron irradiation.

P L A T E S 1 A and B

Area of purified natural graphite before and after 1 hr. 40 min. in carbon dioxide irradiated by a proton beam. x 195,000

P L A T E S 2 A and B

Area of purified natural graphite before and after 1 hr. 40 min. in carbon dioxide irradiated by a proton beam. x 210,000

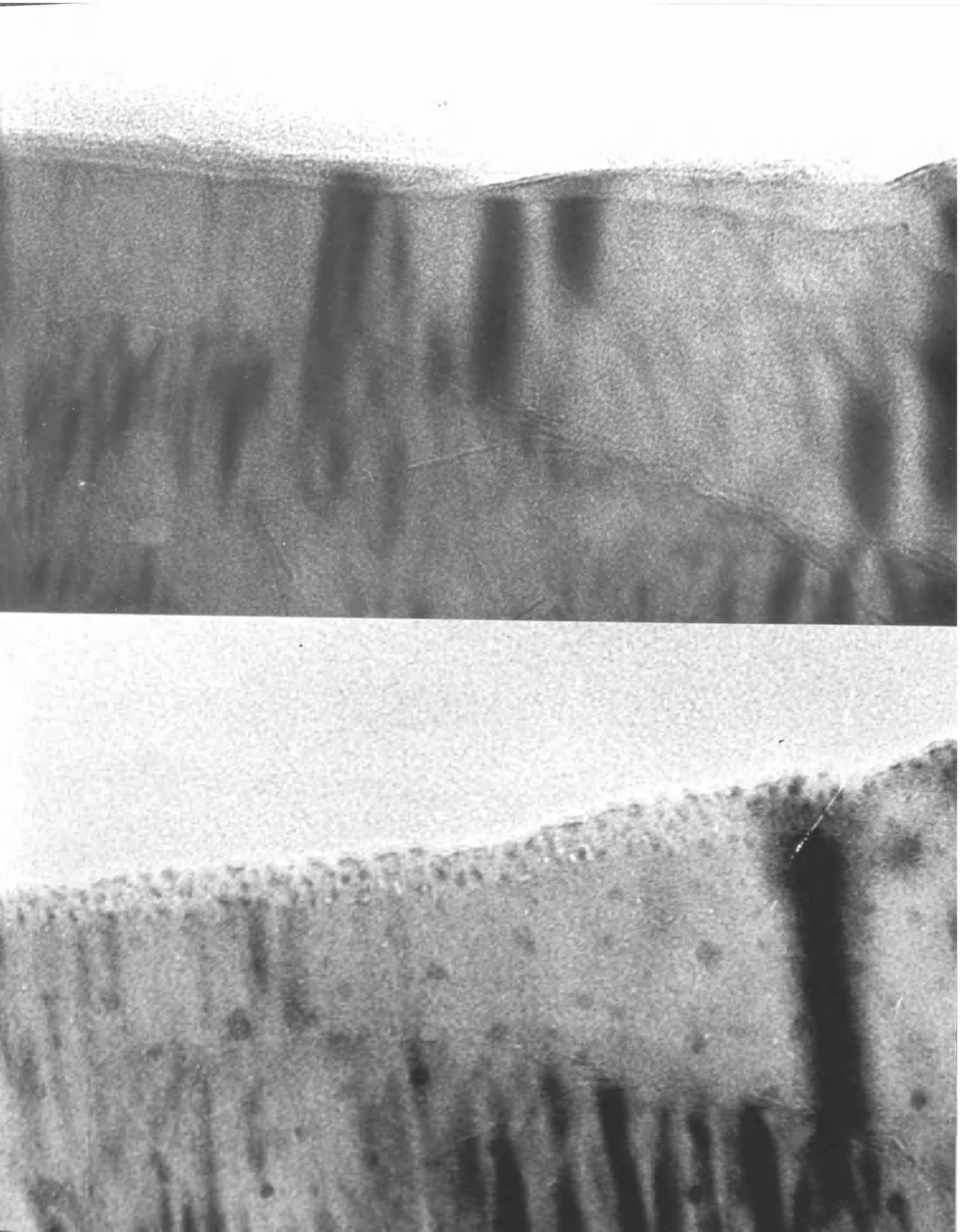

P L A T E S 3 A and B

Area of natural graphite, extracted from dolomite, before and after 6 hrs. in carbon dioxide irradiated by a proton beam. x 120,000

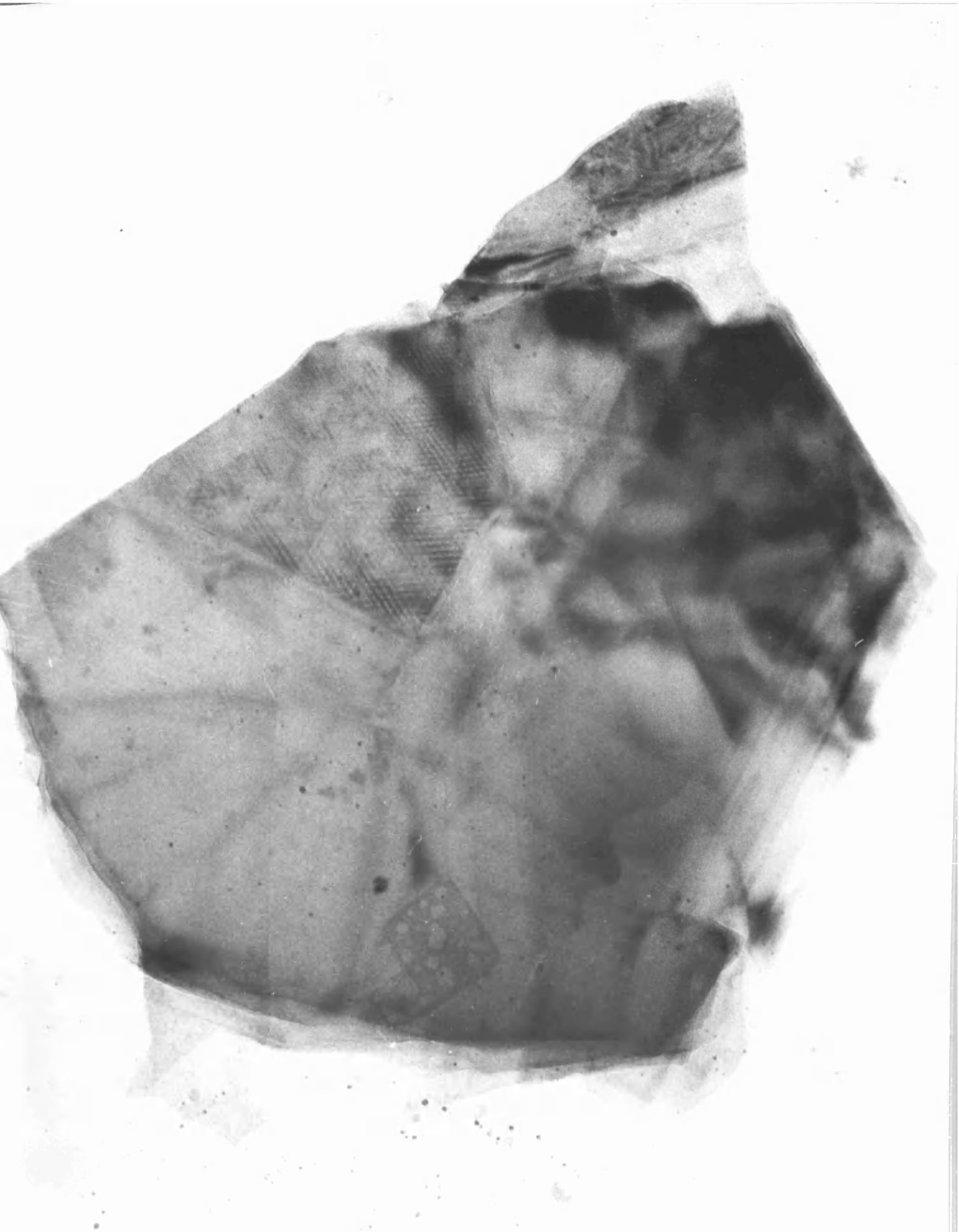

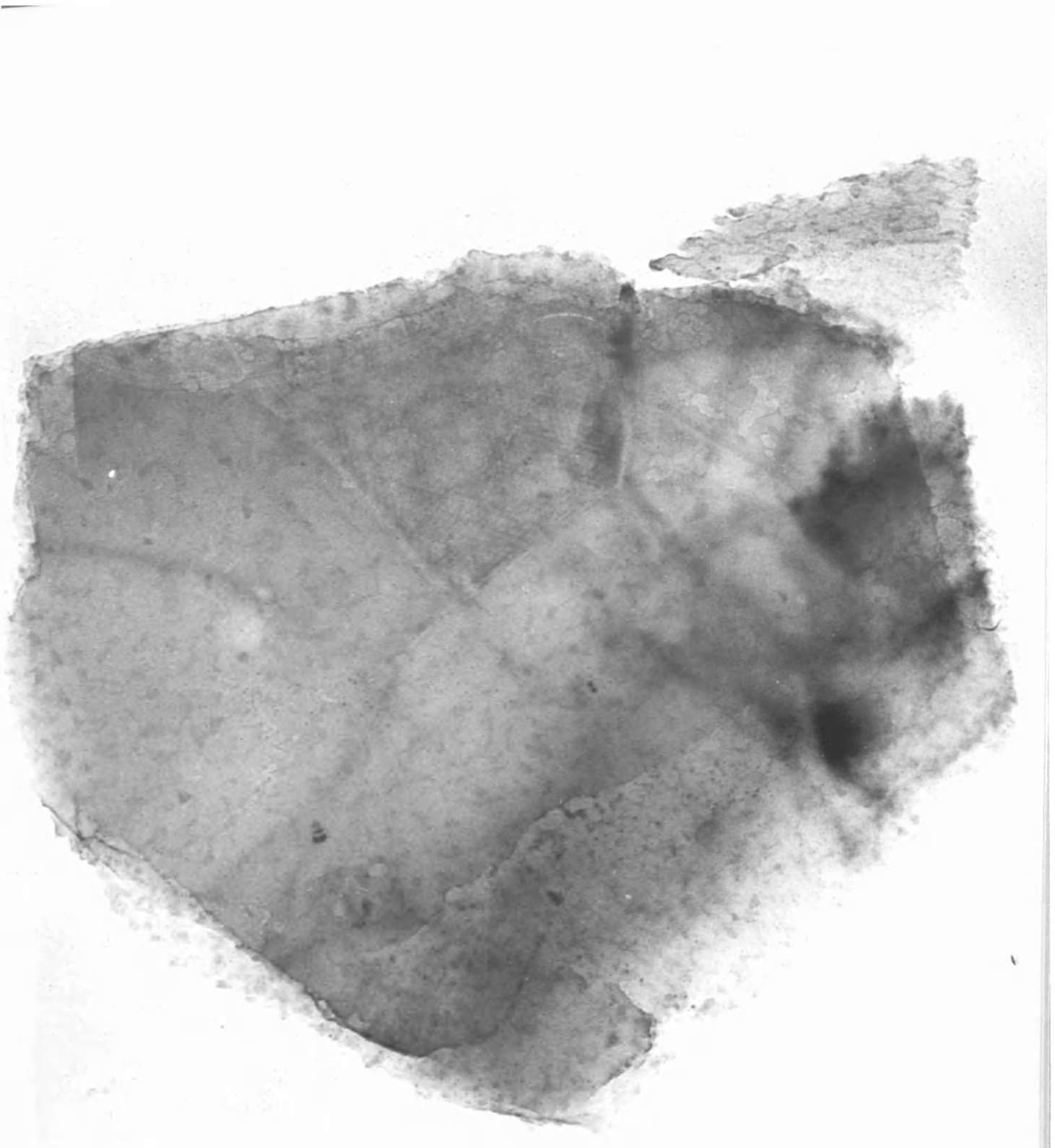

P L A T E 4

Area of nuclear grade graphite after 2 hrs. in carbon dioxide irradiated by a proton beam. x 120,000

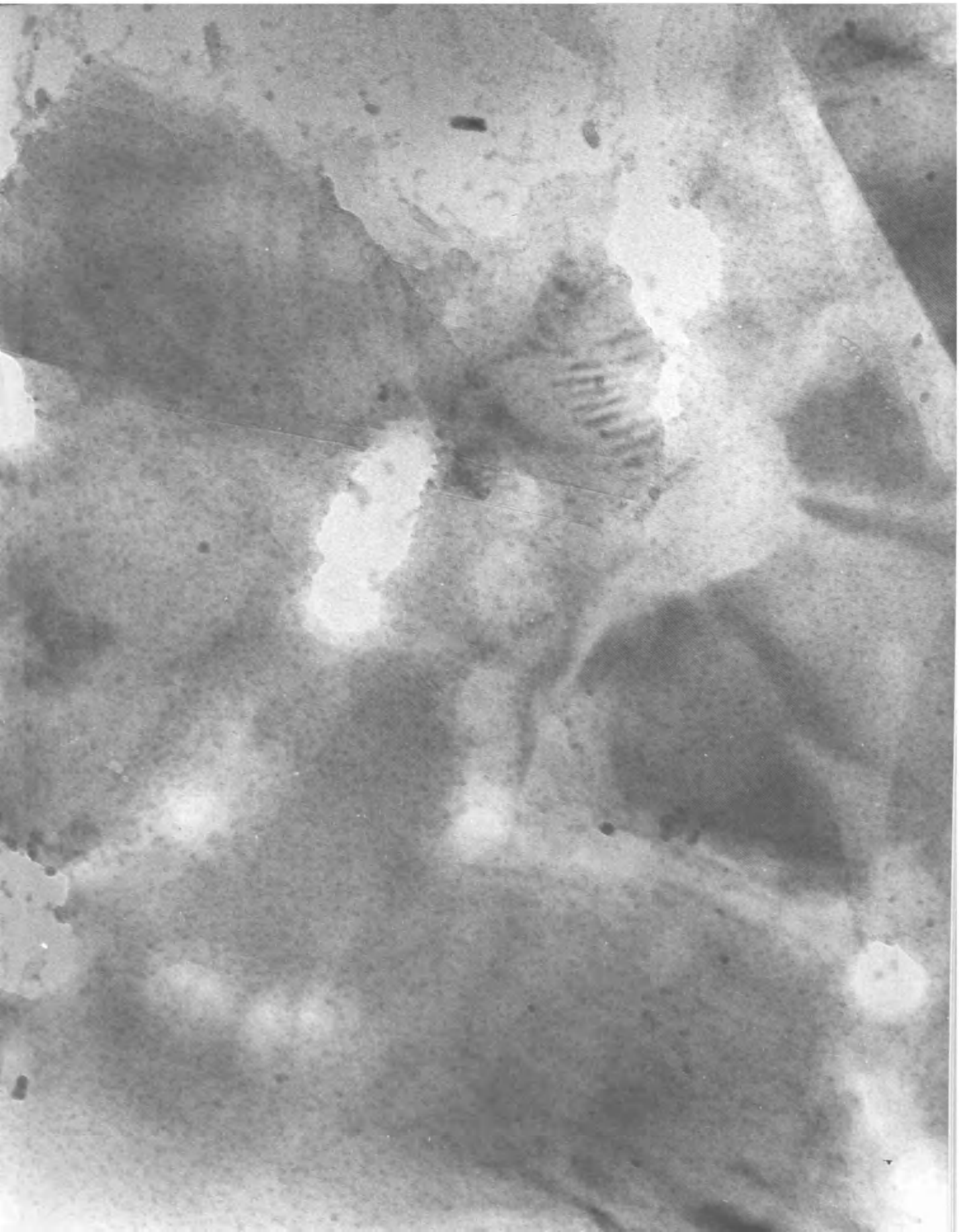

P L A T E S 5 A and B

Area of nuclear grade graphite before and after 4 hrs. in carbon dioxide irradiated by a proton beam. x 120,000


R
X

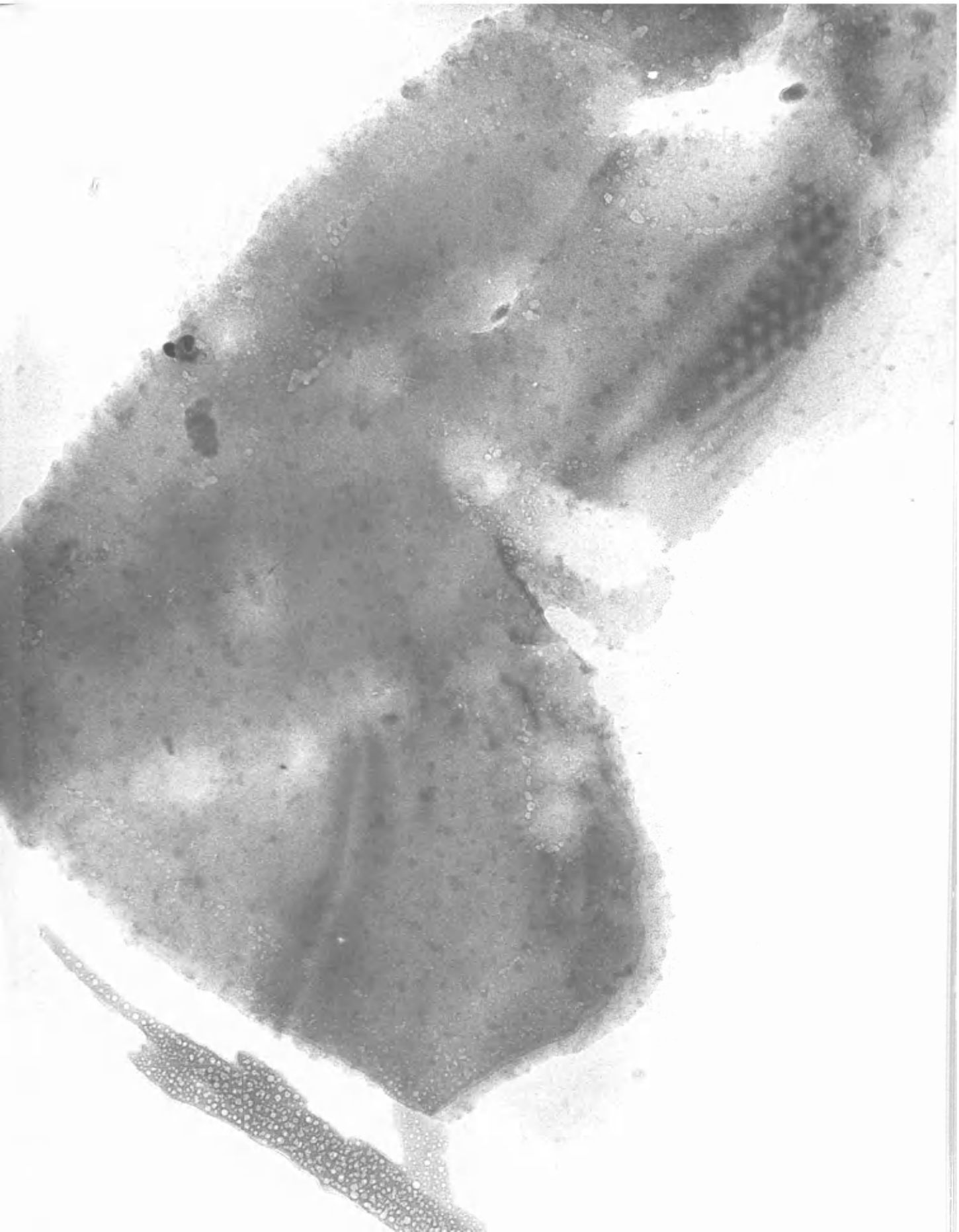

2. Experiments Using Neutron Irradiation

Preliminary experiments were carried out in the DIDO reactor where samples of natural and nuclear graphites were subjected to neutron irradiation in carbon dioxide. After reaction times of up to 3 months, which corresponds to a dose above 10^{20} n/cm^2, the specimens were re-examined and it was found that the graphite was completely destroyed. In some cases the supporting film and the mounts themselves were damaged.

Subsequent irradiations were carried out in BEPO where a few weeks reaction produced doses around 10^{18} n/cm^2 and gave satisfactory results. Zircalloy mounts were used in this work, and experiments were carried out at 350°C.

(a) Irradiation in Carbon Dioxide

In general, doses of 1 x 10^{18} n/cm^2 were found to produce no visible effect on any graphite sample examined. This dose was achieved after approximately 2 weeks reaction time. The actual time varied slightly due to variation in reactor shut-down time, since it was only during this period that the samples could be inserted or removed. In some cases slight reaction was noticed and some favourable areas gave indications of incipient attack. This was noticeable in samples of both natural and synthetic graphites after 1.10 x 10^{18} n/cm^2.

The natural graphite after reaction was slightly etched at thin edges particularly where grain boundaries emerged. In addition to this, the nuclear grade material showed some shallow surface pitting which

penetrated the surface at thin regions, as illustrated in Plate 6. From the pitting pattern, it can be seen that much of the reaction has occurred at grain boundaries in the material and the individual grains tend to be shown up by contrast differences due to the increased transmission through the boundary regions.

Greater reactivity was found when the dose was increased to 2.01×10^{18} n/cm^2, which was obtained after 4 weeks irradiation. A typical area of purified natural graphite before and after reaction is illustrated by Plates 7A and B. Carbon gasification has taken place almost exclusively at the flake edge. Comparison studies show that the attack was greatest at thin flake edges. At areas marked 'X' and 'Y' on the original area, grain boundaries emerge at the flake edge, and after reaction, these areas show most attack and penetration into the flake is substantial. At one area in the centre of the flake, there is evidence of surface attack with the appearance of a pit. This shows that there must be a small number of active sites on the surface of this material.

In contrast, when a sample of nuclear graphite, which was irradiated simultaneously, was examined, a different mode of oxidative attack was found. Gasification had taken place to such an extent that all the thin areas which were originally suitable for microscopy had been completely oxidised and only thick areas remained. A typical area is illustrated by Plate 8. There has been extensive surface pitting, with complete penetration of the surface at many points.

P L A T E 6

Area of nuclear grade graphite after 1.10×10^{18} n/cm^2 in carbon dioxide in BEPO x 120,000

P L A T E S 7 A and B

Area of purified natural graphite before and after 2.01 x 10^{18} n/cm^2 in carbon dioxide in BEPO. x 120,000

Y
X

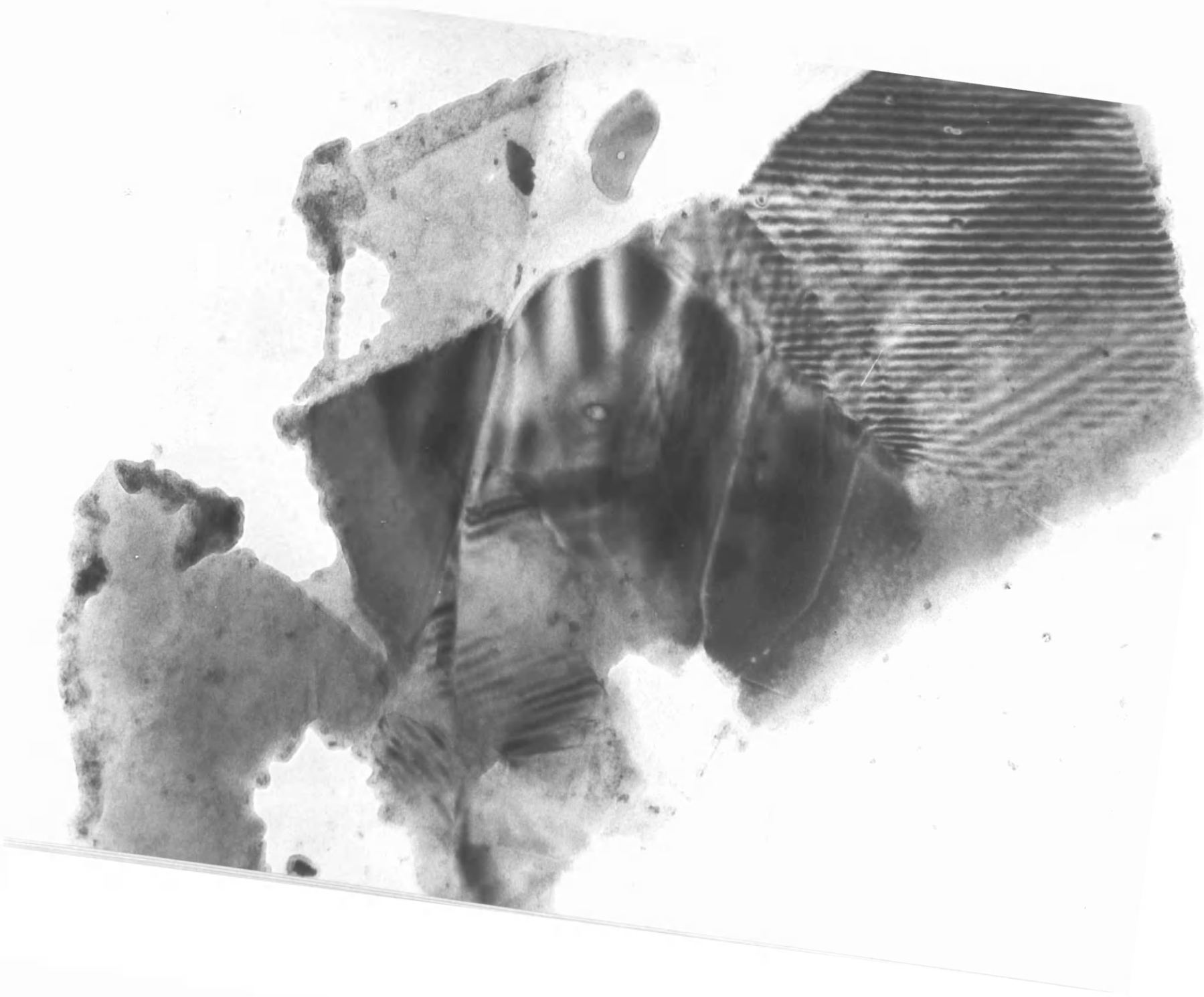

PLATE 8

Area of nuclear grade graphite after 2.01 x 10^{18} n/cm^2 in carbon dioxide in BEPO. x 120,000

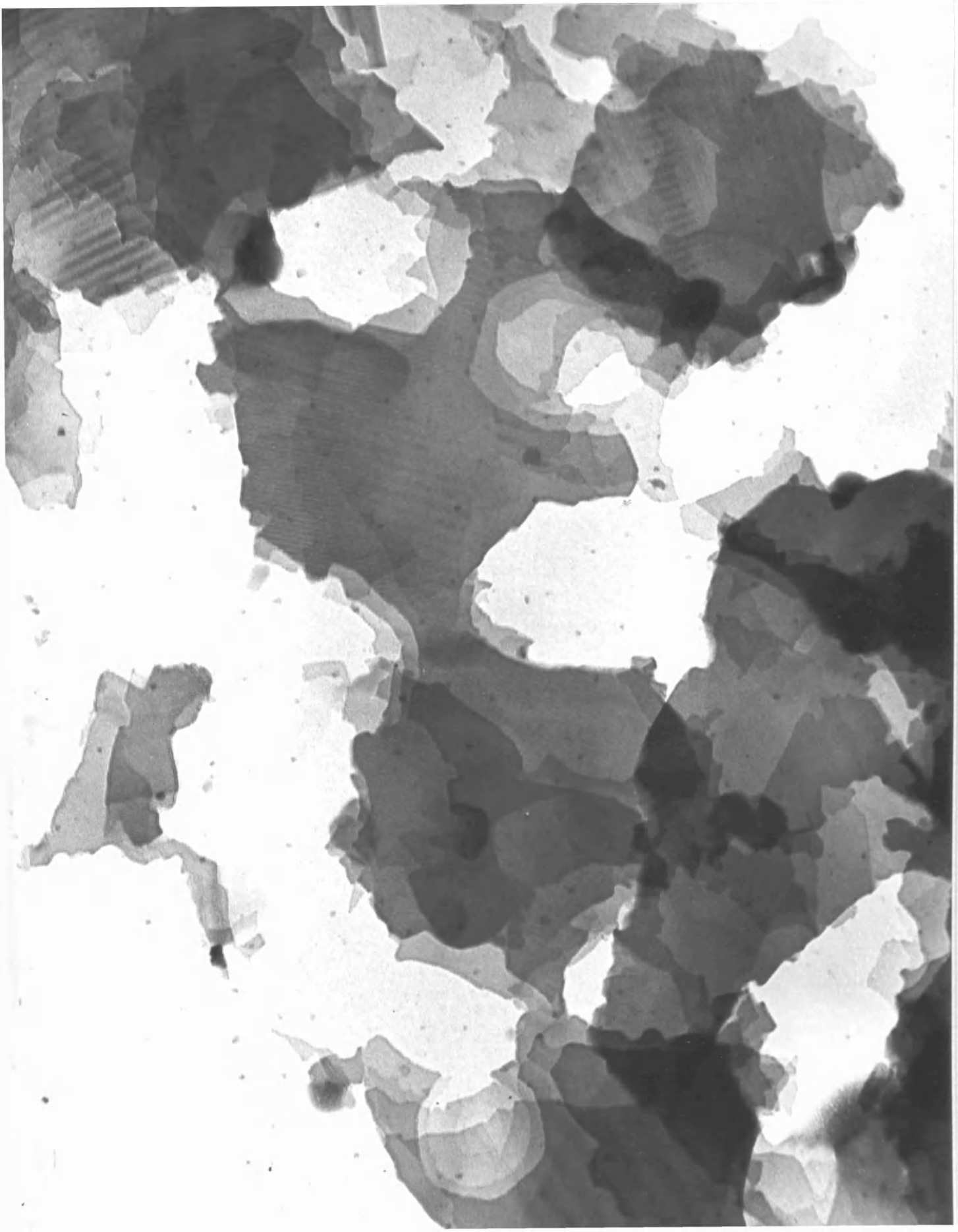

Although attack is too far advanced to derive much information on the pitting characteristics, many pits, however, on this and other areas show some linearity of pit edge, which occasionally can be shown to follow a hexagonal contour. The origin of these pits cannot be completely attributed to defect and impurity centres at grain boundaries but must also include similar sites randomly located on the graphite surface. As sites are attacked and carbon is removed from one layer, fresh active sites will be exposed on the layer underneath, so that a continual pitting process will ensue until the graphite has been penetrated.

Since these two samples were alongside each other in the apparatus, the different features of attack cannot be due to radiation effects and damage, but must be due to the properties of the graphite samples. The fact that many moiré patterns are still in evidence after reaction also indicates that little damage has occurred since authors including Dawson and Follett (1959) have shown that damaged graphite appears as low contrast material with few moiré patterns.

The difference in number and location of active sites in both graphites has led to the conclusion that either defect sites or impurity sites, or an association of both, are responsible for carbon removal. These sites are difficult to distinguish. They tend to occur together, since impurity atoms take up some of the spare bonding electrons of defect sites. During crystal growth, both impurity and defect sites tend to migrate to crystallite edges,

and so appear in quantity at crystal edges and grain boundaries. In the synthesis of nuclear grade material such defects can also be incorporated at crystallite surface sites. In order to try and differentiate between the impurity and defect sites as centres for the initiation of reaction, samples of graphite containing increased impurity and defect content were prepared.

In the preparation of graphite with increased impurity content, samples of natural and nuclear materials were set up in the usual way. A reduced quantity of gold was evaporated onto them by the method described for decoration. In this way both samples were decorated in a single evaporation and then simultaneously reacted in BEPO. By this means, conditions were identical for both materials throughout the experiment and the final results could be subjected to strict comparison. Since the gold particles were expected to act catalytically, the samples were given a dose of 1×10^{18} n/cm^2. Under normal conditions, this dose did not produce any visible reaction, but in this case re-examination revealed that reactivity was increased in both graphite samples. Original areas were photographed after decoration and a typical area of natural graphite is illustrated by Plate 9A. In this micrograph, the gold particles are seen to form clusters and also broken lines along edges and other surface features. The mean particle diameter on all samples was 40Å. These samples had been heated to 300°C. for a few minutes after metal evaporation.

After irradiation in carbon dioxide at 1 x 10^{18} n/cm^2, the same area was rephotographed and is illustrated by Plate 9B. The conditions of irradiation and the temperature of 350°C. have produced greatly increased mobility of gold particles over the graphite surface, and after reaction the particle diameter had increased so that the diameter varied from 600 - 1100Å. From this pair of micrographs, it can be seen that graphite attack has taken place at the flake edge and is also particularly noticeable at a surface flake edge where a large gold particle appears to be active. A surface pit has arisen at the other large particle in the field of view and successive layer edges can be distinguished. Both the edge of the gold particle and the pit are hexagonal. Another typical area of this purified natural graphite is shown in Plate 10. This again illustrates edge attack. Some channels start at edges and proceed into the graphite with a dark gold particle at the channel head. This is similar to the attack features found by Presland and Hedley (1963). Any attack on the surface is associated with edge attack of surface flakes, but at random points on the surface, particles can be seen with no activity associated with them. This is a good indication that impurity alone will not catalyse carbon gasification but will only do so when it acts in conjunction with a normally active site to produce reaction at a lower dose than in the case where no impurity was added. The production of channels is a feature of attack catalysed by a mobile catalyst. The particle initially

stimulates attack at the flake edge or other defect site and as carbon is removed, the metal particle can migrate along any reaction front so catalysing carbon removal in its path. After gasification at any site, the neighbouring sites will then become identical to edge sites so reaction can proceed further and widen the deepen the channel.

Nuclear graphite does not exhibit much channelling but again shows surface pitting as illustrated by Plate 11. After reaction the gold particles were not as large as those on the natural graphite but their number was greater. The measured size was 300 - 400Å. Many of the pits have no visible gold particles, some contain gold particles at pit edges, and many have gold particles associated with shallow pits which do not penetrate the specimen. The contours of the pits show considerable linearity, and in many cases hexagonal outlines can be recognised. The appearance of this specimen is similar to that of specimens of nuclear graphite subjected to twice the dose without added impurity e.g. Plate 8, where however the pitting had proceeded much farther. This again illustrates that catalysis by gold has not influenced the sites for reaction but has merely accelerated gasification at those sites which would be attacked later under normal circumstances.

Samples were then prepared using two nuclear grade graphites which had previously been irradiated to doses of 1×10^{18} n/cm^2 and 4×10^{20} n/cm^2. It is well known that irradiation produces damaged

P L A T E S 9 A and B

Area of purified natural graphite with gold catalyst, before and after 1 x 10^{18} n/cm^2 in carbon dioxide in BEPO. x 100,000

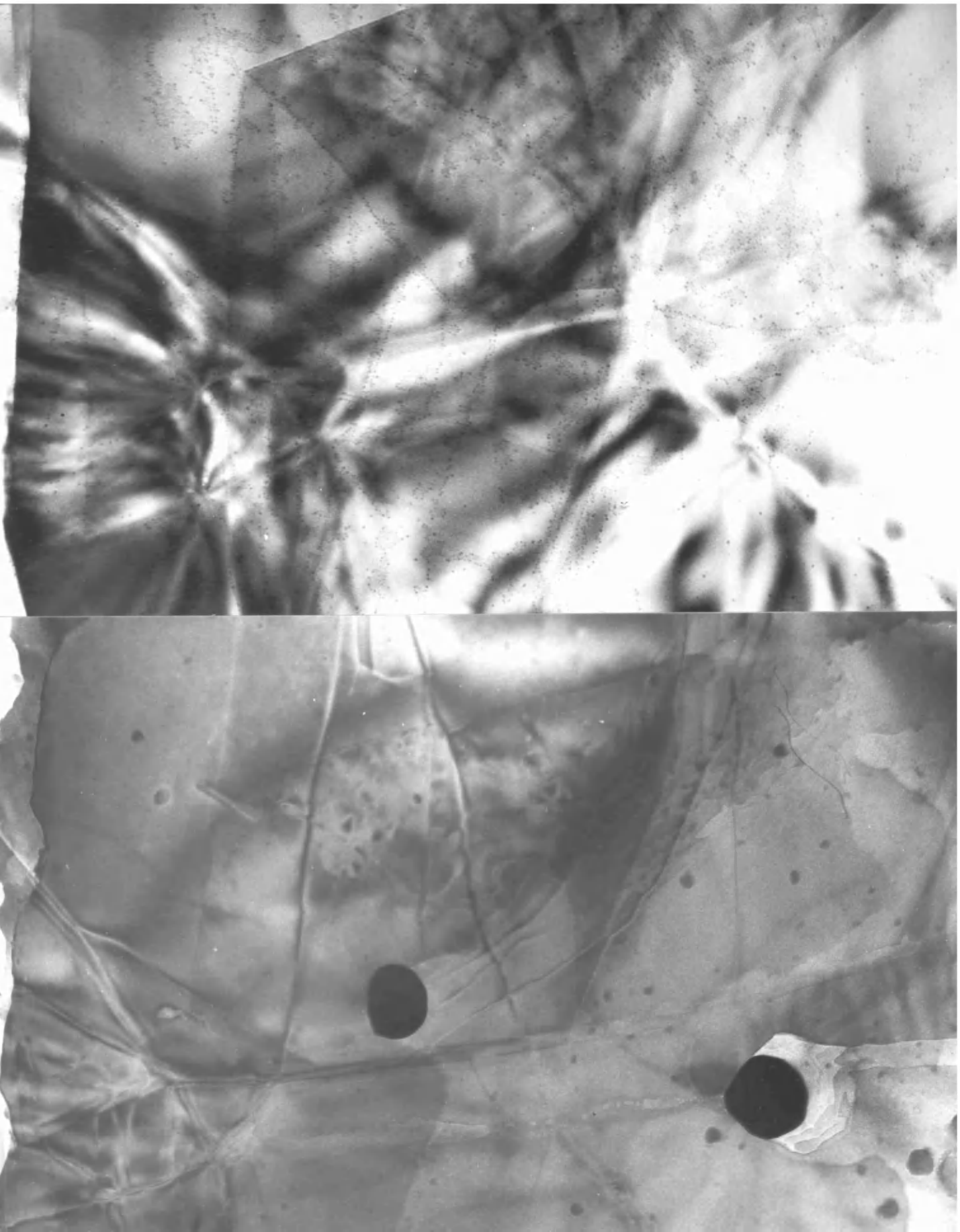

PLATE 10

Area of purified natural graphite with gold catalyst, after 1×10^{18} n/cm^2 in carbon dioxide in BEPO. x 120,000

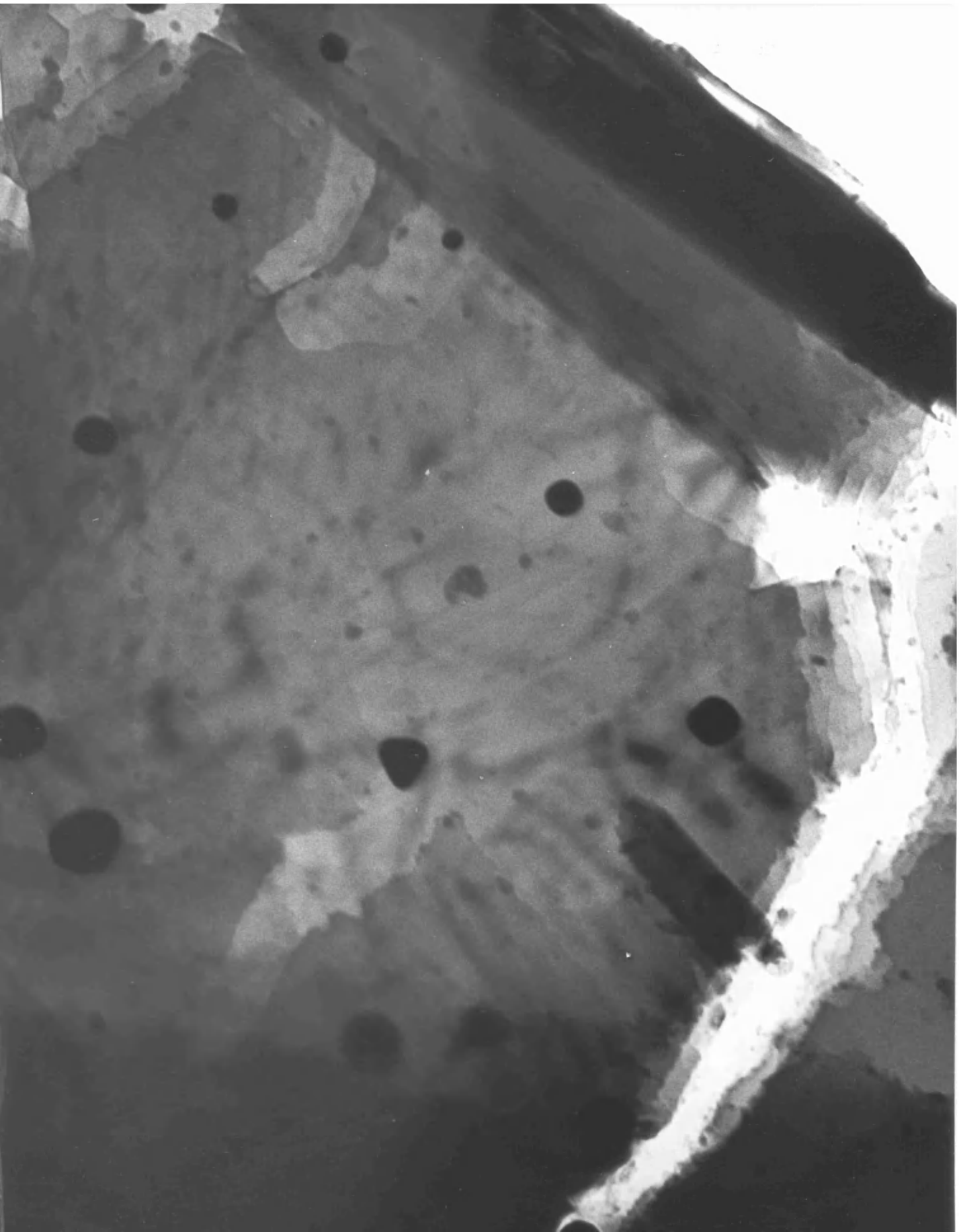

PLATE 11

Area of nuclear grade graphite with gold catalyst, after 1 x 10^{18} n/cm^2 in carbon dioxide in BEPO. x 120,000

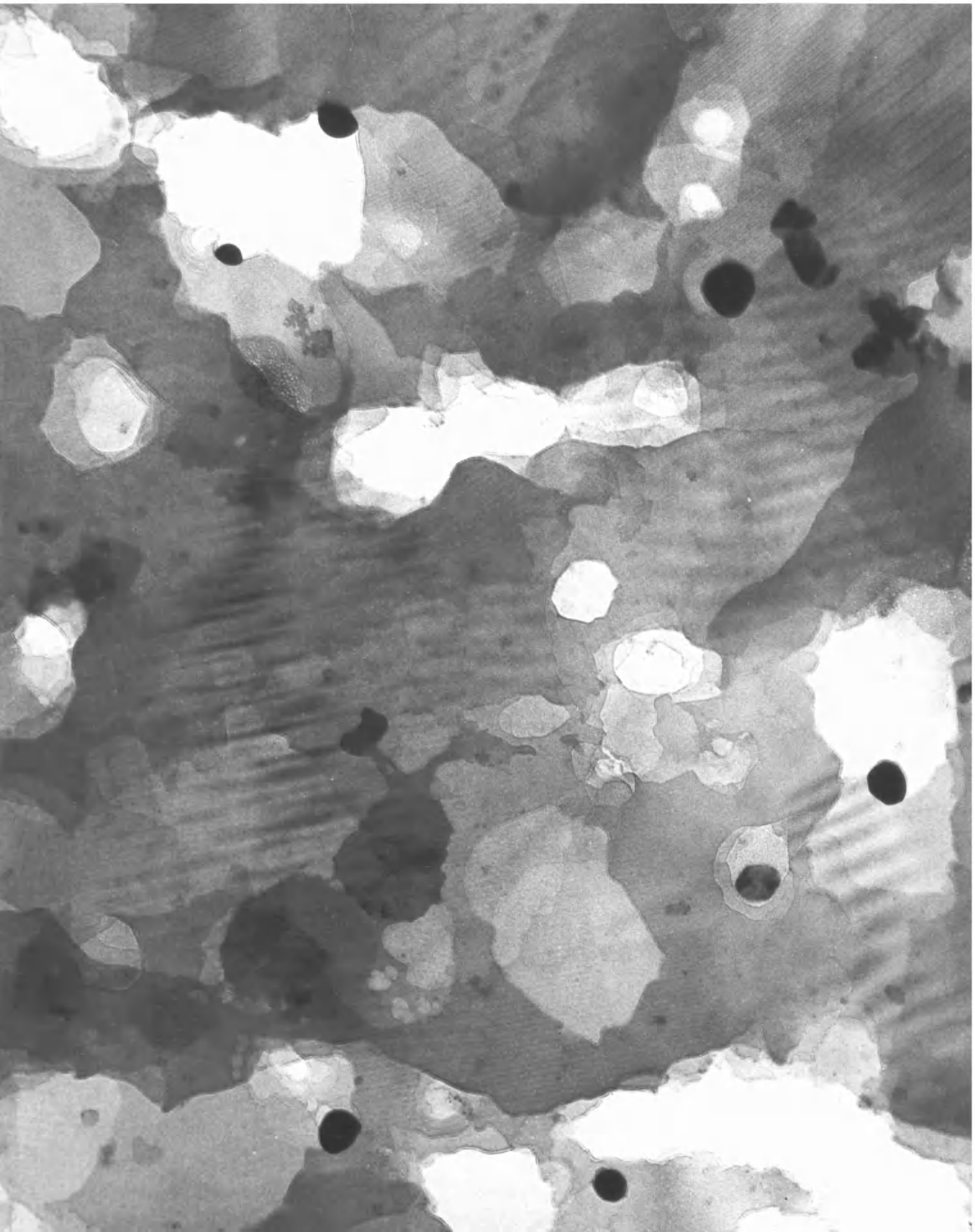

regions in the graphite which occur as vacancies and interstitial defects, the samples used therefore represent graphite with an increased defect concentration. Plate 12 illustrates an area of this graphite after 1 x 10^{18} n/cm^2 then a further 1 x 10^{18} n/cm^2 in carbon dioxide. Plate 13 shows an area after 4 x 10^{20} n/cm^2 then 1 x 10^{18} n/cm^2 in carbon dioxide. This second treatment on normal unirradiated nuclear graphite produces no attack but as shown here the increased defect concentration has significantly increased carbon gasification. It can be seen that the higher initial dose produced the greater attack. Since these samples had a greater defect content than samples which received their damage during the normal oxidation cycle, the reactivity increase can be attributed to the extra defects, and it can therefore be concluded that defects alone can stimulate reaction. Because the reaction rate increases with pre-irradiation dose, the possible explanation that a combined impurity-defect mechanism is operating, in this case, can be overruled.

Examination of the pit contours shows the presence of pits which are not as well defined as those found on normal graphite or on graphite with added impurity. When additional defects are present, and so presumably when graphite is attacked at vacancy sites, the pit edges appear more ragged and non-linear. From this visual evidence it can be proposed that the normal pitting of graphite after approximately 2 x 10^{18} n/cm^2 shows more resemblence to that produced by a known

P L A T E 12

Area of nuclear grade graphite, pre-irradiated to 1 x 10^{18} n/cm^2, after a further 1 x 10^{18} n/cm^2 in carbon dioxide in BEPO.

x 150,000

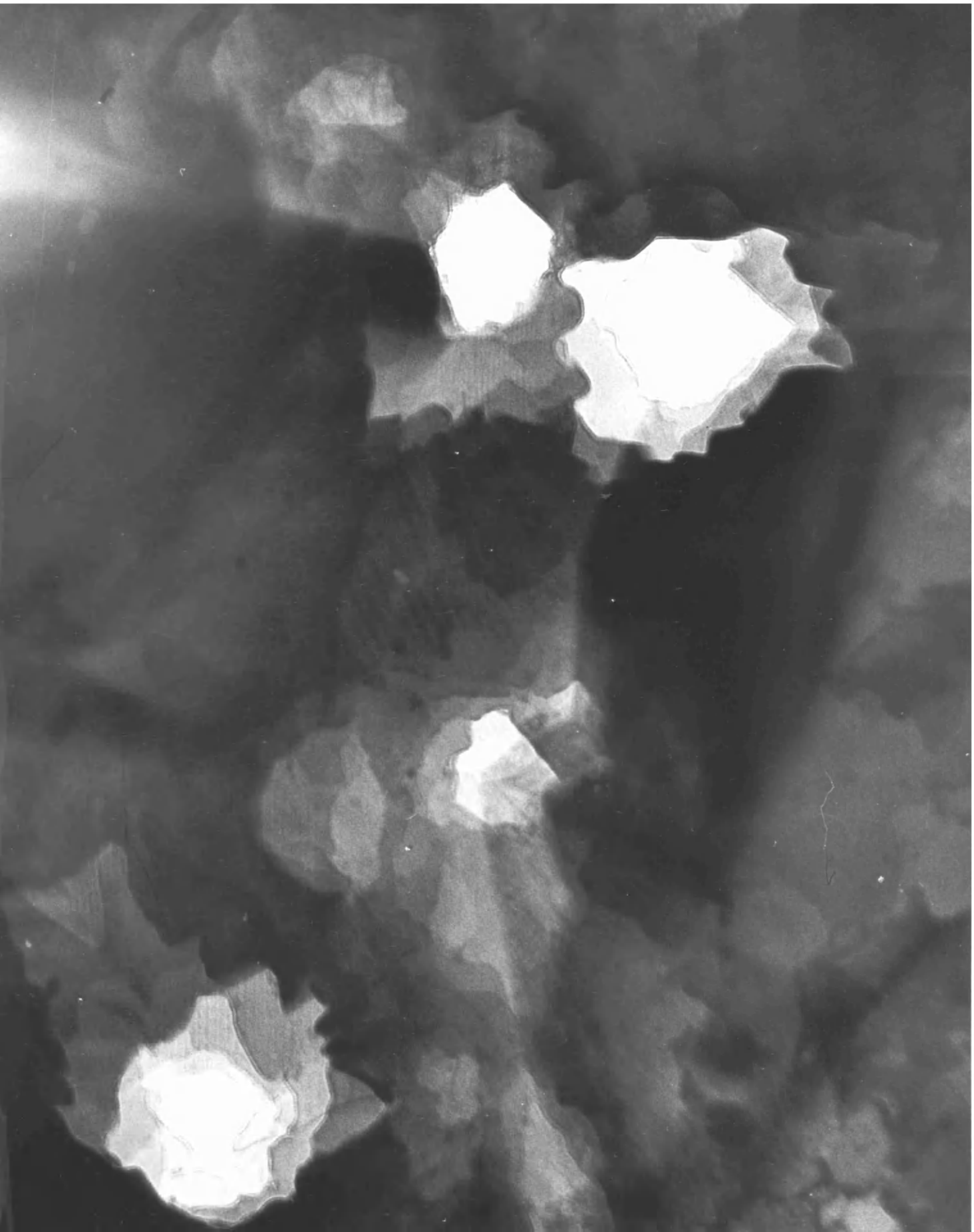

PLATE 13

Area of nuclear grade graphite, pre-irradiated to 4×10^{20} n/cm^2, after a further 1×10^{18} n/cm^2 in carbon dioxide in BEPO.

x 120,000

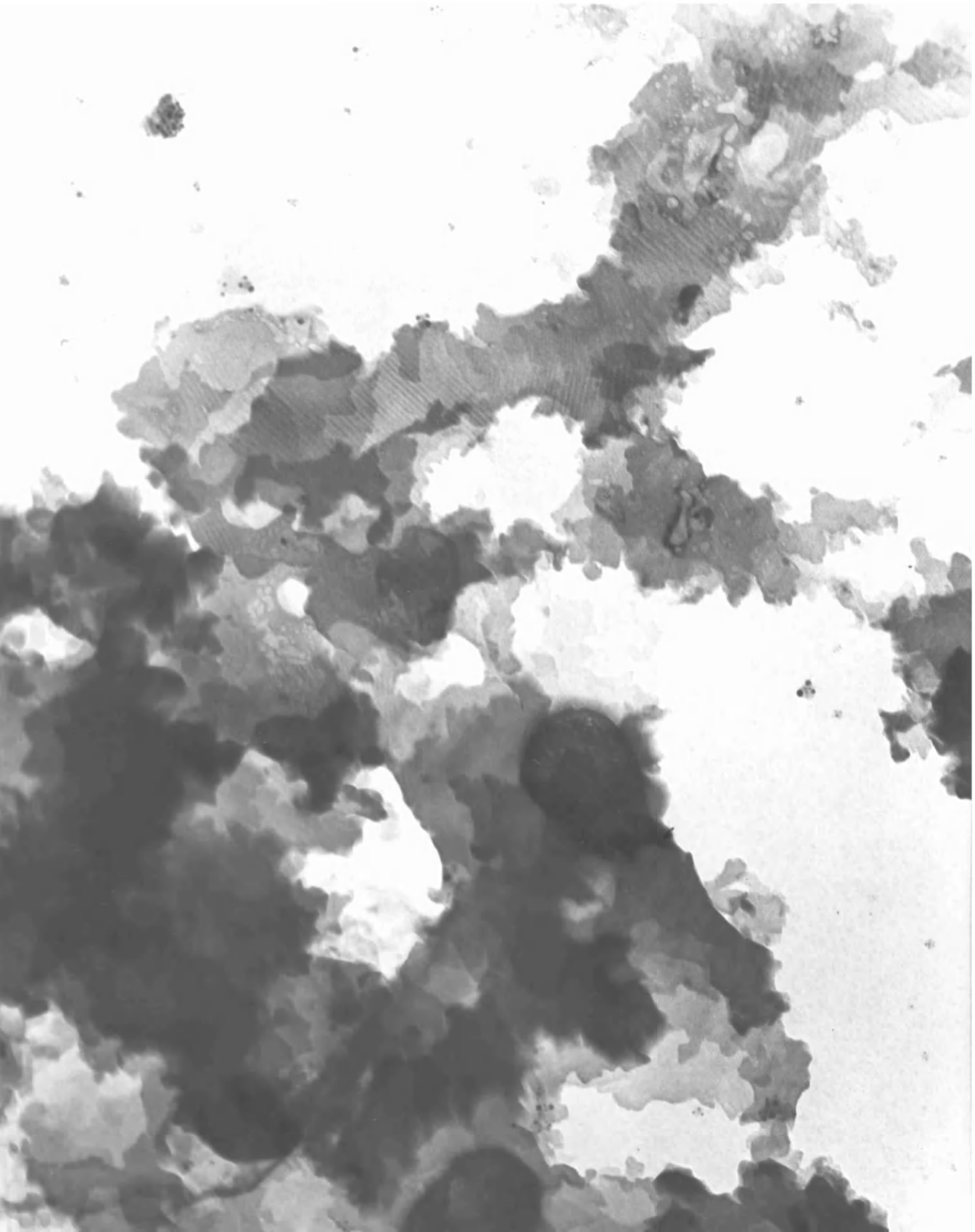

defect plus impurity mechanism. The conclusion can therefore be drawn that normal graphite attack takes place at defect and impurity sites which are originally present in the graphite in varying amounts depending on the type of graphite used. This constitutes gasification at the basic structural features of the graphite, and not at the defect centres induced by the irradiation conditions. In order to have some means of comparison between these results and those obtained by proton Van de Graff irradiations, the dose rate received by the gas was measured. It was known that in this reaction rig the dose rate was 4.6 milliwatts/gm. which is equivalent to 2.1×10^{-6} ev/mol CO_2/sec. Since reaction time for appreciable gasification was 4 weeks, the total dose received was 4.7 ev/mol. This is approximately 200 times less than the unreliable figures quoted for the proton irradiations, but even although the BEPO irradiations were done at a higher temperature, this decrease in dose rate could explain the non-appearance of any deposited material in these neutron irradiated samples. If previously, deposits were blocking reaction sites and slowing down the reaction, this would explain the higher attack rate obtained in BEPO where no deposition took place, even allowing for the temperature increase.

These above results were obtained from a flow system. When a static system was used at a dose of 2.1×10^{18} n/cm^2 there was an appreciable reduction in reactivity, in fact most samples examined

showed no signs of attack. This can be attributed to the inhibiting effect of carbon monoxide produced by the radiolytic decomposition of the carbon dioxide. In the normal flow system, most of the carbon monoxide produced would either recombine with an oxygen atom to regenerate carbon dioxide or else it would flow away in the gas stream. Only a very small proportion of the gas produced near the graphite surface could play any part in the reaction mechanism. In a static system, however, there will be much more carbon monoxide continually in contact with the graphite surface, and where it is chemisorbed at active sites in preference to the oxygen atoms, it can inhibit gasification. Further reactor experiments were carried out under gas flow conditions.

(b) Irradiations in Inhibition Mixtures

In attempts to inhibit the carbon gasification in the flow system, a mixture of 1% carbon monoxide plus ·1% methane was added to pure carbon dioxide, and graphite samples were prepared for reaction as usual. Times of 2 and 4 weeks were used, giving doses up to 2.14 x 10^{18} n/cm^2. In all experiments tried, no evidence was found for carbon gasification on either nuclear or natural graphites. An area of nuclear graphite, which has been established as the more reactive, is shown in Plates 14A and B before and after 2.01 x 10^{18} n/cm^2 in the gas mixture. The usual reactive areas at flake edges and points of emergence of grain boundaries have been completely untouched and

P L A T E S 14 A and B

Area of nuclear grade graphite before and after 2.01 x 10^{18} n/cm^2 in the carbon dioxide, carbon monoxide, methane mixture in BEPO.

x 90,000

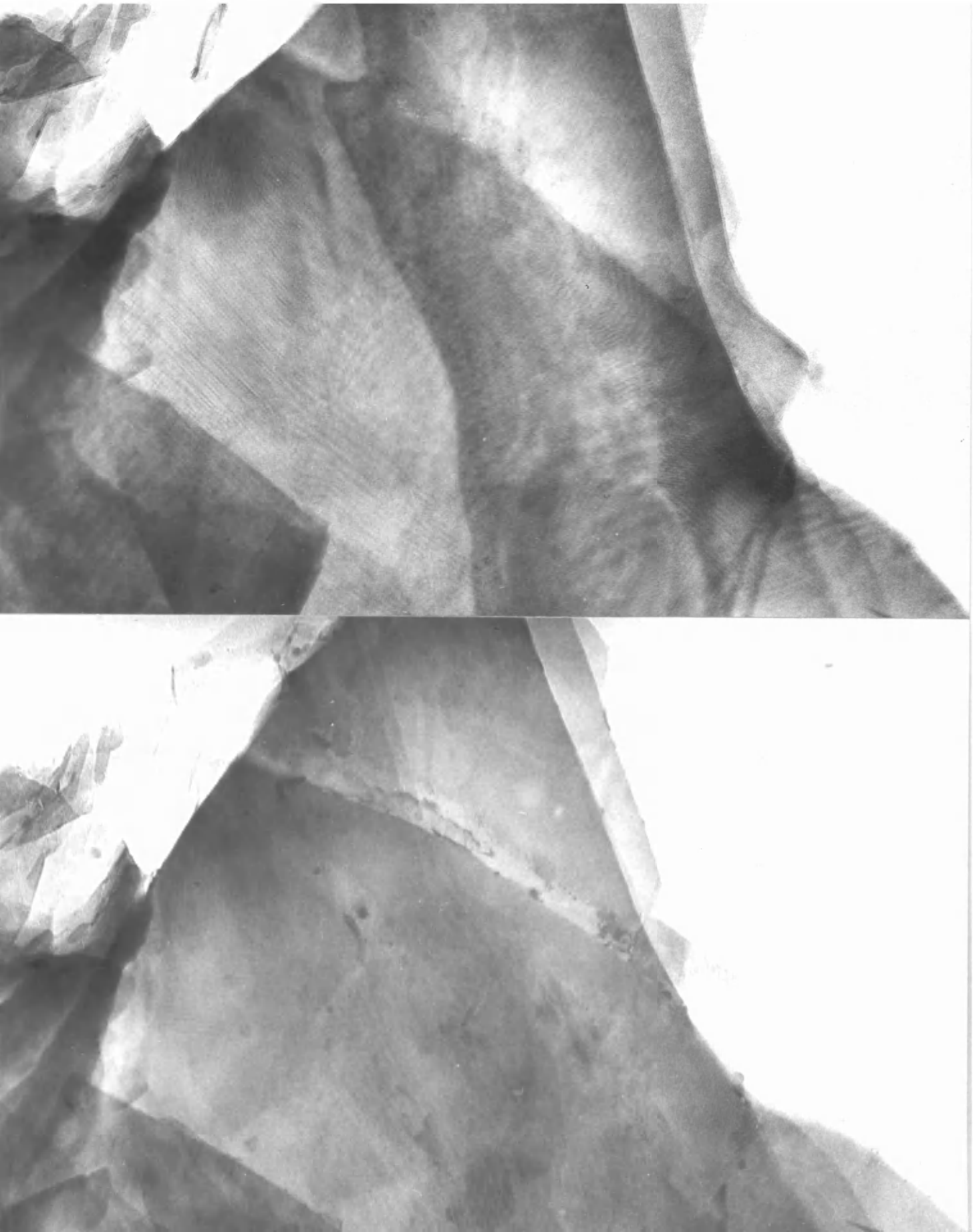

P L A T E S 15 A and B

Area of purified natural graphite before and after 2.04×10^{18} n/cm^2 in the carbon dioxide, ketene mixture in BEPO. x 90,000

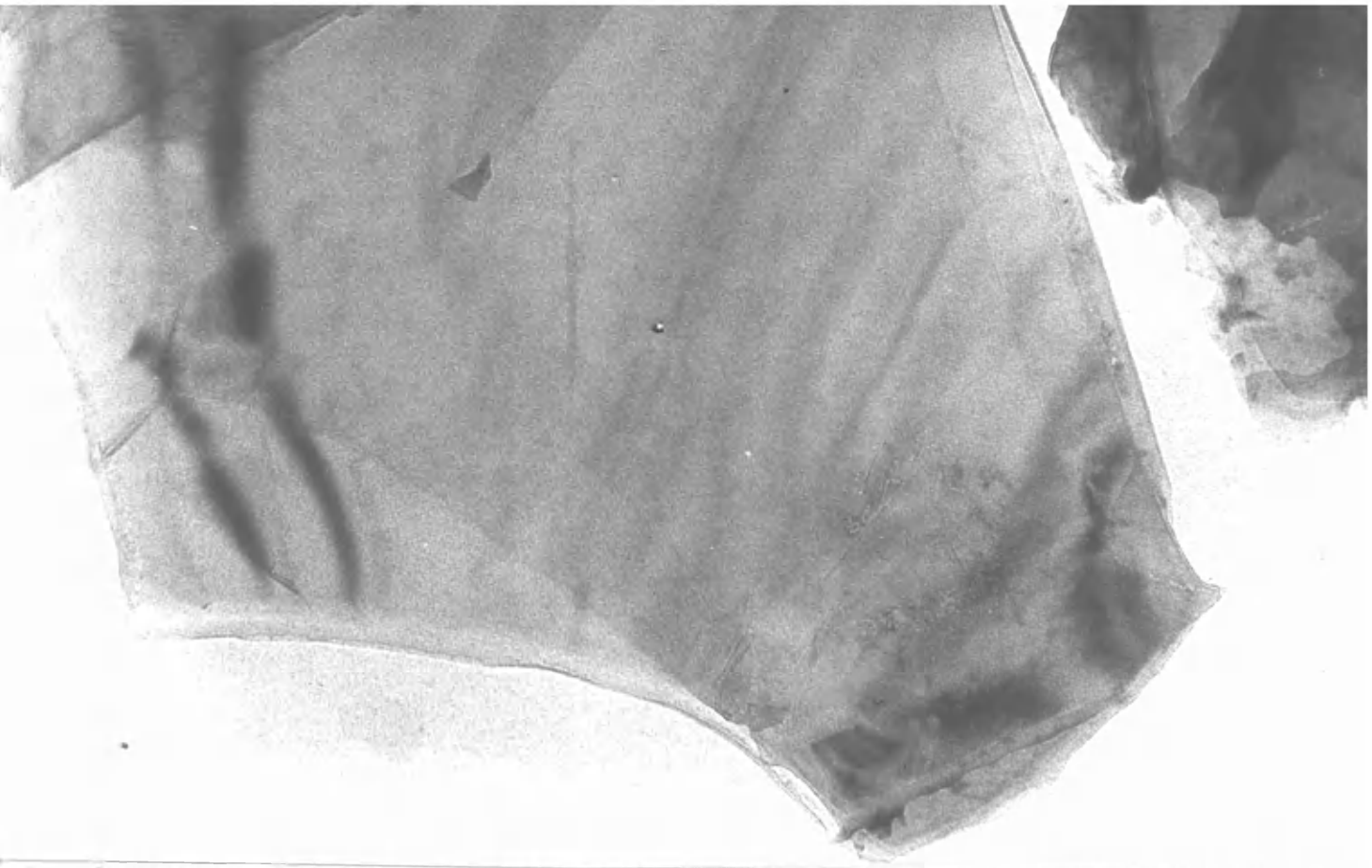

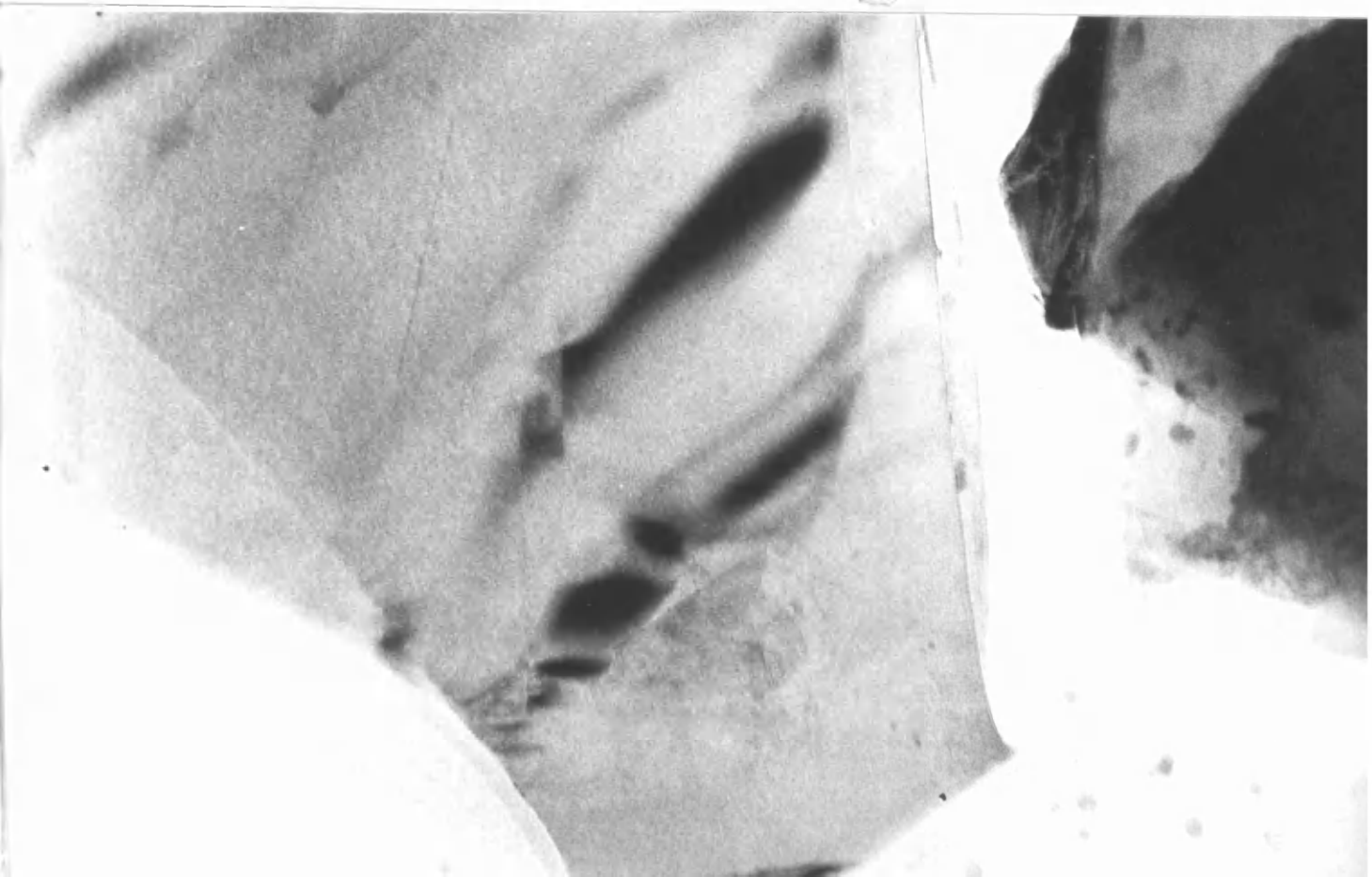

the only changes in the area after reaction are moiré pattern changes and some slight contamination.

Similar experiments were performed using .9% carbon monoxide + .3% ketene in carbon dioxide at 2.04 x 10^{18} n/cm^2 and again this resulted in complete inhibition of gasification. This is illustrated by an area of natural graphite before and after this treatment, Plates 15A and B. The only change this time is in the background silica film.

It was also found that there was no visible evidence of deposition of any material on any sample using these two gas mixtures under the above conditions.

(c) Interrupted Irradiations

Some specimens which were examined after 2 weeks irradiation at a dose around 1 x 10^{18} n/cm^2 and exhibited no evidence of reaction, were subsequently given a further 4 weeks reaction at a dose of approximately 2 x 10^{18} n/cm^2 although not always in the same gas as the first irradiation. The effect of this treatment was to produce a series of results which tended to contradict predictions based on the previous results.

The first series to be considered are samples which had undergone irradiation in 1% carbon monoxide, .1% methane in carbon dioxide at doses of first 1.06 x 10^{18} n/cm^2 and later 2.14 x 10^{18} n/cm^2 under the same conditions. As usual, a temperature of 350°C. was used. This total dose of over 3 x 10^{18} n/cm^2 was sufficient to produce

incipient attack in both purified natural and nuclear grade graphites. A typical area of natural graphite before and after this treatment is illustrated by Plates 16A and B. Carbon gasification has taken place at the sites expected from previous studies. These are the thin edge regions mainly at the sides of this flake and in particular along a grain boundary where a channel has been formed. The edges of some surface flakes have also been attacked. These edges usually consist of a succession of thin steps and attack has taken place there instead of at the thicker edges which show no visible signs of attack. After attack, the micrograph 16B was seen to contain many dislocation lines. These must have resulted from the irradiation conditions, although they do not seem to have played any part in the oxidation process. There is also evidence of some contamination which does not seem to have affected the slight reaction.

Samples of nuclear graphite show a greater degree of attack. An area before and after the identical treatment to that received by the natural graphite is shown in Plates 17A and B. Edge attack is most noticeable at the thinnest edge regions, at the main flake edges and also at any flakes superimposed on the graphite surface. At some points, channelling along grain boundaries has taken place and after a general examination it can be seen that grain boundaries on the surface have been made more distinct by carbon gasification along them. This improves their contrast compared with that of surrounding regions.

P L A T E S 16 A and B

Area of purified natural graphite before and after two BEPO irradiation cycles.

i) 1.06×10^{18} n/cm^2 in the carbon dioxide, carbon monoxide, methane mixture.

ii) 2.14×10^{18} n/cm^2 in the same conditions. x 120,000

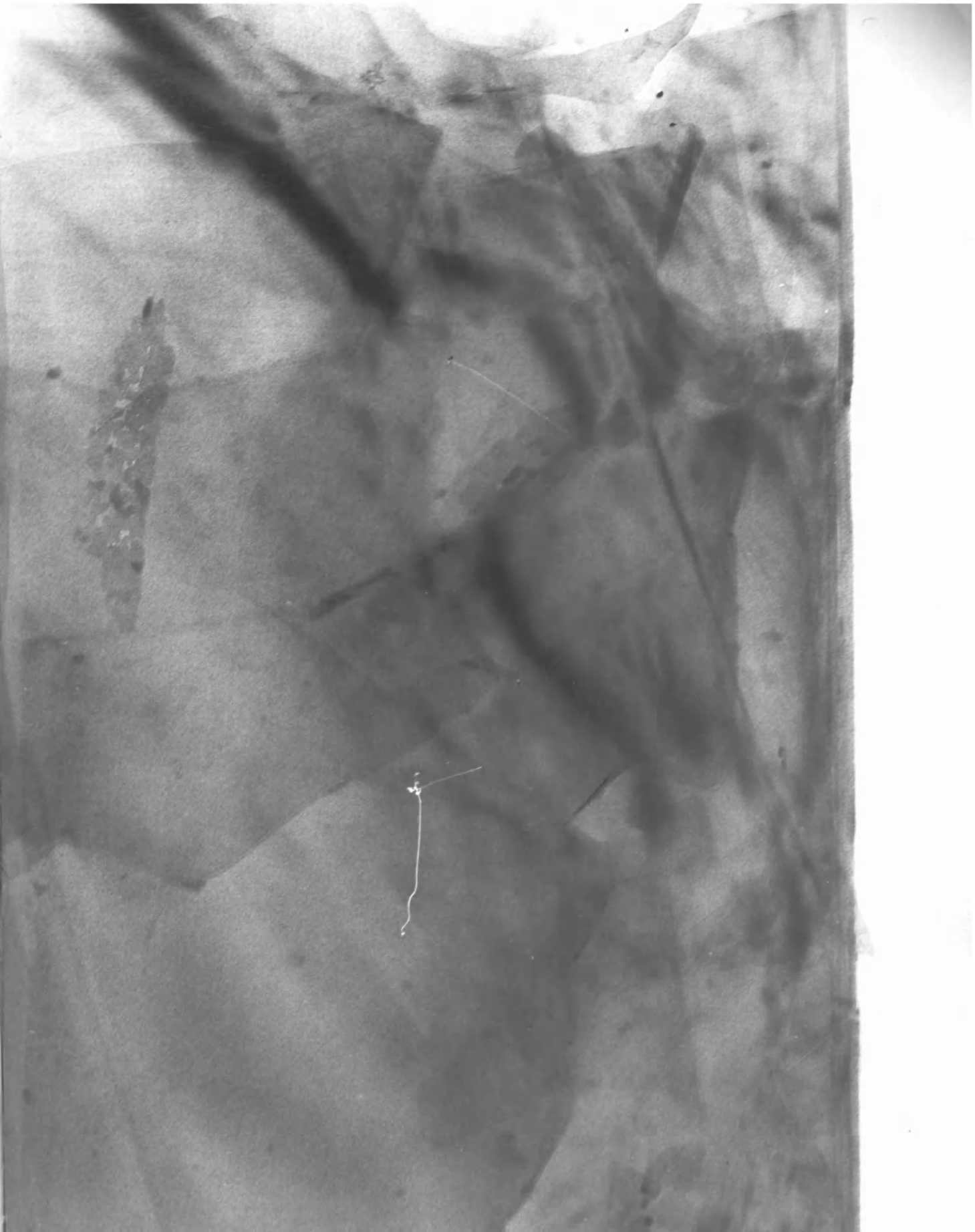

P L A T E S 17 A and B

Area of nuclear grade graphite before and after two BEPO irradiation cycles.

i) 1.06 x 10^{18} n/cm^2 in the carbon dioxide, carbon monoxide, methane mixture.

ii) 2.14 x 10^{18} n/cm^2 in the same conditions. x 120,000

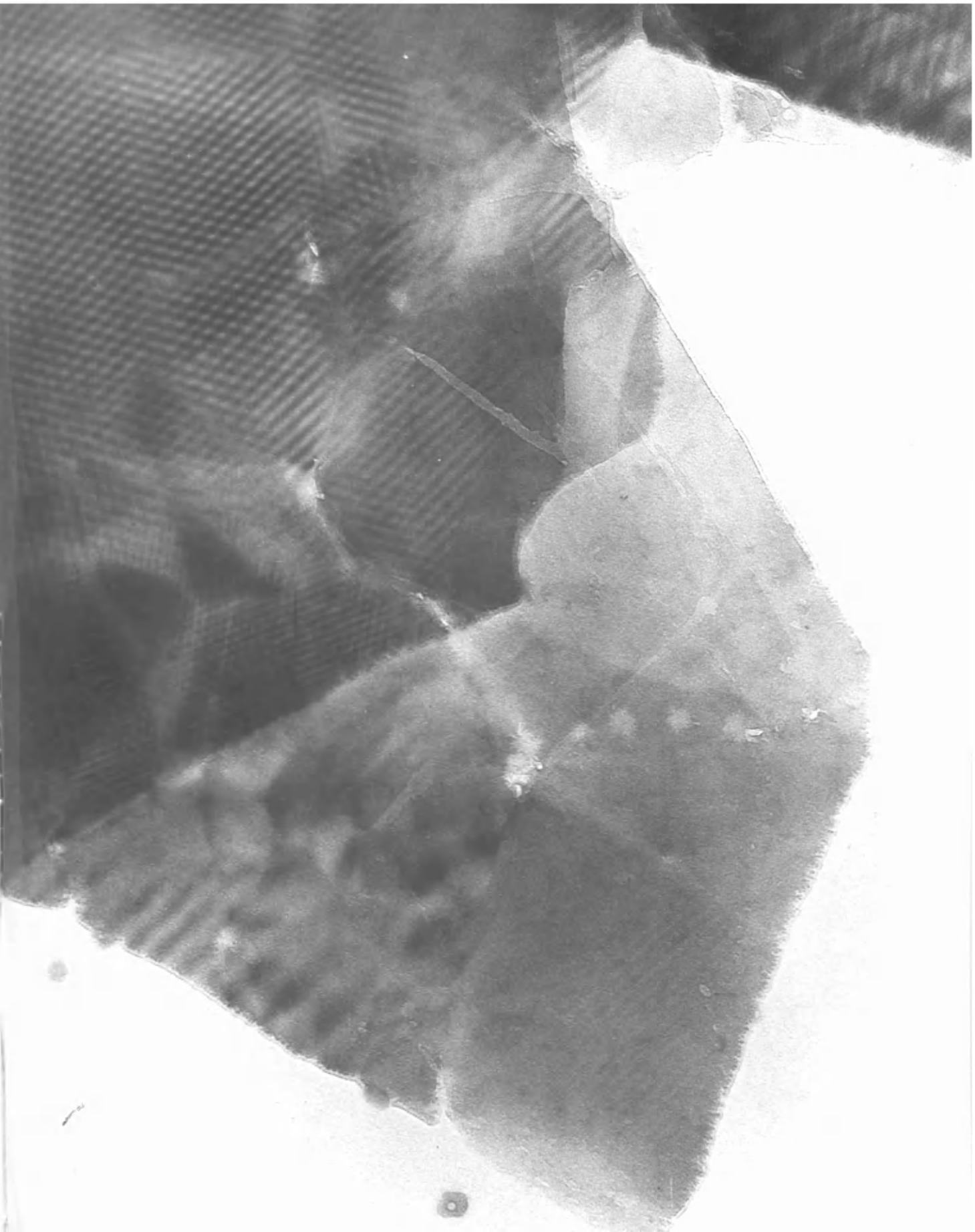

As well as general etching at these sites, some particularly active surface sites have been sufficiently attacked to produce pits which occasionally penetrate the specimen.

In the next set of experiments to be considered, the graphite samples received identical radiation doses to the above set, but in the first irradiation pure carbon dioxide was used as oxidant, while in the second irradiation the methane, carbon monoxide mixture in carbon dioxide was used. Again no reaction was found after the initial irradiation in carbon dioxide, but after the second treatment, graphite oxidation was noticed in both materials. It could logically be expected that since the initial treatment gave no reaction and a treatment similar to the second exposure had already been found to give no reaction (see Plates 14A and B), then the combination of both experimental conditions should also result in no carbon gasification, but this was not the case.

Samples of the natural graphite reacted characteristically with edge attack predominant, and penetration into the flake was found at grain boundaries. Micrographs obtained were very similar to that of Plate 16B, and thus no illustration is given. Nuclear grade material showed its customary edge attack with many instances of surface pitting, but the pits produced were not all similar in appearance and this seemed to depend on the presence or absence of a dark particulate impurity. In cases where this material was in evidence,

pitting of the type illustrated by Plate 18 was found. The pits in this case are rounded and it can be deduced from the pit edge contrast that the sides slope gradually. At some points these pits linked up, and channel formation was sometimes found. On samples where no such impurity particles were found, attack took place at points along grain boundaries and pitting was produced. Pits often linked up to give an etched outline of many crystallites. This is illustrated by Plate 19. Many isolated surface pits were also seen. Here the pit contours had a definite linearity associated with them and in many cases, e.g. area 'X', definite hexagonal outlines can be recognised. This micrograph shows a great resemblence to the pitting pattern produced by air oxidation of nuclear graphite as shown by Dawson and Follett (1963).

It can be deduced that the difference in pit formation must be due to the impurity. It is reasonable to expect a contamination layer on those specimens which had received two oxidation cycles. Before the second reaction stage, the samples had two microscope examinations, two loading and unloading procedures as well as exposure to the atmosphere not only during transit, but for the total time after preparation. Some areas may be contaminated more than others and this would seem to be shown by the appearance of the dark particles which could form part of a more extensive contaminant layer. In this way, samples with this contamination would evidently give a different

PLATE 18

Area of nuclear grade graphite after two BEPO irradiation cycles.

i) 1.06×10^{18} n/cm^2 in carbon dioxide.

ii) 2.14×10^{18} n/cm^2 in the carbon dioxide, carbon monoxide, methane mixture.

This area shows the presence of visible contaminant. x 120,000

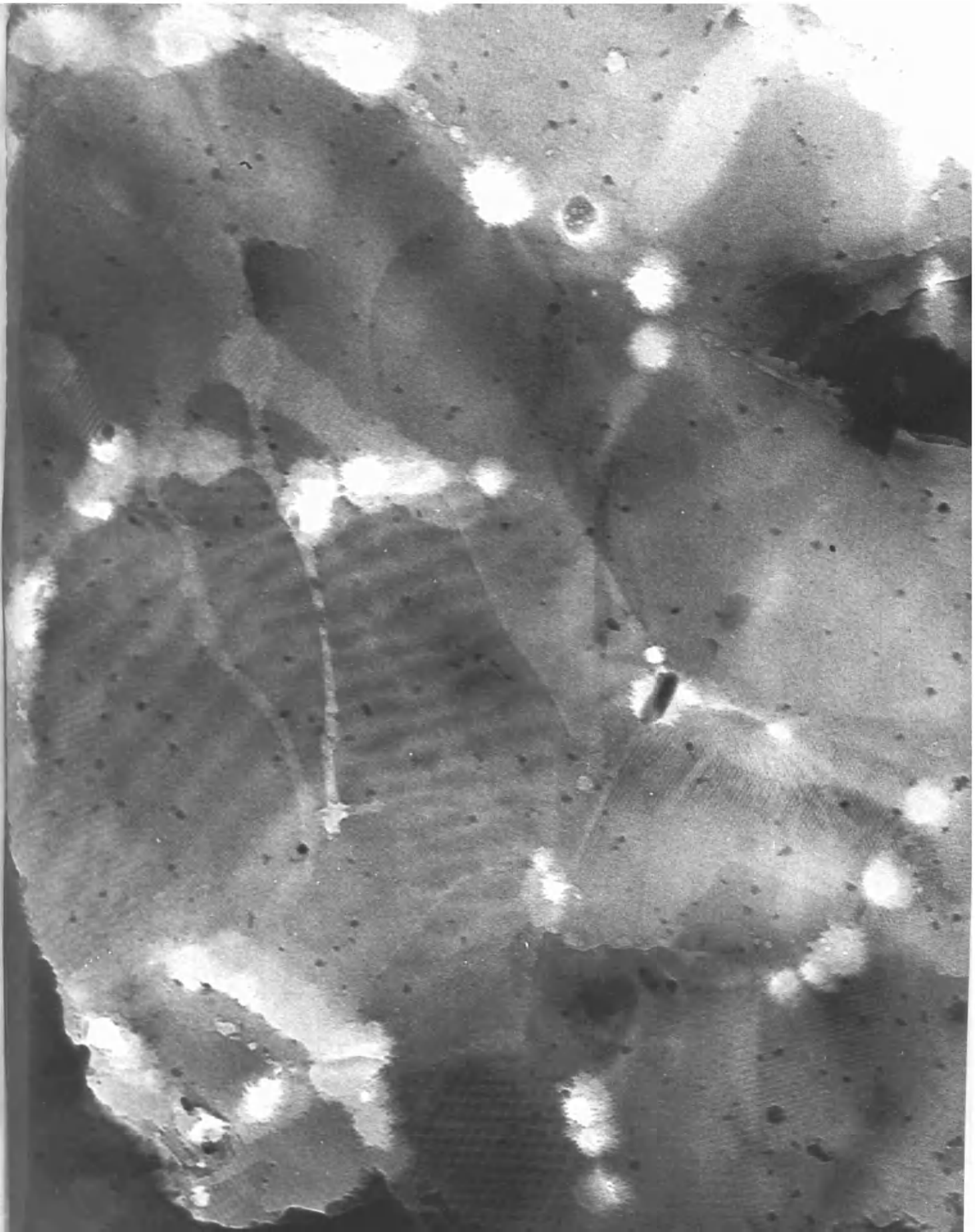

PLATE 19

Area of nuclear grade graphite after two BEPO irradiation cycles.

i) 1.06×10^{18} n/cm^2 in carbon dioxide.

ii) 2.14×10^{18} n/cm^2 in the carbon dioxide, carbon monoxide, methane mixture.

This area is free from visible contaminant. x 120,000

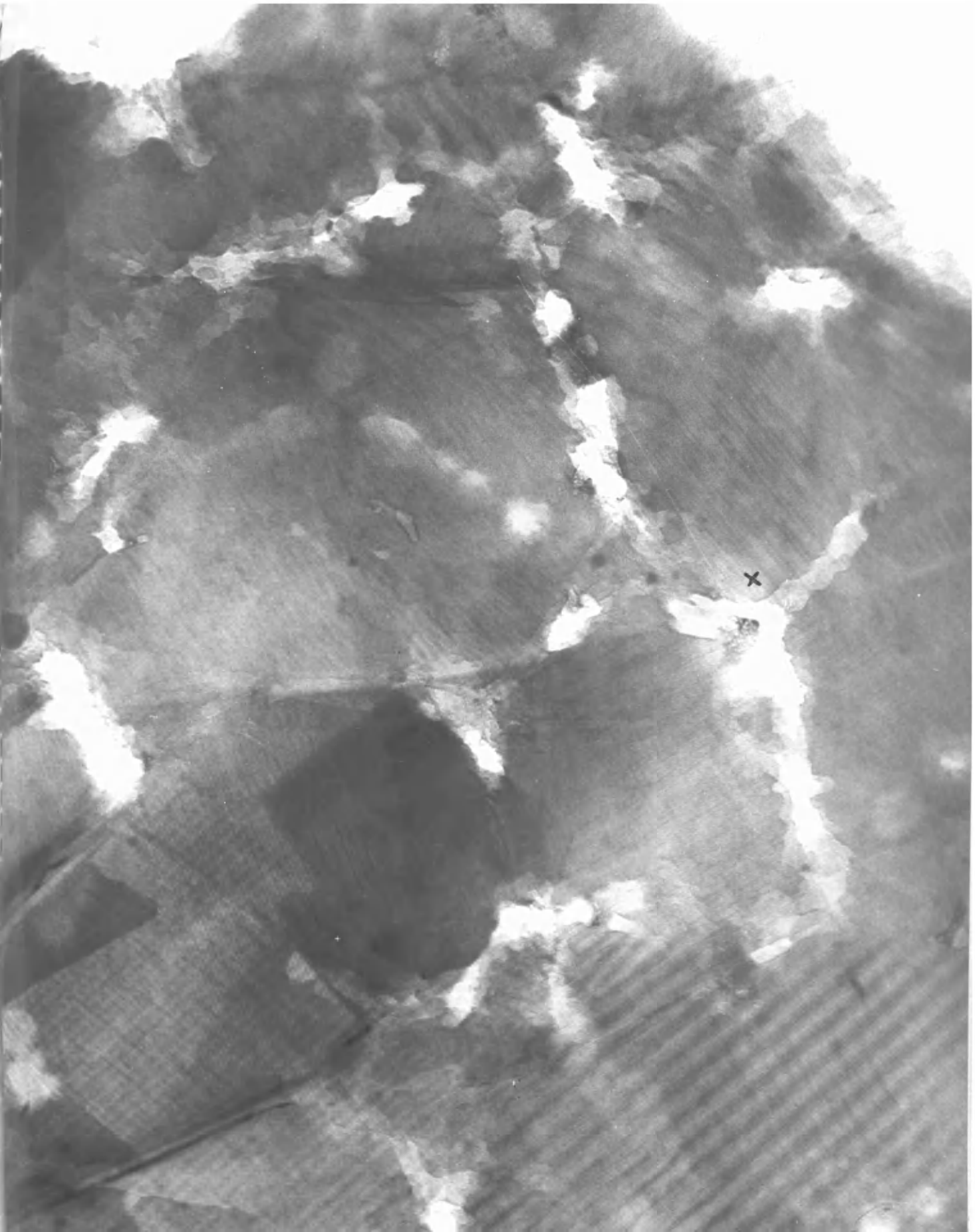

mechanism of attack. Plate 19 shows the uncontaminated specimen where pitting shows a fair resemblence to that found in Plates 7B and 11 which demonstrate attack in pure carbon dioxide and impurity induced attack respectively. It would then appear that the attack of the uncontaminated specimen had occurred by the normal pitting procedure.

Samples were also examined after interrupted irradiations at the same doses as before but this time only pure carbon dioxide was used. Natural graphite samples showed the same features of attack as have been described previously, although some demonstrated a more advanced gasification reaction. Again some samples were found to have particulate material on the surface, and in these cases attack was reduced and was confined to edges and some points of emergence of grain boundaries. In areas where no visible impurity was seen, attack had proceeded further at the normal active sites, and grain boundaries in particular widened considerably. At a few points surface attack did produce shallow areas along certain grain boundaries.

Nuclear graphite samples were all found to have impurity particles on their surfaces and the samples showed appreciable pitting of the basal planes. This is illustrated by Plates 20A and B. The pits have smooth rounded edges and are generally oval shaped. Since the transmission through the graphite around any pit decreases on moving away from the pit edge, it can be deduced that the pit edge drops gradually and uniformly to the background film in the pit centre.

The same contrast change can also be seen at some parts of the flake edge so it can be concluded that all carbon gasification has taken place by the same mechanism. These pits are similar to those shown on Plate 18 which was representative of a contaminated specimen area. In both Plates 18 and 20B, the surface contained a number of impurity particles but none can be seen to be associated with any pit. From the distribution of the particles, it was proposed that impurity must have been present initially at some sites which later gave rise to pits. Good evidence for this can be obtained from counts of pits and particles. Particle distribution counts on unreacted areas of both natural and nuclear graphite, gave good agreement and the mean value was found to be 9.6×10^9 particles per sq. cm. A count of particles on areas such as and including Plate 20B gave counts of 5.5×10^9 per sq. cm. A count of pits on the same samples, where possible, gave pit densities of 2.6×10^9 per sq. cm. This gave a total particle plus pit density of 8.1×10^9 per sq. cm. on areas such as Plate 20B and this shows good agreement with the impurity density on unreactive samples. This indicates that pits on contaminated areas were initiated only at certain sites where an impurity particle had landed. Any discrepancy in the counts can possibly be explained by the fact that some pits which appear single might well be composed of 2 or more small pits, and possibly some pits are too shallow to be observed. These impurity particles were found to be

non-diffracting and therefore consist of a non-crystalline material which was probably 'burned-off' the graphite surface after the initial stages of pitting.

An additional piece of evidence in favour of pitting originated at impurities was obtained from a sample of nuclear graphite which was prepared on a poorly finished zircalloy mount. As a result of the experimental conditions, which were roughly identical to those used above, some zirconium had been removed from the mount and appeared as small crystals on some specimens. These were definitely identified as zirconium by electron diffraction studies. When any of these crystals landed on a graphite surface, pitting was produced on the surface and in most cases the structure of the pits with their sloping edges was identical to that seen in Plate 20B. This time, however, most crystals remained in the centre of the pits, as illustrated by Plate 21. Some pits linked up while others produced channelling effects. It was found that most pits contained crystals and those which did not had in them a depressed film area. This suggests that a crystal had been present in the pit at one stage. The only difference between the Plates 20B and 21 is that in the first case there is no impurity present in the pits, while in the second case the crystalline impurity has remained.

Although all samples in this series showed different reactivity and some different structural features of attack to samples after

continuous irradiation it is still apparent that the mixture tried for inhibition purposes is still effective in controlling attack to some extent. It is also obvious that these conditions do not alter the general conclusion that the properties of each graphite are still the main factor in determining the mode of attack.

P L A T E S 20 A and B

Area of nuclear grade graphite before and after two BEPO irradiation cycles.

i) 1.06×10^{18} n/cm^2 in carbon dioxide.

ii) 2.14×10^{18} n/cm^2 in the same conditions. x 120,000

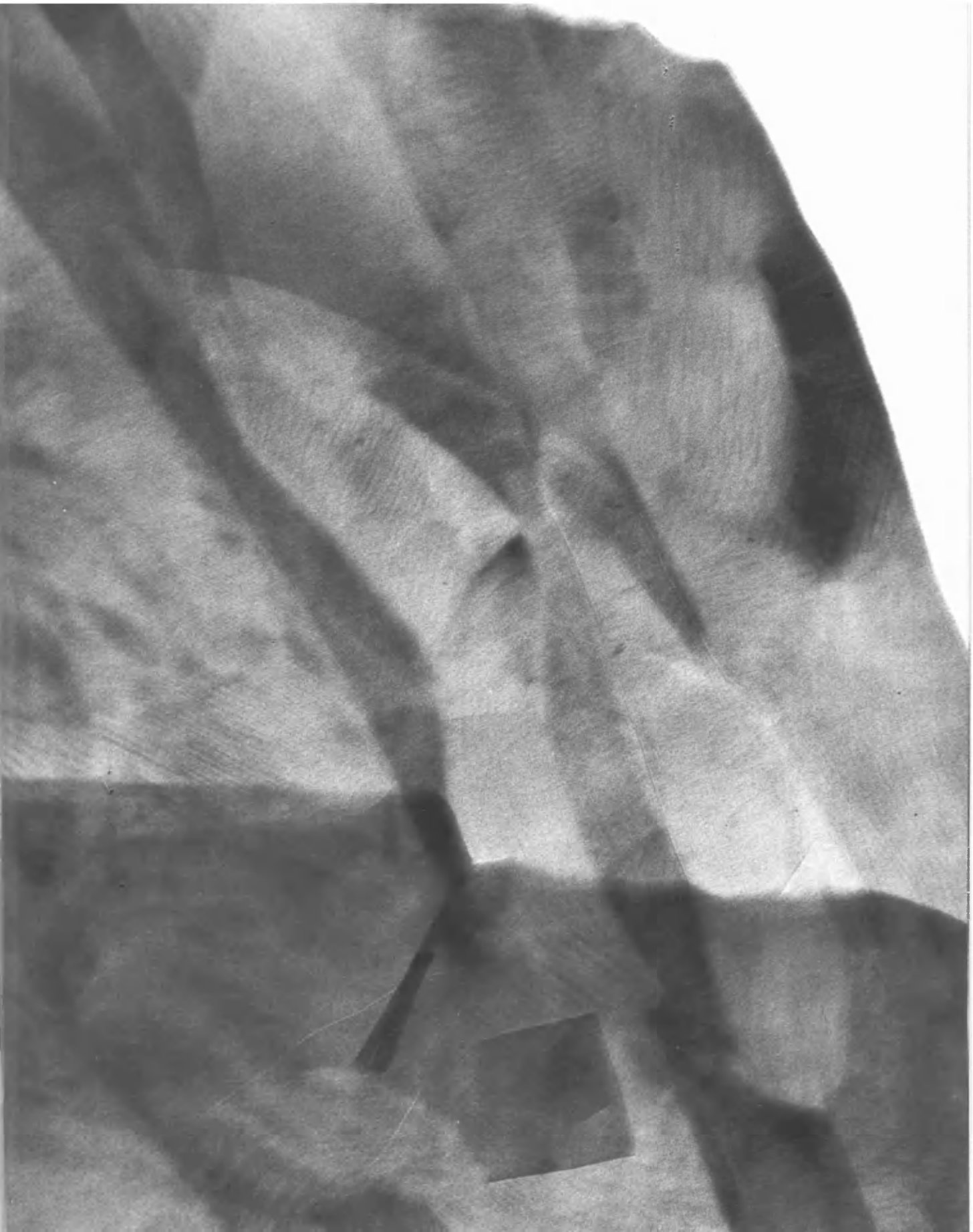

P L A T E 21

Area of nuclear grade graphite after two BEPO irradiation cycles.

i) 1.06 x 10^{18} n/cm^2 in carbon dioxide.

ii) 2.14 x 10^{18} n/cm^2 in the same conditions.

This area shows the presence of zirconium impurity. x 120,000

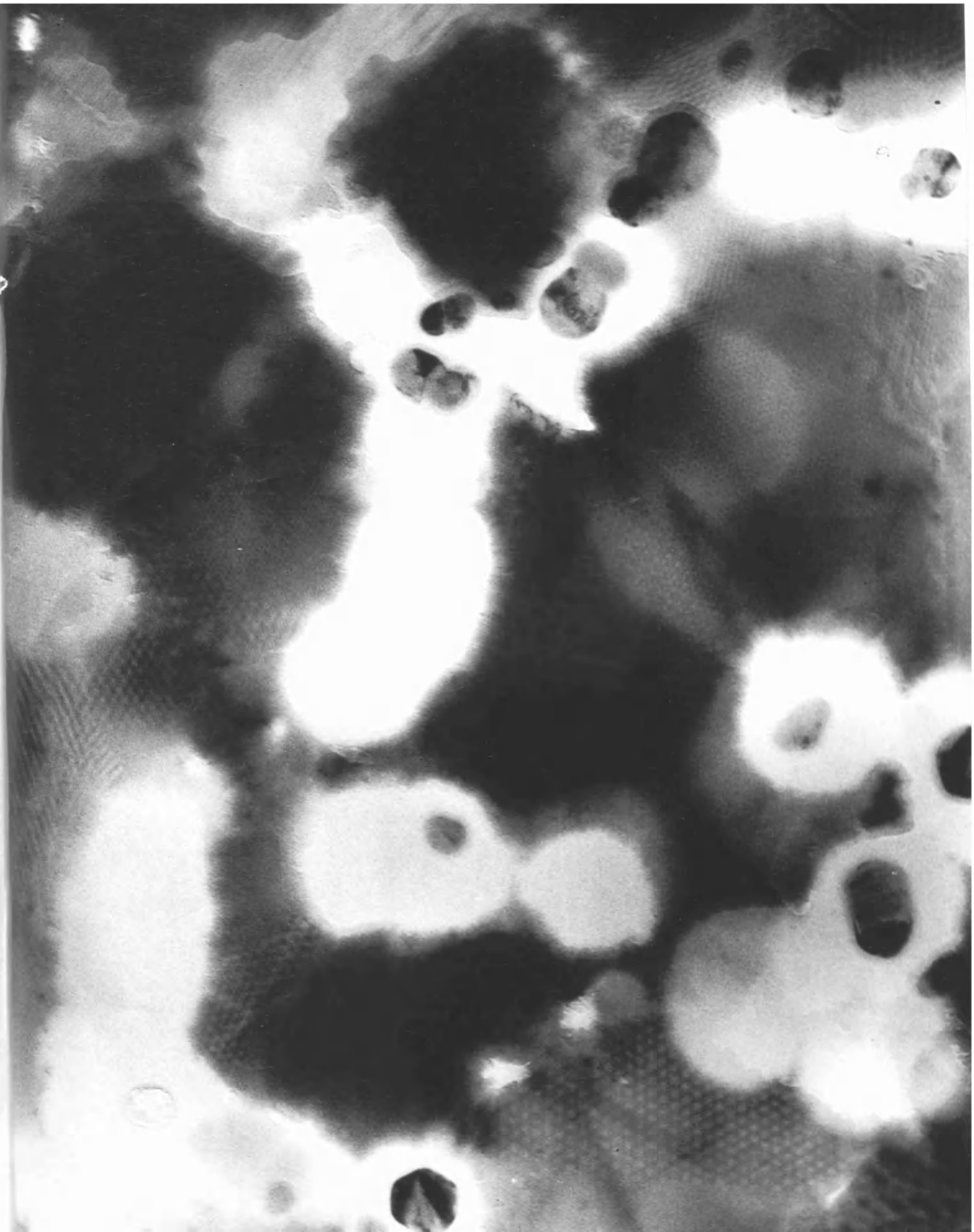

3. Experiments Using Vacuum Ultra Violet Irradiation

(a) Irradiation in Carbon Dioxide at Low Temperature

Preliminary investigations using both krypton and xenon lamps in short period irradiations of up to 30 minutes in carbon dioxide, produced only a slight change in the edge appearance of thin graphite flakes. This exposure time gave a dose received of about 10^{18} quanta, which was usually obtained after a minimum of 2 hours irradiation. The temperature used was around $25^{\circ}C$.

These experiments showed that whichever inert gas was used, there was no difference in graphite attack. The krypton lamp was mostly used since its wavelength for radiation is lower than that of xenon, and by the equation $E = h\nu$, the energy produced will be higher since the frequency $\nu = {}^{1}/\lambda$. From the table given by Feates and Sach (1965), the energy difference in the two gas irradiations results in the production of O(1d) atoms by the xenon lamp while krypton gives O(1s) atoms, in addition to CO(ground state). Thus, if these two active oxygen atoms constitute the attacking species, their mechanism of attack must be identical to give the similar results observed.

An area of purified natural graphite is illustrated before and after 1.1×10^{19} quanta by Plates 22A and B. The only evidence of reaction is seen at flake edges. The thin flake edge has become very uneven as carbon has been removed and areas along this edge contain

dark regions which resemble areas of particulate deposit. This can also be seen at the edge of an attacked surface flake, marked 'XY' on Plate 22B. Other natural graphite samples showed the same features of attack, with deposition apparently at sites of attack.

The attack on nuclear graphite at the same dose is illustrated by Plates 23 A and B. Oxidation at flake edges has proceeded to a greater extent at thin edges rather than thick areas. The main attack has taken place at the central thin triangular region which has been etched back to a thicker edge. The attack at this region, marked 'XYZ', can be contrasted to that at thicker edge areas, in particular 'YP' which shows little sign of attack. Surface flake edges have also been attacked and an obvious feature after reaction is the appearance of a dark particulate material exclusive to the graphite. In contrast to the natural grade, the deposit is randomly distributed over the surface, and, as in the case of the proton irradiation experiments, its presence can be attributed to deposition at attacked sites. Nuclear graphite in addition to its active edge sites also contains many more active surface sites than natural graphite. Again, attack at these points could result in a carbon monoxide product being bonded at nearby sites and subsequently a polymer product could be deposited there. The absence of any deposit on areas where there was originally graphite present, suggests that the deposit-forming species had been mobile over the surface and had

collected at certain sites behind the attack front where polymerisation had taken place.

To find the distribution of the particles, counts were made on this area. It was found that there was 2.3×10^{11} particles per sq. cm. on the bulk of the graphite but 3.4×10^{11} per sq. cm. at the edge, which was taken as the 1000Å nearest the flake edge. These figures give additional evidence for the theory that deposit is found at attacked sites since, near the edge, the count will be made up of particles produced by edge reaction plus surface reaction particles produced at sites close to the edge. A similar particle distribution was found on other graphite areas under the same conditions. Particle size was also measured on a number of areas and was found to be 56.6 ± 6Å.

The effect of increasing the dose was to increase reaction at the same sites as before. A dose of 2.5×10^{19} quanta was used, and typical results are illustrated by Plates 24A and B which show an area of nuclear grade graphite. Although reaction was appreciable, it was less than would be expected when it is considered that this sample had $2\frac{1}{2}$ times the dose of that sample, illustrated by the previous micrographs. This small increase in reactivity could be due to the inhibiting effect of the deposit which was located at active sites. By a deposit blocking mechanism, reaction could slow down or stop. The main areas of attack are the flake edges, and in

P L A T E S 22 A and B

Area of purified natural graphite before and after 1 x 10^{19} q.u. in carbon dioxide at 25°C. x 120,000

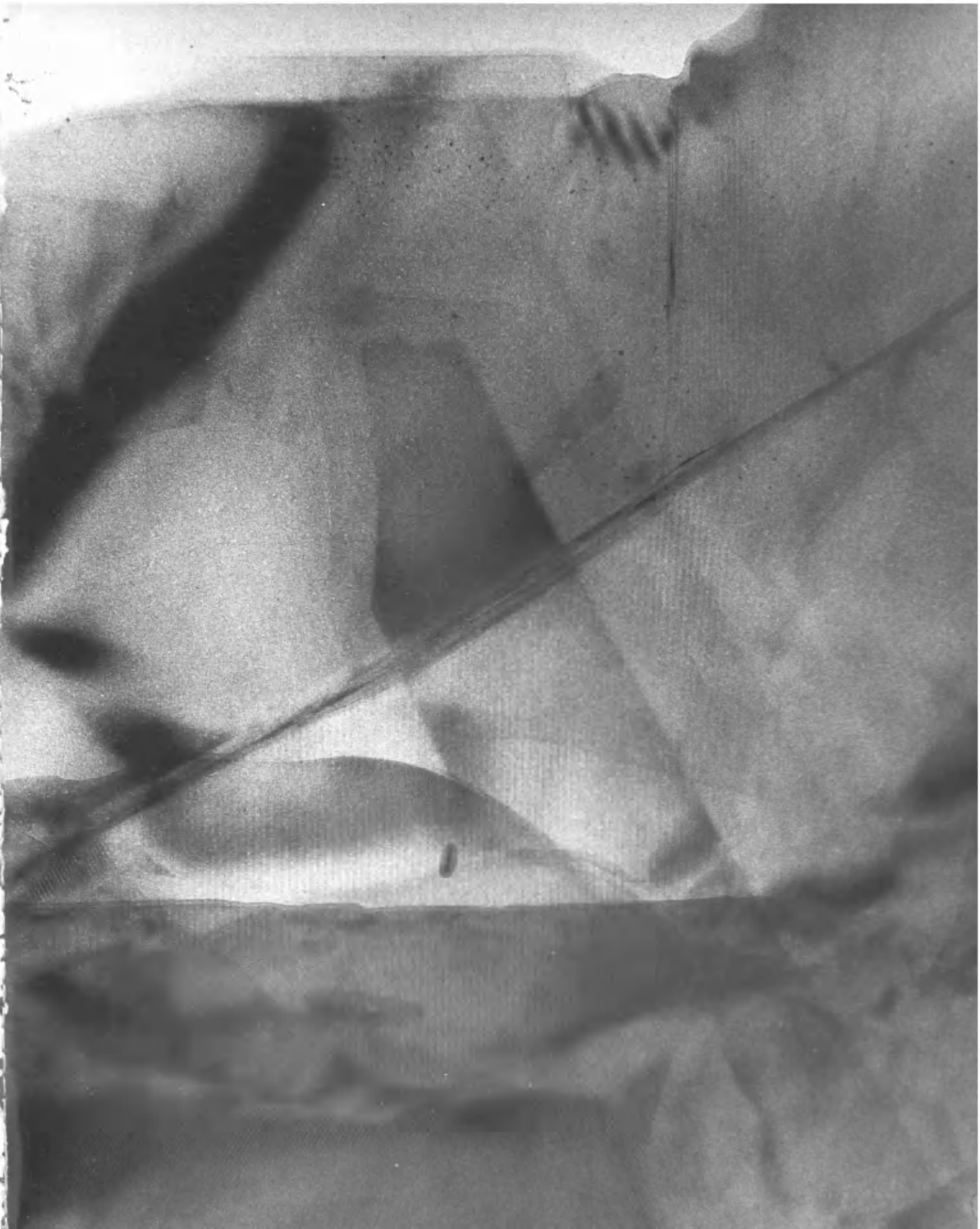

X
Y

P L A T E S 23 A and B

Area of nuclear grade graphite before and after 1 x 10^{19} q.u. in carbon dioxide at 25°C. x 120,000

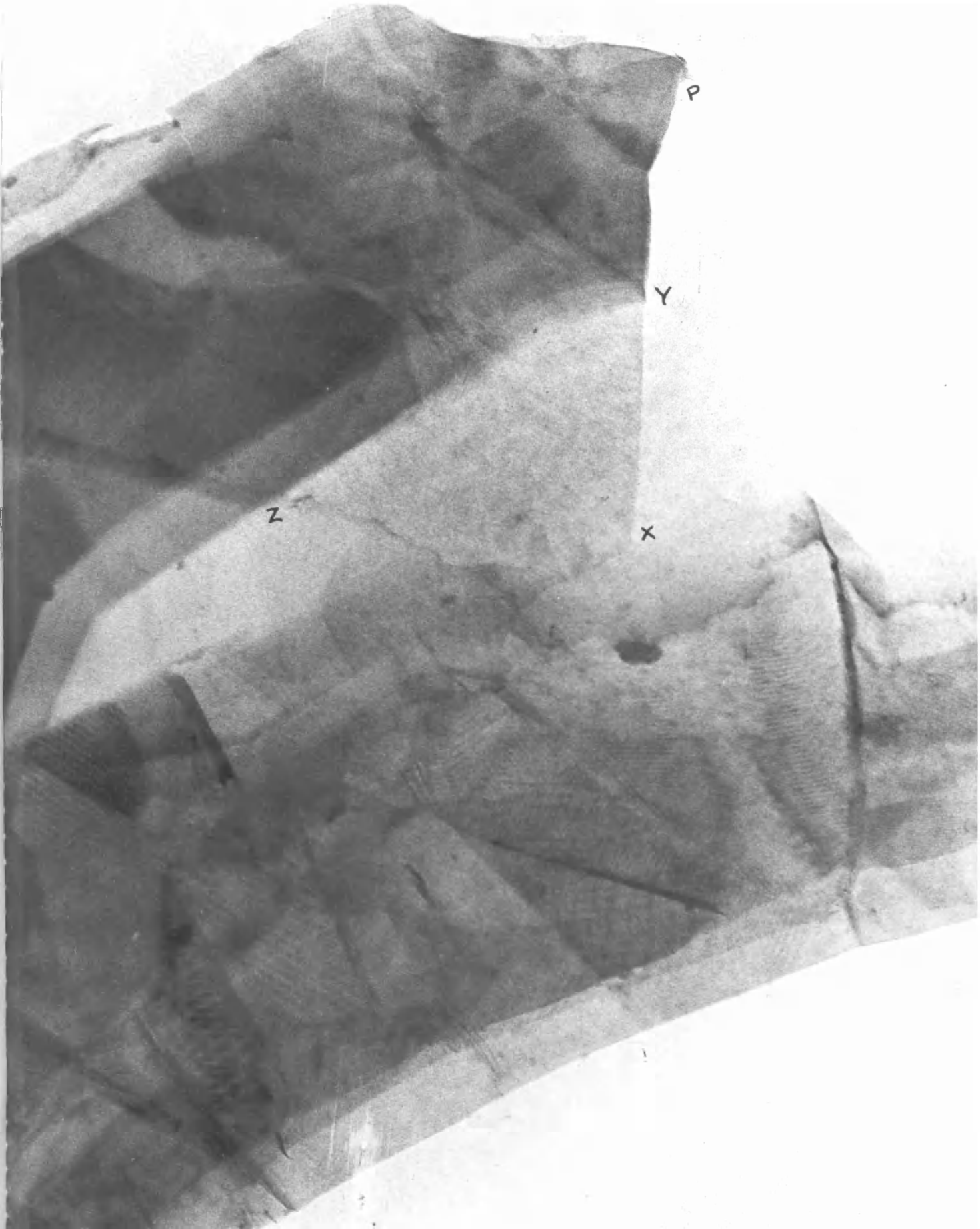
P
Y
Z
X

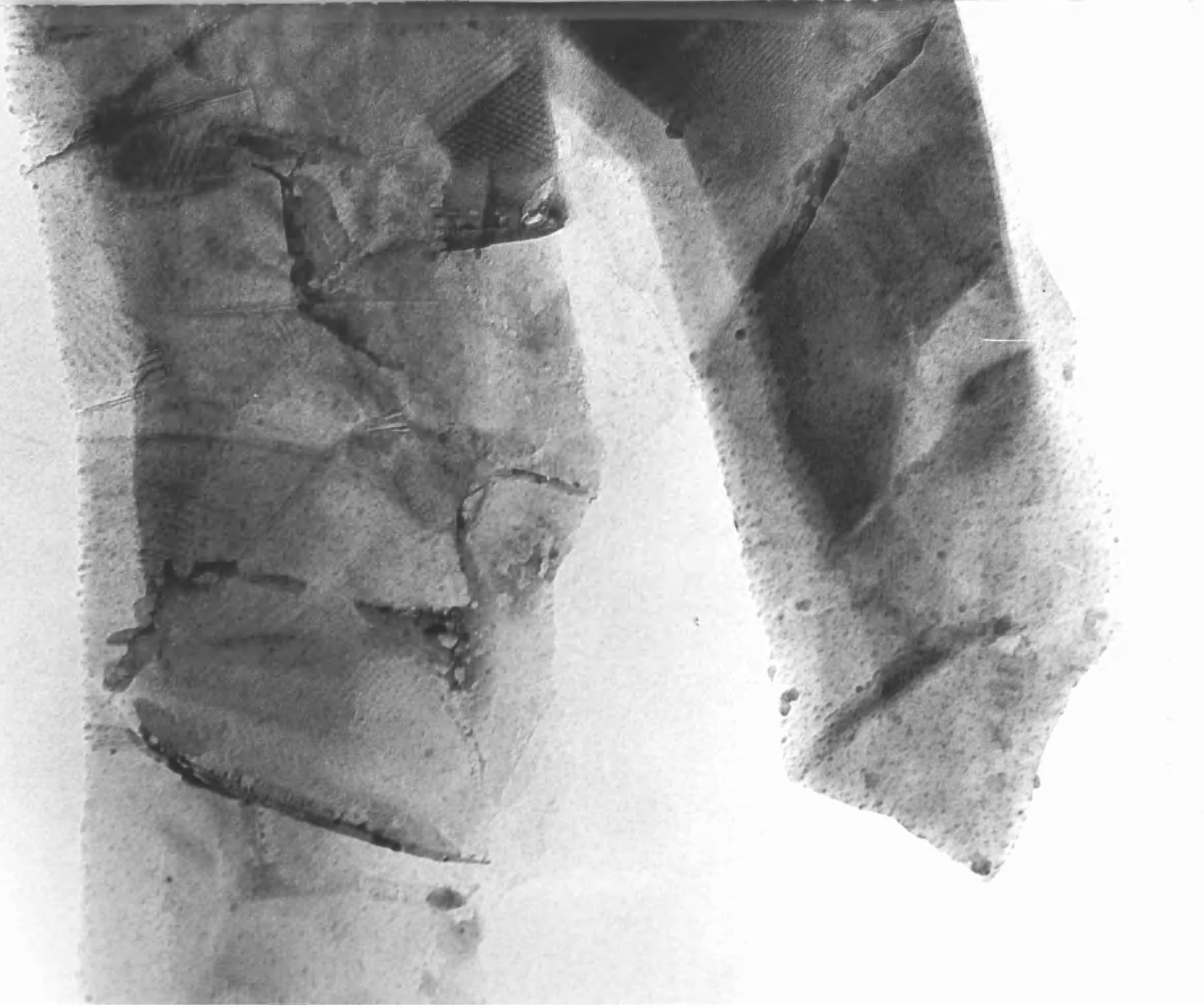

P L A T E S 24 A and B

Area of nuclear grade graphite before and after 2.5×10^{19} q.u. in carbon dioxide at 25°C. x 120,000

particular the thin stepped edges which have been etched back to a thicker region. There is also extensive attack at the surface but this is confined to surface flake edges and is therefore due to edge site gasification. Once again the difference in reactivity of thick and thin edges is well illustrated. Due to the poorer contrast on this particular area, fewer particles than usual were measured but their diameters were in good agreement with the above figure, and the mean for this series of experiments was 57.4 ± 7Å.

It can therefore be seen that graphite attack in these experiments is similar to that found in proton irradiation experiments where a deposit of the same size was produced. It is therefore necessary to compare the dose rates for these experiments.

By using the equation $E = h\nu$, the energy in ergs of 1 quantum of energy emitted at a particular wavelength can be found. An average value for the krypton and xenon emission is 1.6×10^{-11} ergs. Since 10^{19} quanta were passed in an experiment which gave reasonable attack, the total ergs received by the system is 1.6×10^{8}. This was received by .5 c.c. of carbon dioxide at 30 cms. pressure which is equivalent to 5.32×10^{18} molecules. Since 1 ev = 1.6×10^{-12} erg, the dose rate is therefore 18.8 ev/mol. of carbon dioxide. This is approximately 4 times the dose rate of an average BEPO reactor irradiation, which could account for the lack of visible deposit on the BEPO irradiated samples. Since this rate is a good deal below the proton irradiation

dose rate, this can be used to account for the appearance of pits in the nuclear graphite after proton irradiation experiments but not after the vacuum ultra violet irradiations. Although the dose rate is less than for proton irradiation, it is obviously high enough to promote polymerisation and deposition effects.

(b) Irradiation in Carbon Dioxide at High Temperature

By using a heating coil wrapped round the specimen chamber, temperatures around 350°C. were produced. The experiments to be described were carried out under krypton irradiation and received 2.3×10^{19} quanta.

When the specimens were re-examined after reaction, it could be seen that an entirely different mode of gasification had taken place. Both graphites now gave similar results, which were attack perpendicular to the basal plane and deposition, which this time appeared as large agglomerations.

A typical area of purified natural graphite is shown before and after the above conditions by Plates 25A and B. Certain letters have been written on the micrographs to help to identify the same regions before and after reaction. Instead of the usual edge attack, there has been widespread carbon gasification with deposition over the whole graphite surface and particularly at thin areas where only isolated deposit masses remained. The deposit formed large clusters and chains which probably resulted from the greater mobility of the

deposit-forming species at this elevated temperature. This species is probably a carbon monoxide molecule produced by carbon gasification, and these molecules could collect and polymerise at certain sites where a radiolysis product could be formed. The appearance of this sample with the presence of deposit on the surface is strong evidence in favour of attack and carbon removal at random points on the basal plane.

An area of nuclear graphite is shown in Plates 26A and B. This has been reacted alongside the above sample so the results are comparable. The original graphite flake has been gasified and only the pattern of deposit at former edges helps the identification of the area. Once again the deposit has clustered to give a small chain-like appearance. Electron diffraction studies were made of such areas, and the patterns and measurements found were proved to be those of graphite. A typical diffraction is illustrated by Plate 27 which was obtained from the area shown in Plate 26B. The strongest spacings were found to be 2.14, 1.24 and 1.07Å, which can be favourably compared with the graphite literature values of 2.13, 1.23 and 1.06Å. This clearly indicates that there must be graphite below the deposit areas and so even under these extreme carbon attack conditions, the deposit is still blocking the gasification of the underlying graphite. It is possible, though unlikely, that there are a few layers of the original graphite present, but indistinguishable from the background film.

P L A T E S 25 A and B

Area of purified natural graphite before and after 2.3 x 10^{19} q.u. in carbon dioxide at 350°C. x 170,000

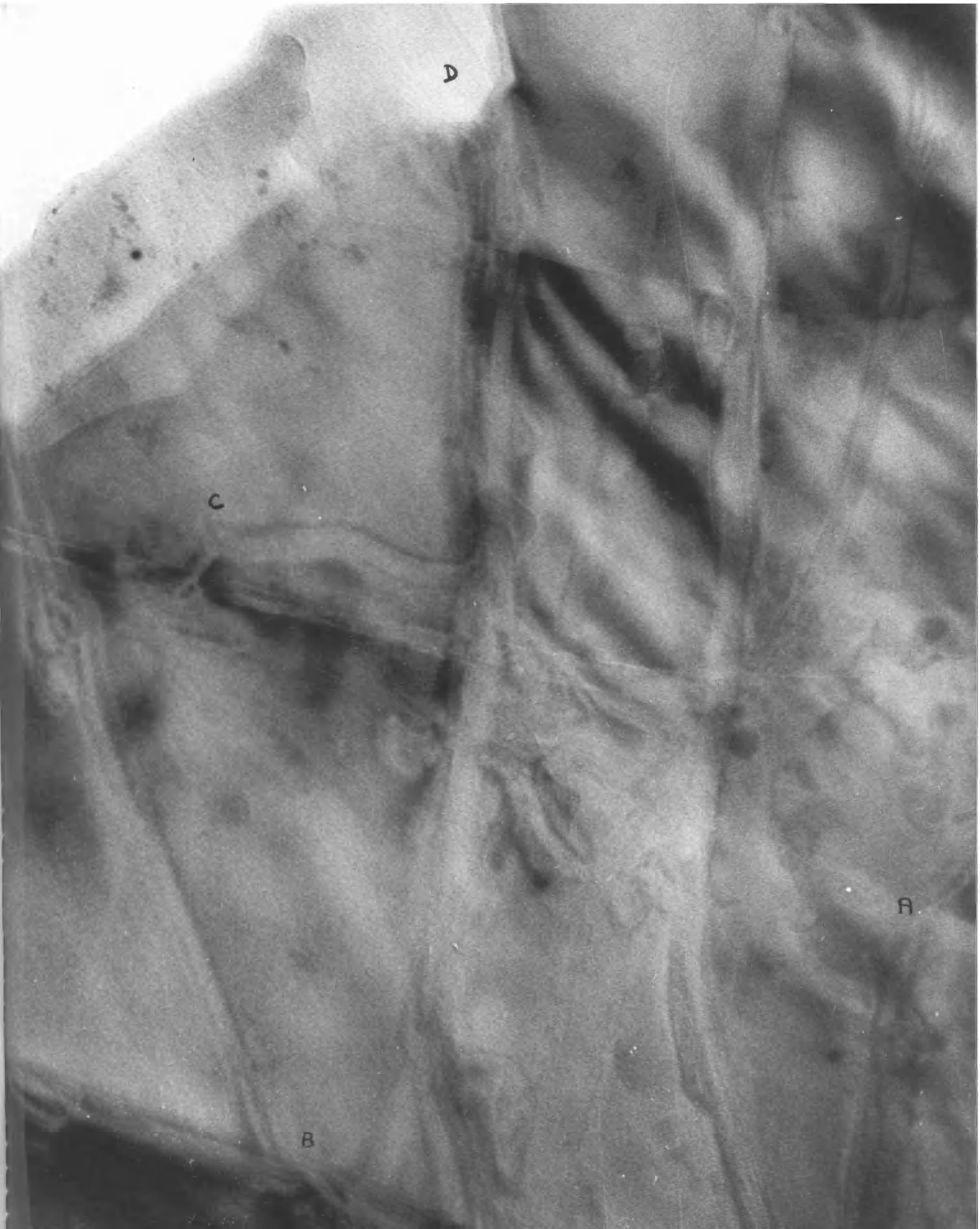
D
C
A
B

D
C
A
B

P L A T E S 26 A and B

Area of nuclear grade graphite before and after 2.3×10^{19} q.u. in carbon dioxide at 350°C. x 120,000

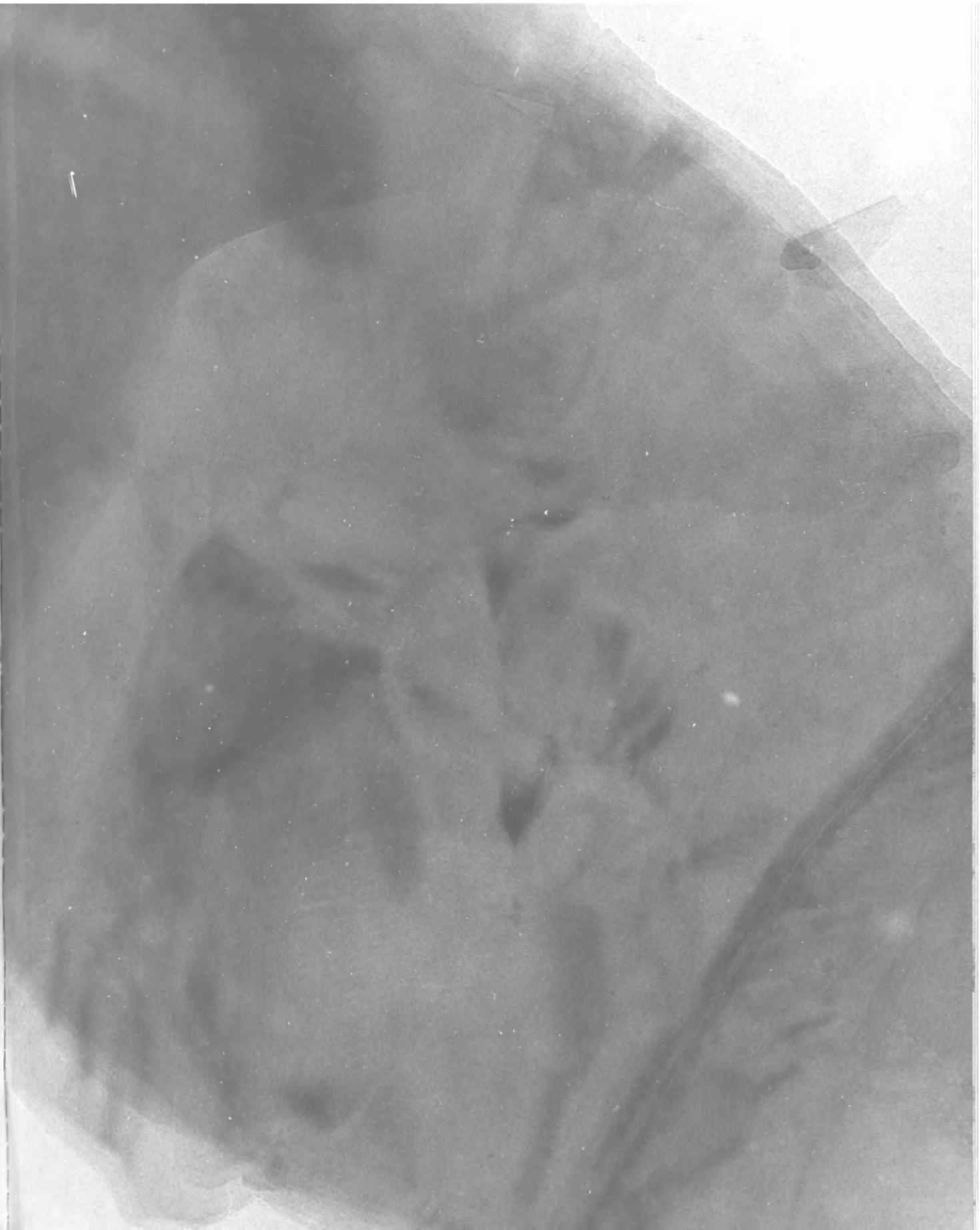

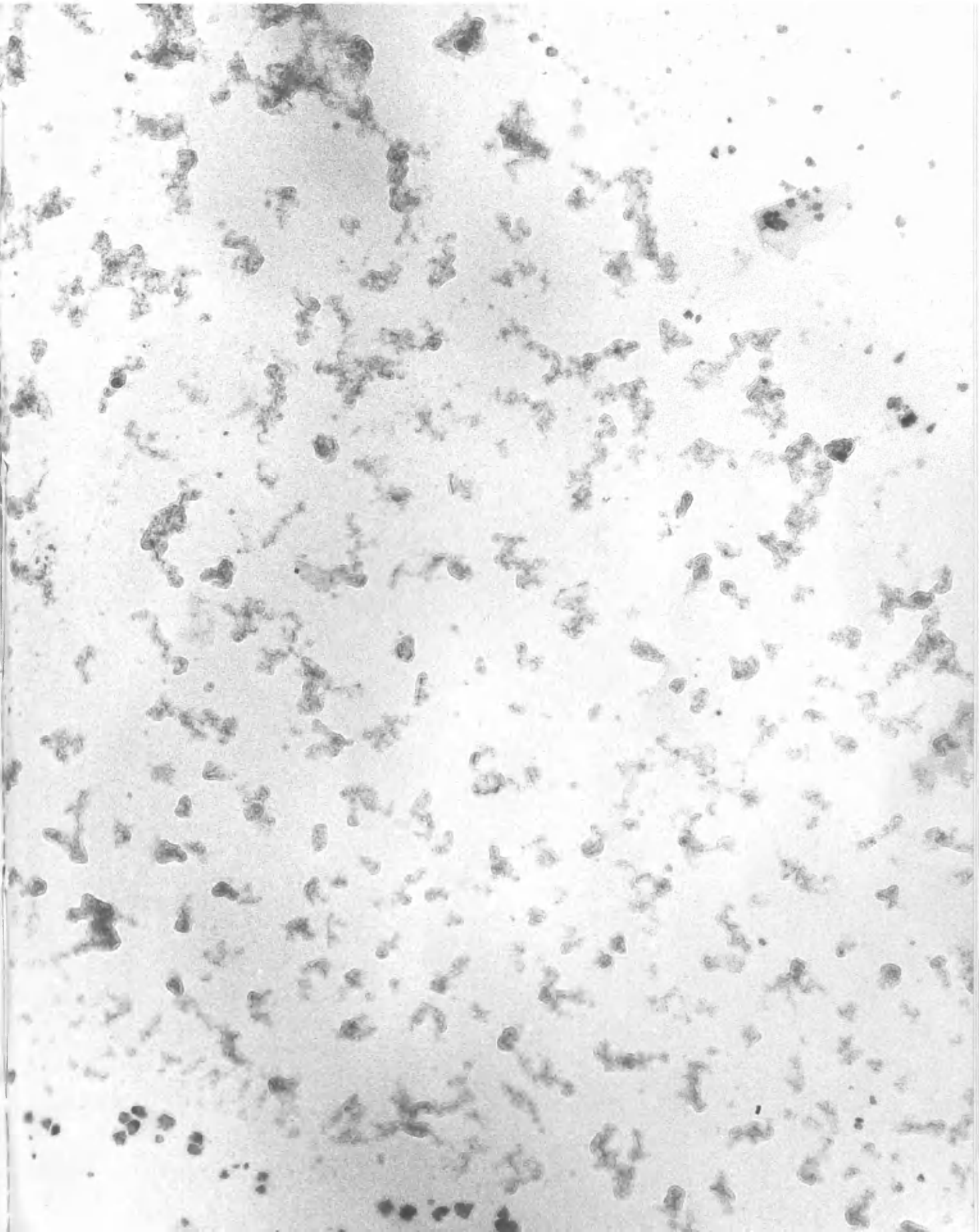

P L A T E 27

Electron diffraction of the deposit area of Plate 26B.

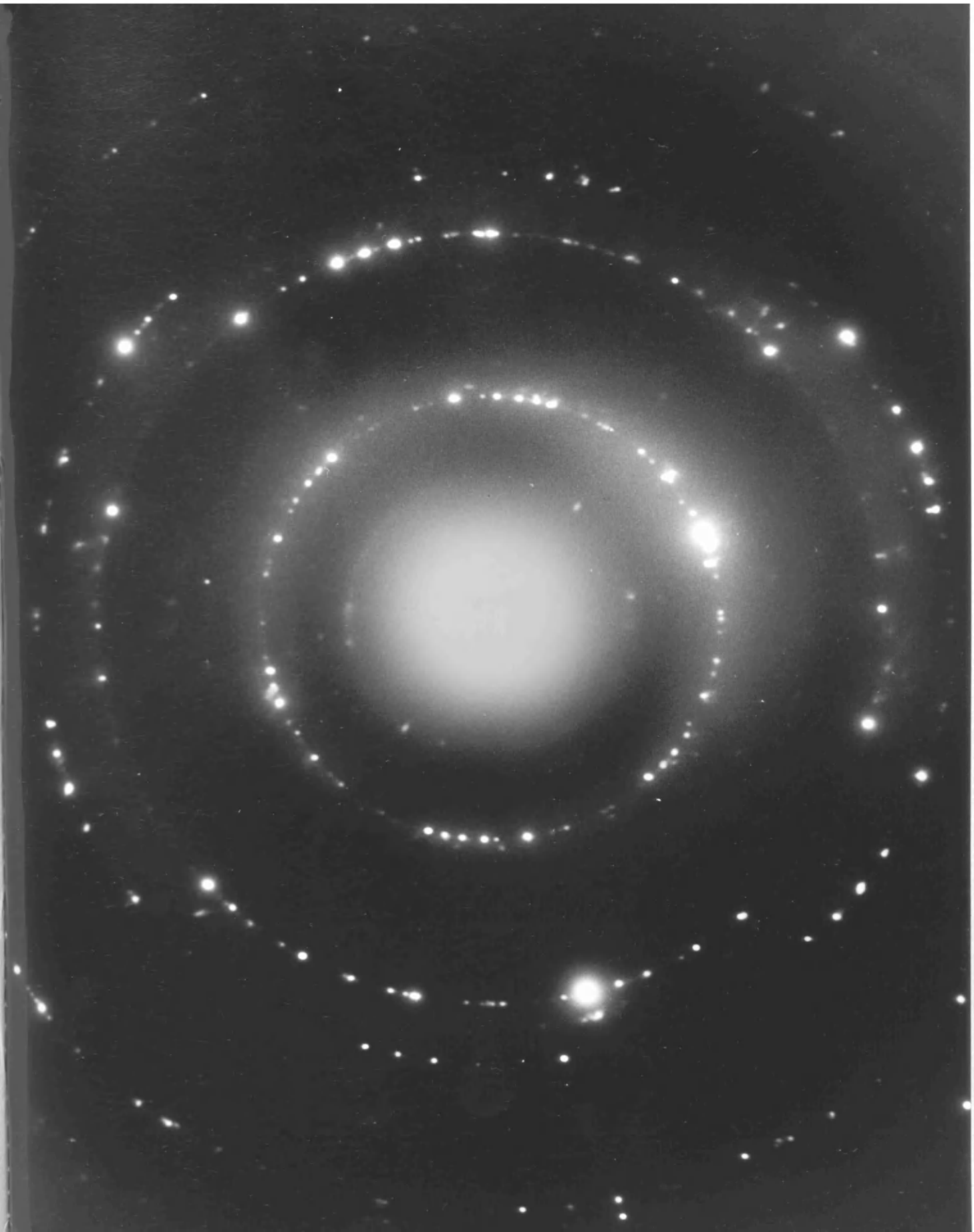

Many areas were photographed where graphites of both types showed all intermediate stages of oxidation which mostly depended on the thickness of the particular flake. In no case examined was there any evidence found of pitting such as had been found in other systems. These two facts support the observation that attack perpendicular to the basal plane had occurred at random sites on the graphite surface. The fact that there is no anisotropy of reaction, with the surfaces parallel and perpendicular to the basal plane showing equal attack, is consistent with the findings of Marsh, O'Hair and Reed (1965). These authors reacted atomic oxygen thermally with various carbons and found that a general background of conical pits was produced on all crystalline graphites, and so they concluded that defects were not essential for the initiation of this type of attack.

This evidence from the literature, taken with the experimental evidence described above, suggests that atomic oxygen is responsible for graphite attack under vacuum ultra violet irradiation at this temperature. The above authors also found some etch pits caused by oxidation at defect structures in addition to the background pitting, and their absence in these studies is likely to be due to the presence of deposit. If this deposit had been formed by a species which migrated and polymerised at a collecting point, probably a defect site, then the resultant deposit particle could block that site from its normal attack process, and no etch pit would be produced there. Nuclear

graphite,which has a greater defect content, will therefore contain more centres for polymer collection and so will contain more deposit areas, although smaller than those on natural graphite. The larger the deposit cover, the greater will be the graphite protection, and so the lower will be the rate of attack.

The appearance of the deposit seems to alter with its surroundings. In Plate 26B, where there is no intervening graphite, the particles are smaller, better defined and appear more granular than most of those particles which lie on a graphite surface as shown in parts of Plate 25. Here,(Plate 25), the particles appear as rounded masses. An even better illustration of this is given by Plate 28, which shows a natural graphite area. This plate shows regions of small chain-like deposit where the graphite has been extensively attacked, but the deposit on the bulk of the graphite resembles a 'semi-liquid' with round areas whose centres appear more dense than their outer regions. The deposit mass marked at the position 'XY' shows a moiré pattern extending to the particle edge where the pattern changes to that of the graphite immediately adjacent to the deposit.

A possible explanation of the pattern change is that there is a different graphite content at the two regions, due to the gasification of a few graphite layers around the deposit mass. However, a more probable explanation can be proposed from physical considerations. On close examination, it can be seen that a moiré pattern similar to

PLATE 28

Area of purified natural graphite after 2.3×10^{19} q.u. in carbon dioxide at 350°C. x 120,000

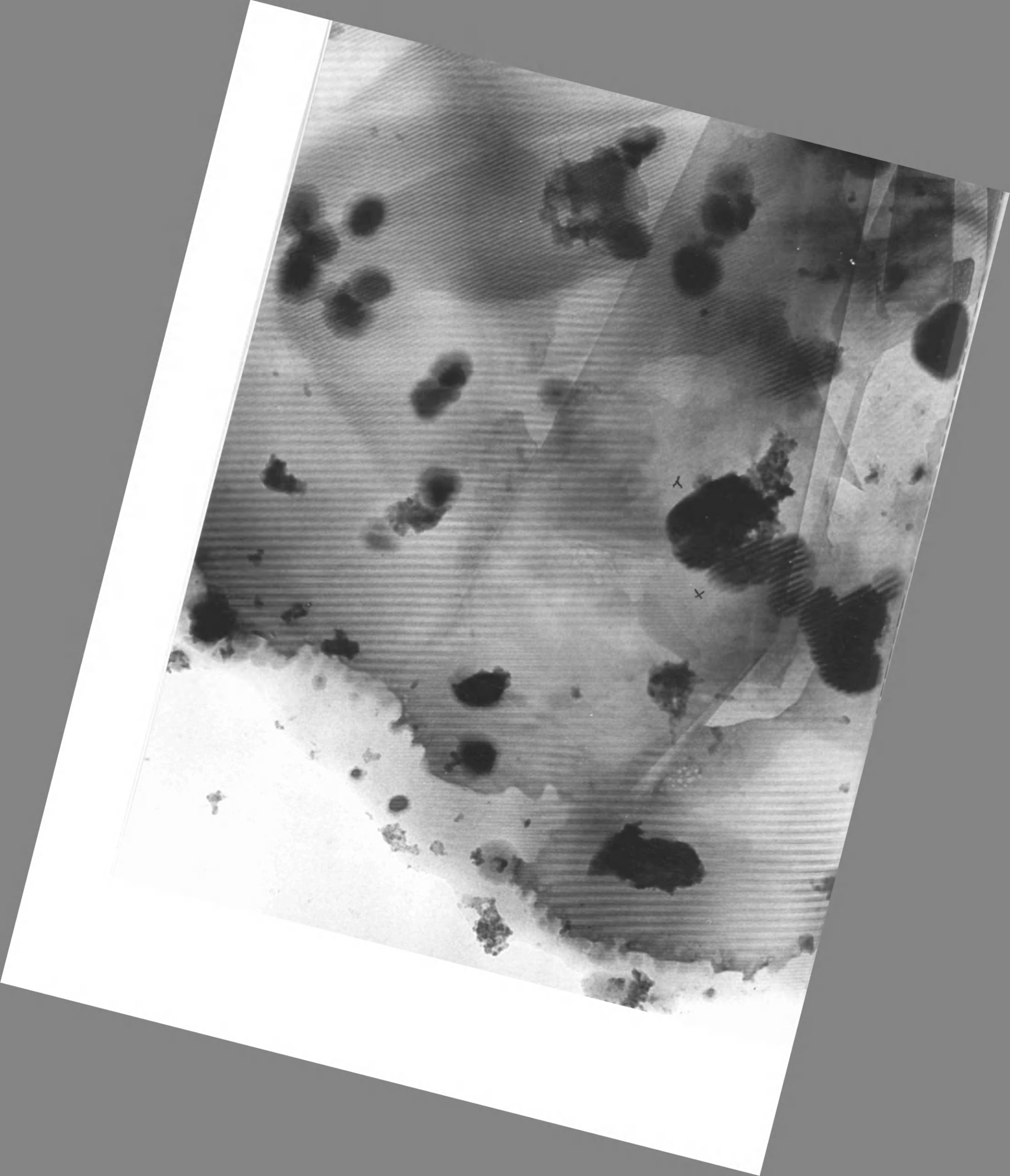

that of the deposit mass 'XY' is visible at other neighbouring areas. It is therefore possible that there are two superimposed different regions of graphite, each of which possesses a different moiré pattern. Depending on local effects, either pattern could become dominant and visible to the exclusion of the other. Several factors could cause an alternation of the patterns. It is possible that a moiré pattern change at the deposit particle could be due to purely a contrast effect produced by the particle itself, which can magnify the image of a pattern which is different to that pattern adjacent to the particle. A moiré change can also be produced by a localised energy effect. As the polymer producing species collects and forms a particle, there will be an energy release at those sites and this localised high energy area below the deposit could cause the moiré pattern to change. This could also result from any annealling effects produced by the higher energy at deposit regions. The difference in deposit appearance at some areas suggests that, as graphite is oxidised, the energy produced could cause any nearby deposit to 'dry-out' and shrink. Also any energy absorbed by the deposit from the system during the gasification process could enhance the solidification rate of the deposit, as well as transmit energy to the graphite below it.

(c) Irradiation in Inhibition Mixtures at Low Temperatures

As reported for the neutron irradiation experiments, the mixture of 1% carbon monoxide and .1% methane in carbon dioxide was used in

attempts to inhibit carbon gasification. Feates and Sach (1965) showed that methane decomposition was most favoured by the emission from the krypton lamp which was therefore used exclusively.

No visible signs of reaction were found on either grade of graphite up to a dose of 2.2×10^{19} quanta. At 2.2×10^{19} quanta the initial states of reaction were identified on nuclear graphite as very slight etching of the flake edges, accompanied by the appearance of some kind of deposit which was too indefinite for measurement. This corresponds to a dose rate of 41.4 ev/mol. for carbon dioxide for the initial deposit formation from the mixture. At a comparable dose in pure carbon dioxide, appreciable gasification had taken place and so the methane, carbon monoxide admixture is therefore effective for inhibition under these conditions.

By increasing the number of quanta passed into the system, a corresponding increase in reactivity was found, particularly on nuclear grade graphite. The extent of the reaction resulted mainly in the production of a large amount of particulate material all over the surface of both graphites but not on the background films. An area of natural graphite is illustrated in Plates 29A and B, before and after 4.1×10^{19} quanta in the above gas mixture. There has been slight carbon gasification at thin edge regions and the surface is covered by the deposited material. This appears as single particles in the bulk of the sample and as irregularly shaped agglomerations

at the edges. Occasionally some of the particles can be seen to form a broken line which corresponds to a surface flake edge on the original micrograph. The deposit masses at the flake edge could be caused by individual particles condensing together but a more likely cause is the opposite process. By examining some of these masses, particularly in the neighbourhood of the discrete particles, it can be seen that the large areas seem to be shrinking and breaking apart to form denser, smaller, individual particles. This is a sort of 'drying-out' process which can be attributed to a liquid polymeric substance condensing to a more dense solid polymer product. This suggests that originally the specimen was completely covered by a species which could induce polymerisation. The 'drying-out' process would be likely to occur more rapidly in the centre of a flake due to the increased energy and heat content of the centre of a thick area rather than thinner edges.

Counts were made on the individual particles and these gave 3×10^{11} particles per sq. cm. and their size was found to be 89 ± 9Å. This proves that the particles are substantially larger than the deposit found when pure carbon dioxide was used under similar conditions and so they probably arise from a different species. This species is most likely to be a methane radiolysis product.

Nuclear graphite produced slightly different results. Although the deposit was still found, graphite attack was not so successfully inhibited at flake edges. An example of this can be seen in Plates

30A and B, which also received 4.1×10^{19} quanta. Only the central thin flake edges have been attacked and particularly the folded area which can expose both sides of the flake to the attacking species, and so it will be attacked faster. Widespread deposition was again found and the particle size on this sample was 92 ± 11Å. Particle distribution counts were made and they gave figures of 2.95×10^{11} per sq. cm. in the bulk of the material but 3.3×10^{11} at the flake edges. This edge increase can be attributed to the normal gasification and deposition which is also producing particles near the edge reaction sites and so increasing the number of particles at these areas. Since there is no evidence of deposit remaining at areas where graphite has been oxidised away, it is probable that migration of the deposit forming species had taken place as attack had commenced and these molecules had subsequently collected together to form a deposit behind the attack front. It is also possible that deposit was formed before attack and subsequent edge attack gasified deposit regions only at the most reactive sites which are likely to be at flake edges, which always have some carbon atoms unprotected by deposit. Plate 31 shows the same area as Plate 30B after an additional dose of 1.3×10^{19} quanta in pure carbon dioxide. The actual bulk surface deposit seems to have changed little and the attacking species attacks preferentially at the thin edges where some areas of graphite together with its deposit have disappeared. This is a good indication that a deposit protection

P L A T E S 29 A and B

Area of purified natural graphite before and after 4.1×10^{19} q.u. in the carbon dioxide, carbon monoxide, methane mixture at 25°C.

x 120,000

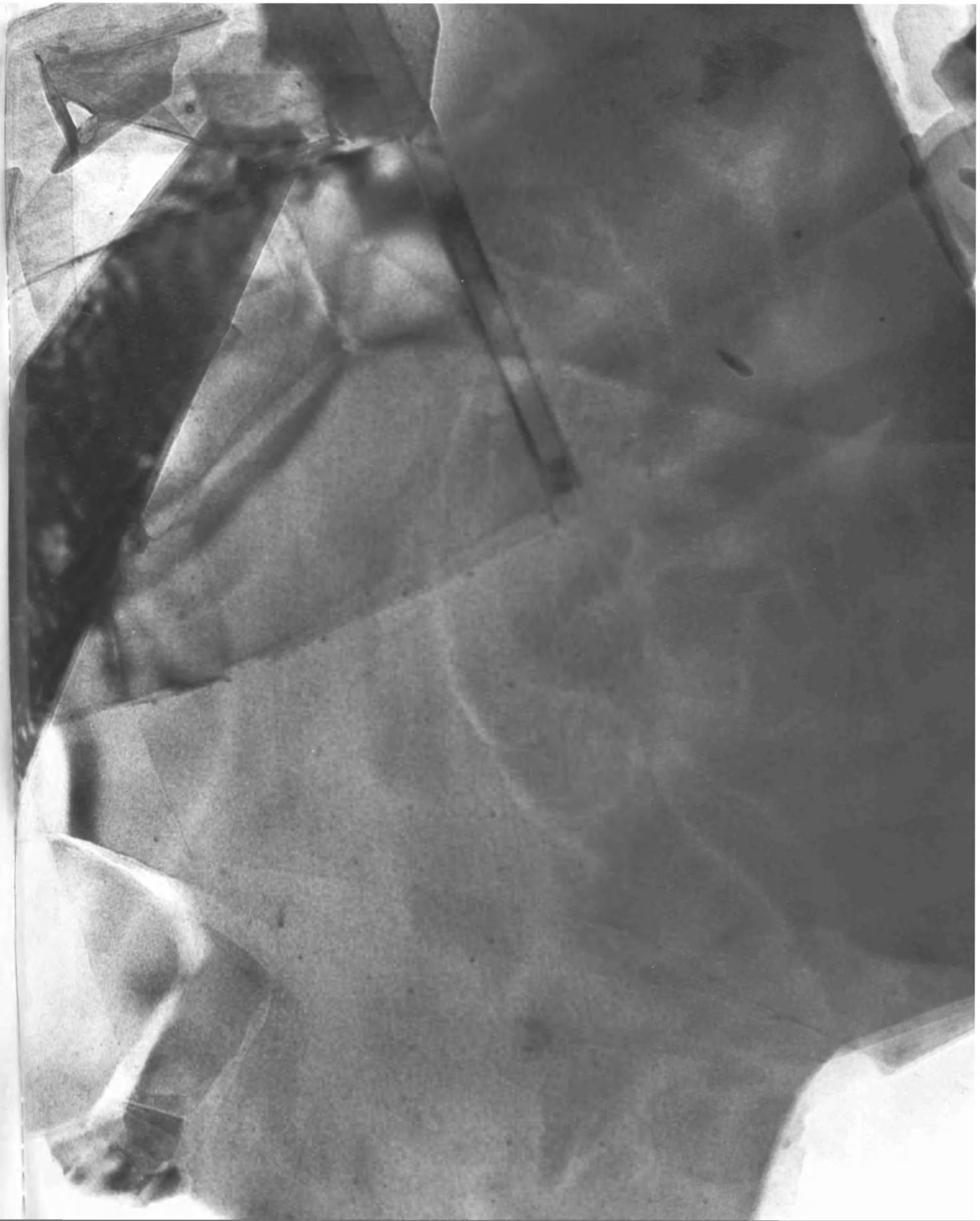

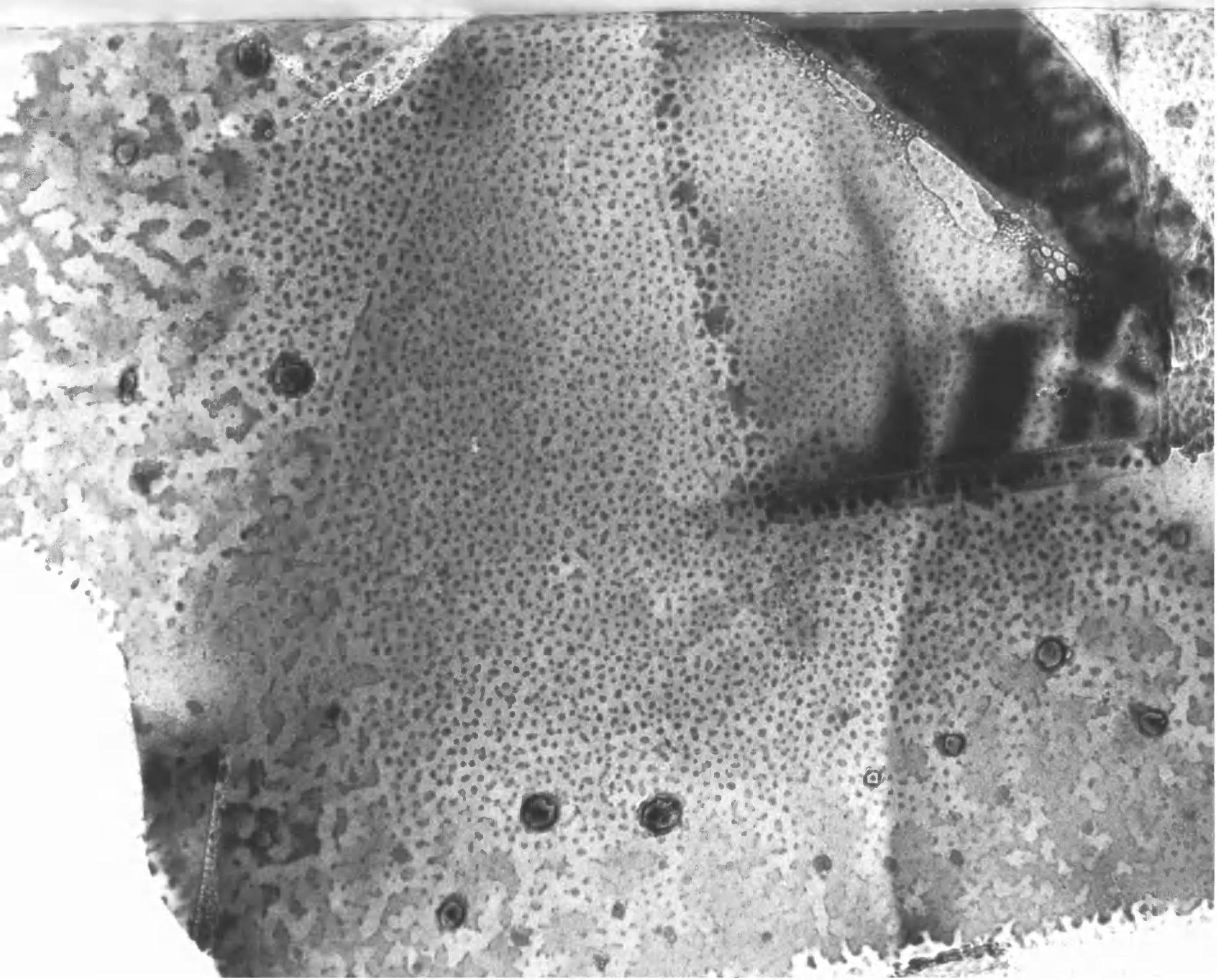

P L A T E S 30 A and B

Area of nuclear grade graphite before and after 4.1 x 10^{19} q.u. in the carbon dioxide, carbon monoxide, methane mixture at 25°C.

x 180,000

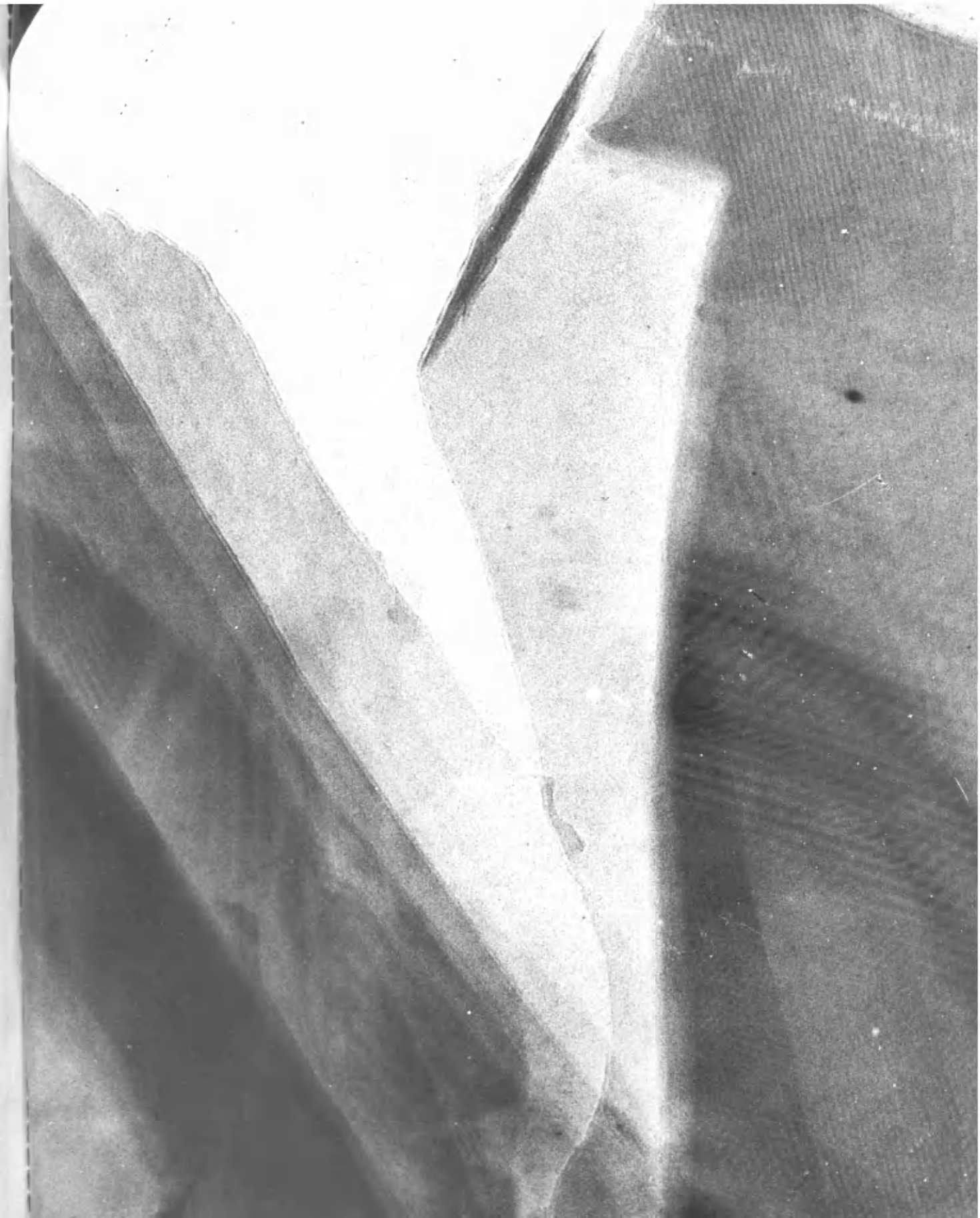

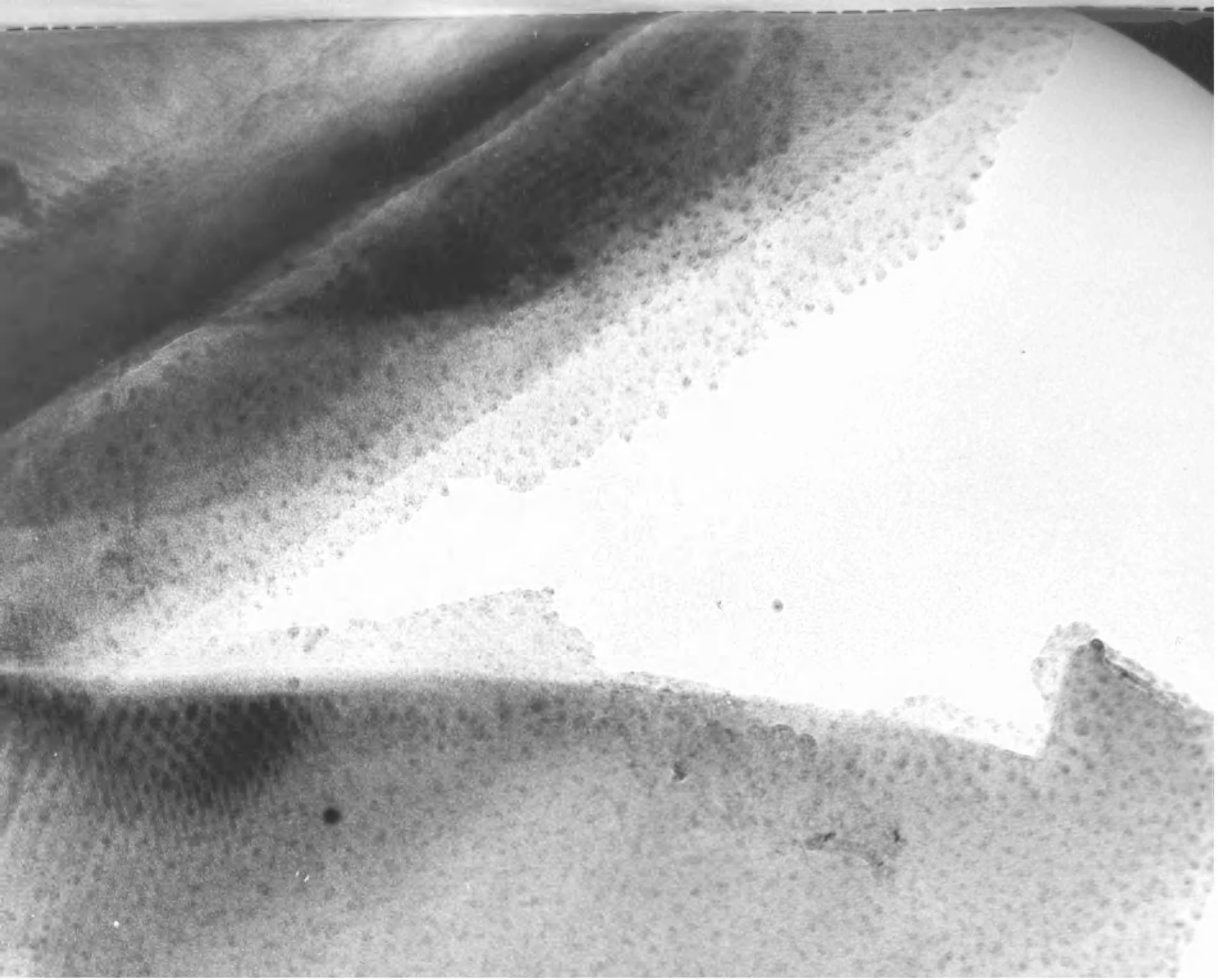

P L A T E 31

Same area as Plate 30 after an additional 1.3×10^{19} q.u. in carbon dioxide at $25^{\circ}C$. x 180,000

mechanism, has, under these conditions, less chance of success in edge attack than in perpendicular attack at active surface sites, since the latter can be completely covered while the former cannot.

Since it was suspected that the origin of the deposit was different with and without methane addition, two groups of experiments were set up to help to elucidate this point. The first run used a mixture of 1% carbon monoxide in carbon dioxide at a dose of 3.6×10^{19} quanta. Both graphites gave similar results and an area of natural graphite is used as an illustration in Plates 32A and B. The gasification reaction has only proceeded slightly at the flake edge at a dose where pure carbon dioxide has been found to give much more attack. The whole surface is covered by a deposit, and particle counts on a few samples gave a distribution of 7.4×10^{11} per sq. cm. The particle diameter was also measured and the mean value found was 56.1 ± 10Å. This shows very good agreement with the particle size found for pure carbon dioxide experiments and so it is a good indication that particles of this size arise from the radiolytic decomposition of carbon monoxide. It can also be deduced that the carbon monoxide must be rapidly adsorbed on the graphite surface at random sites before the attacking gas has sufficient energy content to form a species active enough to initiate gasification. As the carbon monoxide content on the surface increases, it would appear that polymerisation takes place and that a size around 56Å is the preferred

particle size. These particles then block most reaction sites, the exception being some partially covered edge sites. In attack by pure carbon dioxide, only at sites of carbon gasification will carbon monoxide be formed and be bonded nearby, and so form the polymer which could cover the sites of initial graphite oxidation.

A second experiment was carried out using .1% methane in carbon dioxide and again both graphites produced similar results which are illustrated by Plates 33A and B. This is an area of natural graphite before and after 4.3×10^{19} quanta in the above gas mixture. Slight attack has taken place at the main flake edge but gasification is more noticeable along the central crystallite boundary. A particulate material again covers the graphite surface and there were found to be an average of 2.5×10^{11} particles per sq. cm. Although this deposit tends to produce larger particles near the edges, the average size of the individual particles was found to be 95.4 ± 12Å which is in good agreement with the deposit size in the experiments using the methane, carbon monoxide, carbon dioxide mixture. It is therefore likely that the deposit produced in these two experiments is formed from a photolysis product of the decomposition of methane. This means that this product must be adsorbed on the graphite surface more readily than the carbon monoxide from carbon dioxide radiolysis or from the added gas itself, since a deposit, deduced from its size to be of methane origin, was found when both gases were used together.

Samples from this last experiment were shadowed subsequent to the deposition. Platinum-carbon was used and the angle of shadow was 25°. This was done in order to determine whether the particles were lying on the graphite surface, and to eliminate the possibility of the particles being in fact compounds of high electron density or centres of anomalous scattering in the material. The results are illustrated by Plates 34A and B which show an area of natural graphite before and after the above treatment. In Plate 34B, the shadow appears white since no metal has fallen on that area. Since this shadow is visible, it proves that the particulate material is lying on the graphite surface and from shadow length measurements, it can be concluded that the particles are approximately spherical.

Additional experiments were carried out using a mixture of 1% ketene in carbon dioxide to study its inhibition effects. A dose of 3.6×10^{19} quanta produced similar results for both grades of graphite and Plates 35A and B illustrate a nuclear graphite sample. There is no visible sign of graphite attack at any point and no deposition was seen on any sample. This would imply that a photolysis product of ketene was adsorbed on the surface and blocked reaction sites without visible polymerisation and deposit appearance. Any such species seemed to affect the background as these samples were the only ones examined where any change in the silica film was noticed.

Because of the relatively short time needed for reaction in the

P L A T E S 32 A and B

Area of purified natural graphite before and after 3.6×10^{19} q.u. in a carbon dioxide, carbon monoxide mixture at 25°C. x 120,000

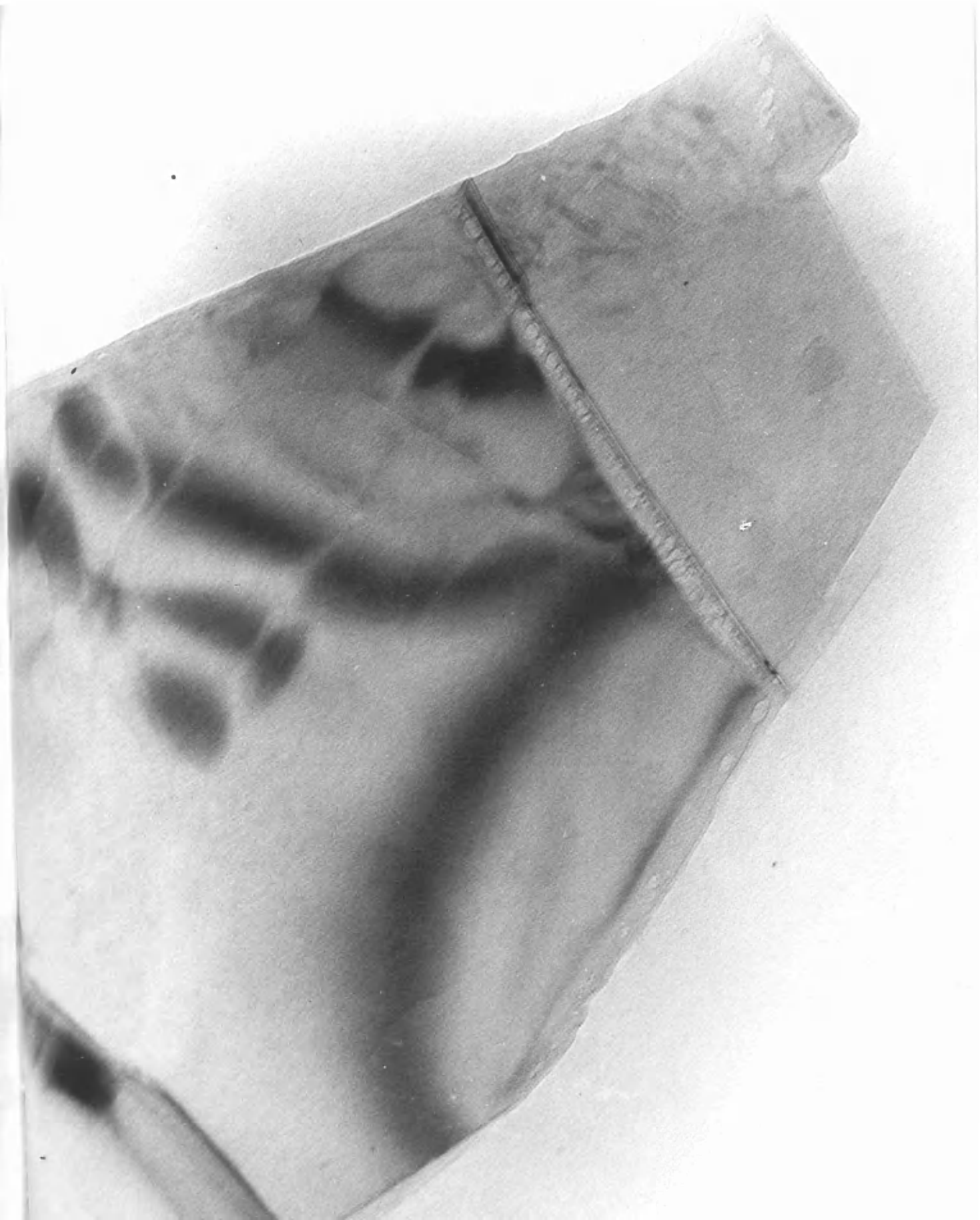

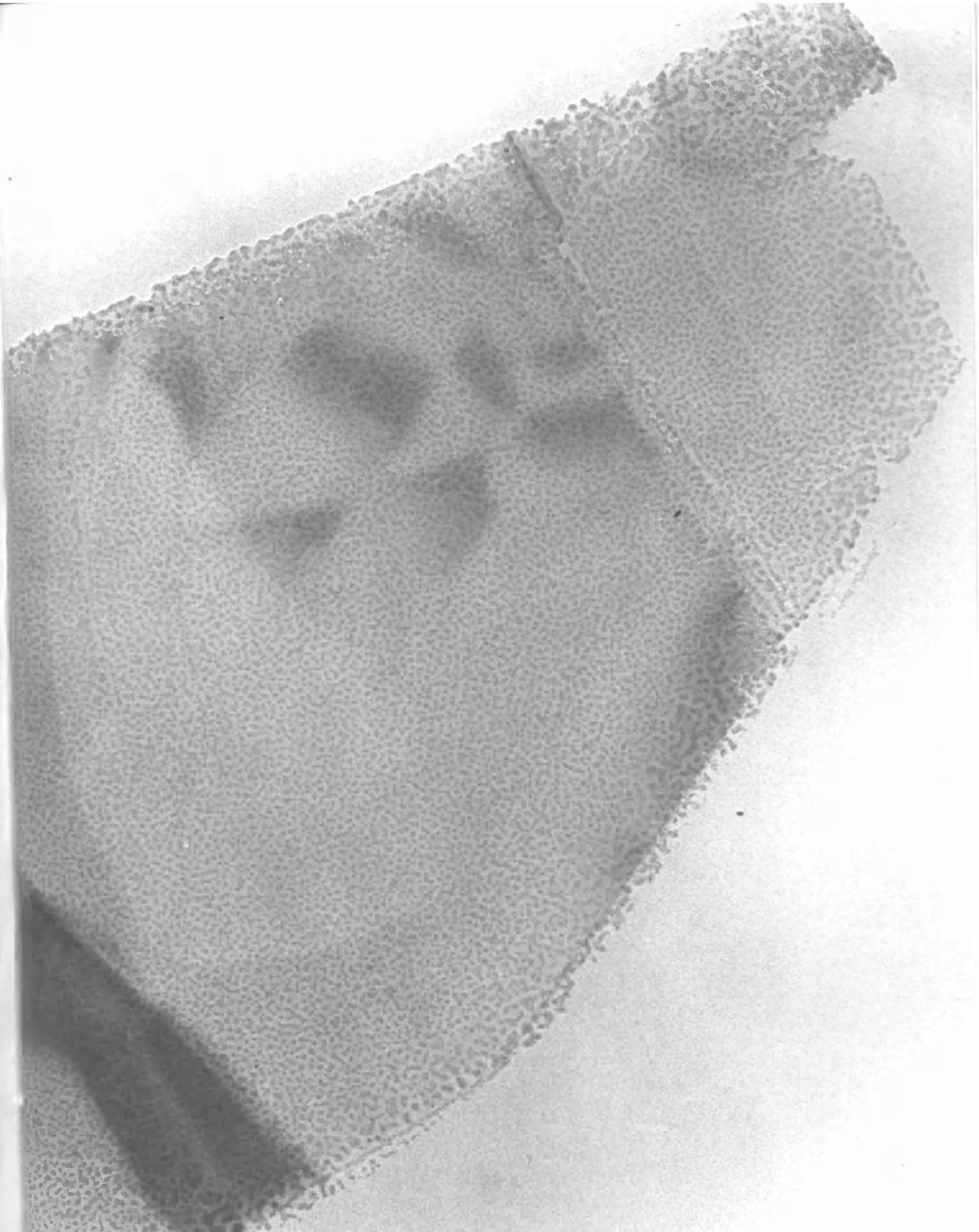

PLATES 33 A and B

Area of purified natural graphite before and after 4.3×10^{19} q.u. in a carbon dioxide, methane mixture at $25^{\circ}C$. x 120,000

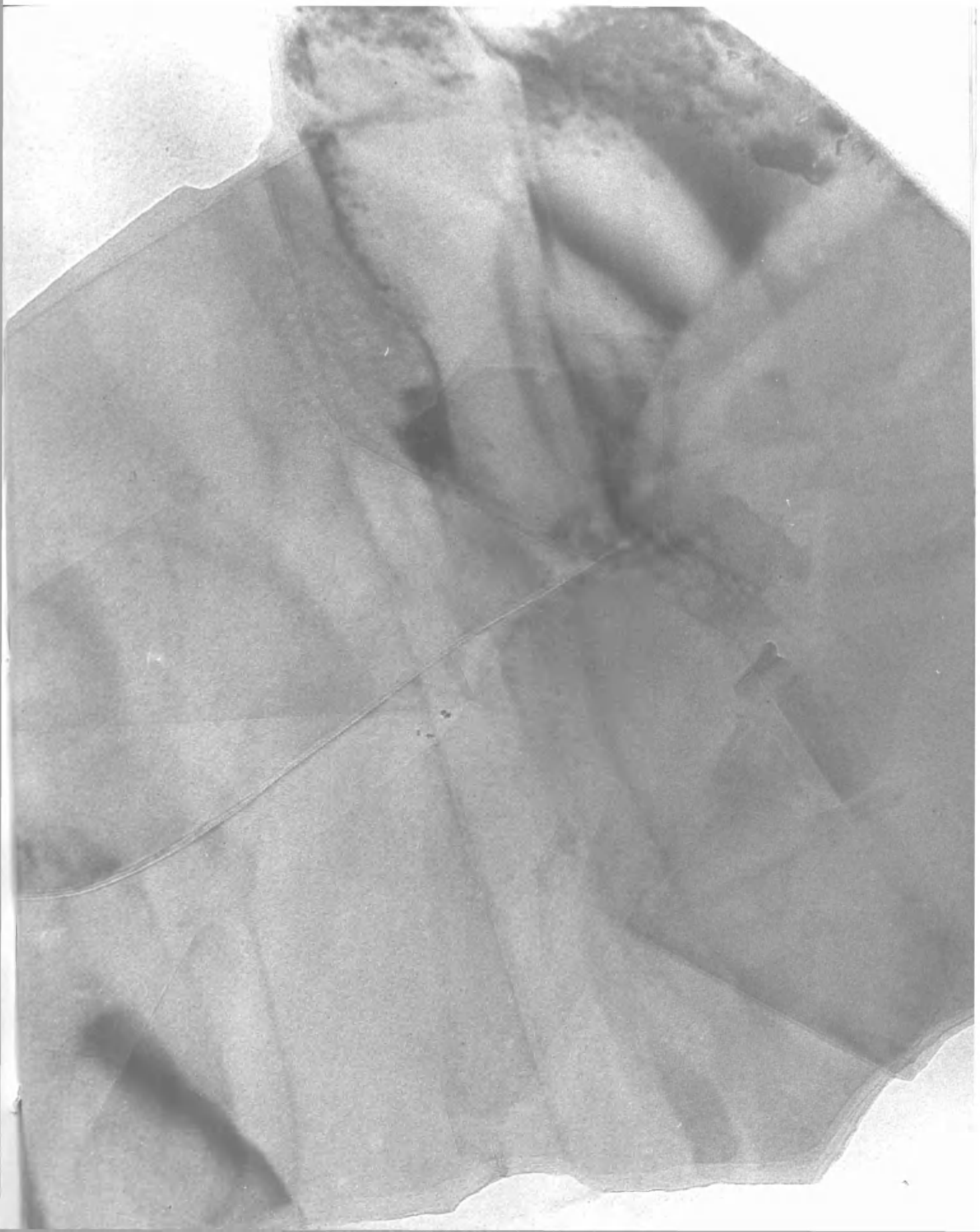

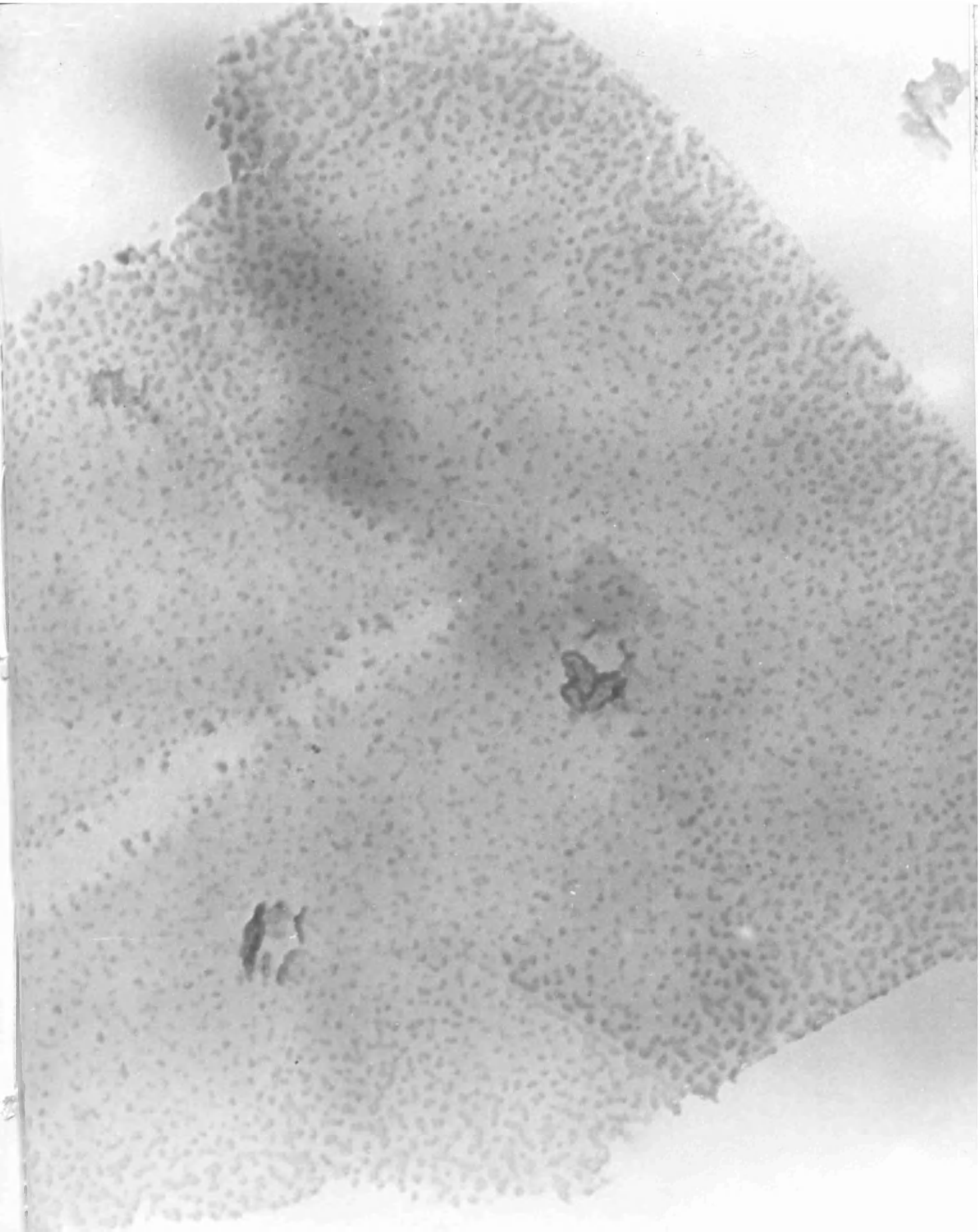

P L A T E 34 A

Area of purified natural graphite after 4.3×10^{19} q.u. in a carbon dioxide, methane mixture at 25°C. x 90,000

P L A T E 34 B

Same area after platinum - carbon shadowing at 25° x 90,000

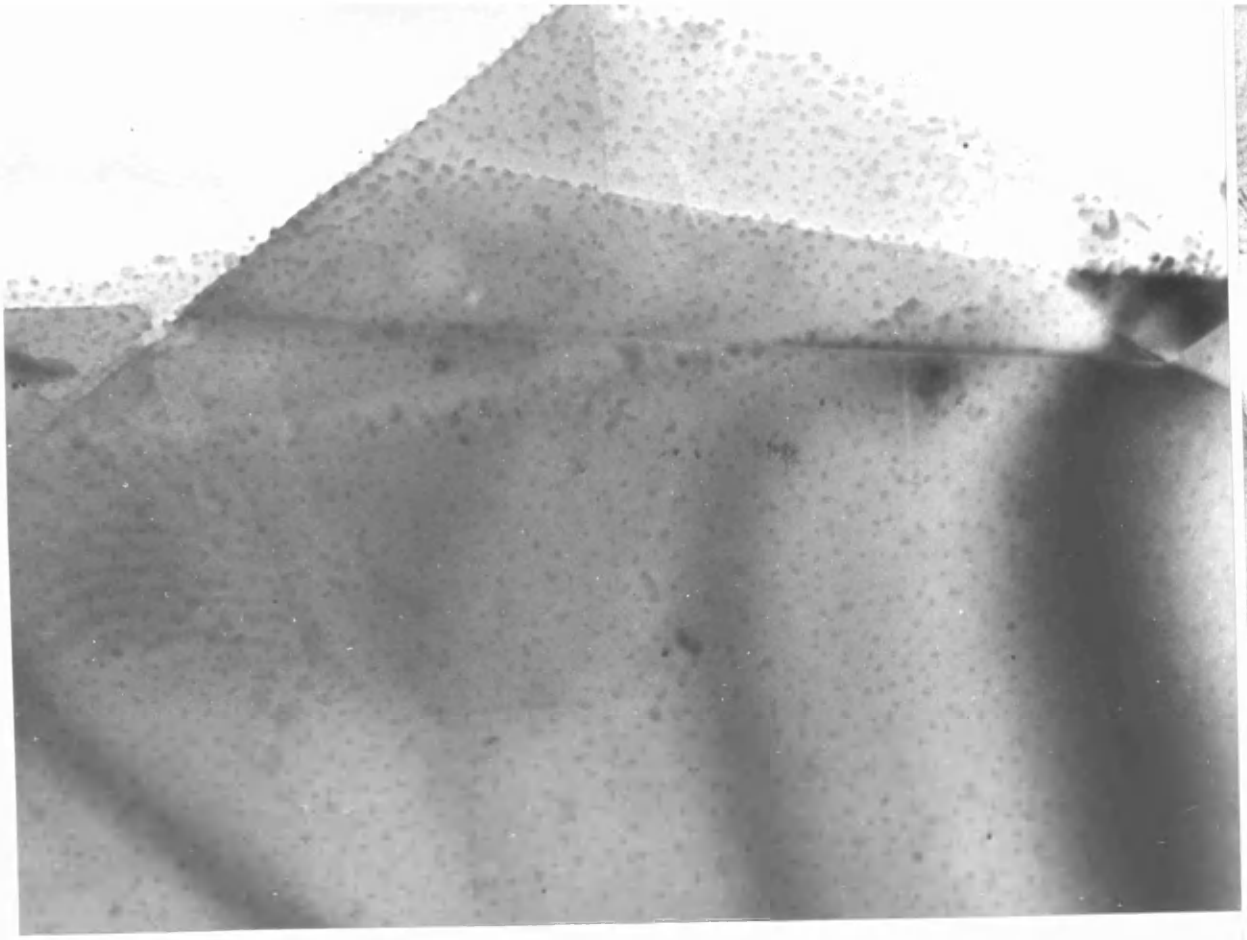

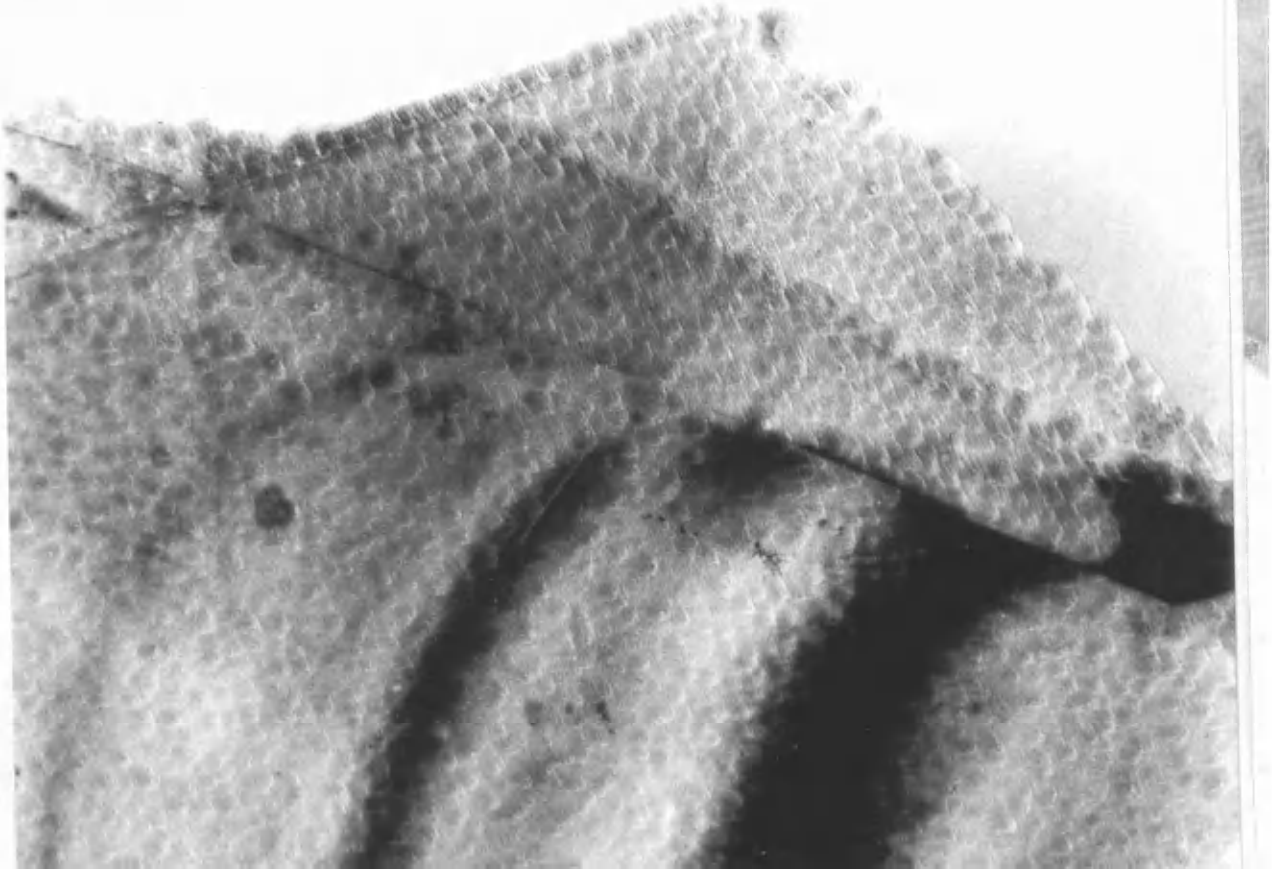

P L A T E S 35 A and B

Area of nuclear grade graphite before and after 3.6×10^{19} q.u. in a carbon dioxide, ketene mixture at $25^{\circ}C$. x 90,000

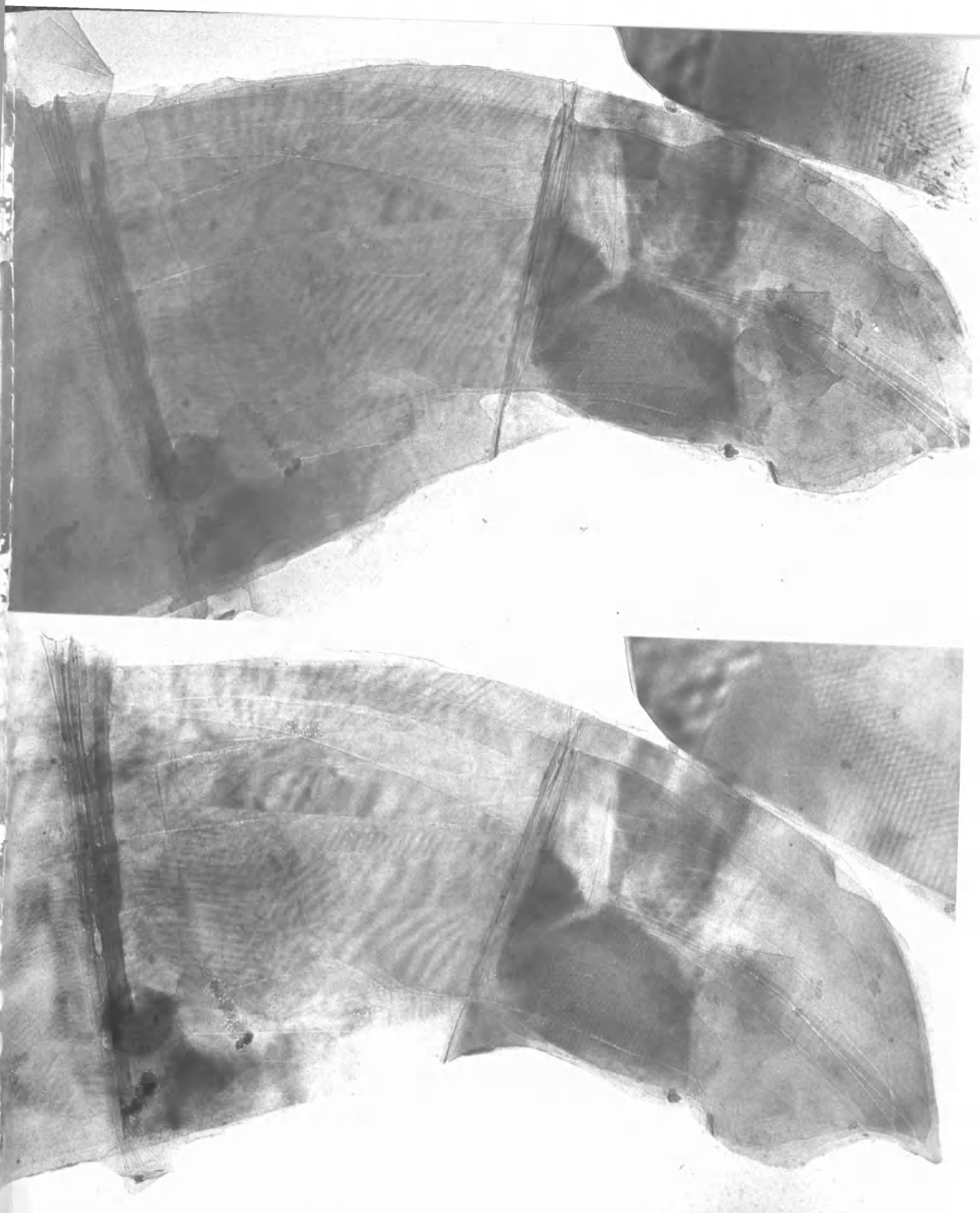

vacuum ultra violet system, additional experiments were performed to try to assess the effects, if any, of the preparation techniques. Samples of graphite were prepared using only dry powdered material so avoiding the use of ultrasonic treatment and water suspension. After reaction in carbon dioxide, these samples showed effects identical to those reported beforehand and this illustrates that the specimen preparation does not affect reaction under these conditions. Similarly, specimens were prepared which had no initial electron bombardment in the microscope, and they also showed no reaction differences. This indicates that the exposure to electrons does not alter the characteristics of attack. This would be expected since any particular area is subjected to the main beam for less than 30 seconds which would allow sufficient time for focussing and photography.

It was also possible by this apparatus to collect a sample of the gas after passing through the reaction zone. This could be analysed by gas chromatography, and a check could be kept for any gaseous impurity as well as analysing the gas products. A typical analysis on the gas from the mixture 1% methane in carbon dioxide showed that approximately 250v.p.m. of carbon monoxide was produced, presumably from the slight carbon gasification, as well as 80v.p.m. of oxygen, probably due to the collision of oxygen atoms at an inactive surface such as the vessel walls.

(d) Irradiation in Inhibition Mixtures at High Temperature

At a temperature of 350°C. and a dose of 1.7×10^{19} quanta in the methane, carbon monoxide, carbon dioxide mixture, the result was still complete inhibition of gasification with no evidence of deposition. When a dose of 2.3×10^{19} quanta was tried, the results showed great contrast to the low temperature experiments but some similarity to the high temperature irradiations in pure carbon dioxide.

An area of natural graphite is illustrated by Plates 36A and B. The oxidation is typical of attack perpendicular to the basal plane and the deposit at this temperature appeared as clusters. This is likely to be due to migration of the deposit forming species at this elevated temperature, followed by collection of the species and polymerisation at certain collecting sites. This micrograph demonstrates how the perpendicular attack has been random over the whole (0001) surface, even between deposit clusters. The bulk of the deposit has a liquid-like appearance but where the graphite has been completely removed around it, the deposit seems to have 'dried out' and solidified to a smaller bulk. This resembles deposit areas on samples after pure carbon dioxide attack. Once again areas which appear to be islands of deposit gave the electron diffraction pattern of graphite, and therefore it is probable that these areas are covering some graphite layers and preventing complete gasification of them.

From this area, it can be seen that thin flake areas have been completely penetrated while thick areas have not. This can also be

seen in Plate 37, which is a nuclear graphite sample reacted alongside the above natural graphite sample. Attack can be seen at flake edges but there is little difference at the bulk of the surface. This could be due to its thickness and also to the increased deposit protection. Nuclear grade graphite was found to have many more areas of deposit, which, although smaller, covered a greater amount of surface and so gave greater protection. Since nuclear graphite has a greater number of deposit collection sites, this can be related to the extra defect content of the surface. It is possible that the surface will behave towards the deposit forming species in the same way as it does towards evaporated metal, which, after heating, can produce mobile particles. These can migrate over the surface and their motion will only be halted by defect regions in the surface. The evidence for this behaviour by deposit species is that natural graphite has less defects and therefore less collecting centres than nuclear graphite. The natural graphite will therefore have more, larger deposit free areas available for the random attack, and so exhibit more oxidation, and this observation has been made.

These last two sets of micrographs represent the extreme cases of both graphite samples, but there are many examples where attack gives an almost identical picture for both materials. Plates 38A and B show an area of nuclear graphite after the same reaction conditions. There has been a great deal of deposit clustering, particularly along

edges of surface flakes seen on the original untreated area. Attack perpendicular to the surface has proceeded between these areas, and at very thin regions complete penetration of the flake has occurred. Plates 39A and B show an area of natural graphite also after the above treatment. After reaction the sample does not contain as much deposit as the nuclear sample and in general more surface attack has taken place. The thin flake edge shows the complete attack. Deposit seems more prominent at its former edge where any collection at defect sites would be expected. As the random basal plane attack proceeded, the deposit at the edge could remain to protect those sites, while the graphite in the bulk of that flake was gasified. The remainder of the flake shows areas where attack has penetrated the surface. On close examination of the deposit on this sample, it can be seen that some particles appear to have moiré patterns associated with them. Also most particles appear to have dense centres with a less dense periphery. It was thought that this was an accumulation of contamination on the dense particles and by leaving the specimen exposed to the atmosphere for a few days and then rephotographing the same area, this was proved. This is shown by Plate 40. Since the magnification is the same as Plate 39B, it can be concluded that the obvious increase in particle size must be due to contamination which had accumulated round each particle. This would probably be some form of carbonaceous atmospheric component. Also this plate shows much more moiré pattern

associated with particles and so it can be deduced that these deposits are giving a magnified image of the moiré pattern of underlying graphite.

Since samples of both graphites have been shown to produce relatively equal attack and gasification, the penetration of any flake will depend largely on its thickness for this type of random perpendicular attack and the extent of the complete penetration will depend on the area of surface not protected by deposit.

P L A T E S 36 A and B

Area of purified natural graphite before and after 2.3 x 10^{19} q.u. in the carbon dioxide, carbon monoxide, methane mixture at 350°C.

x 120,000

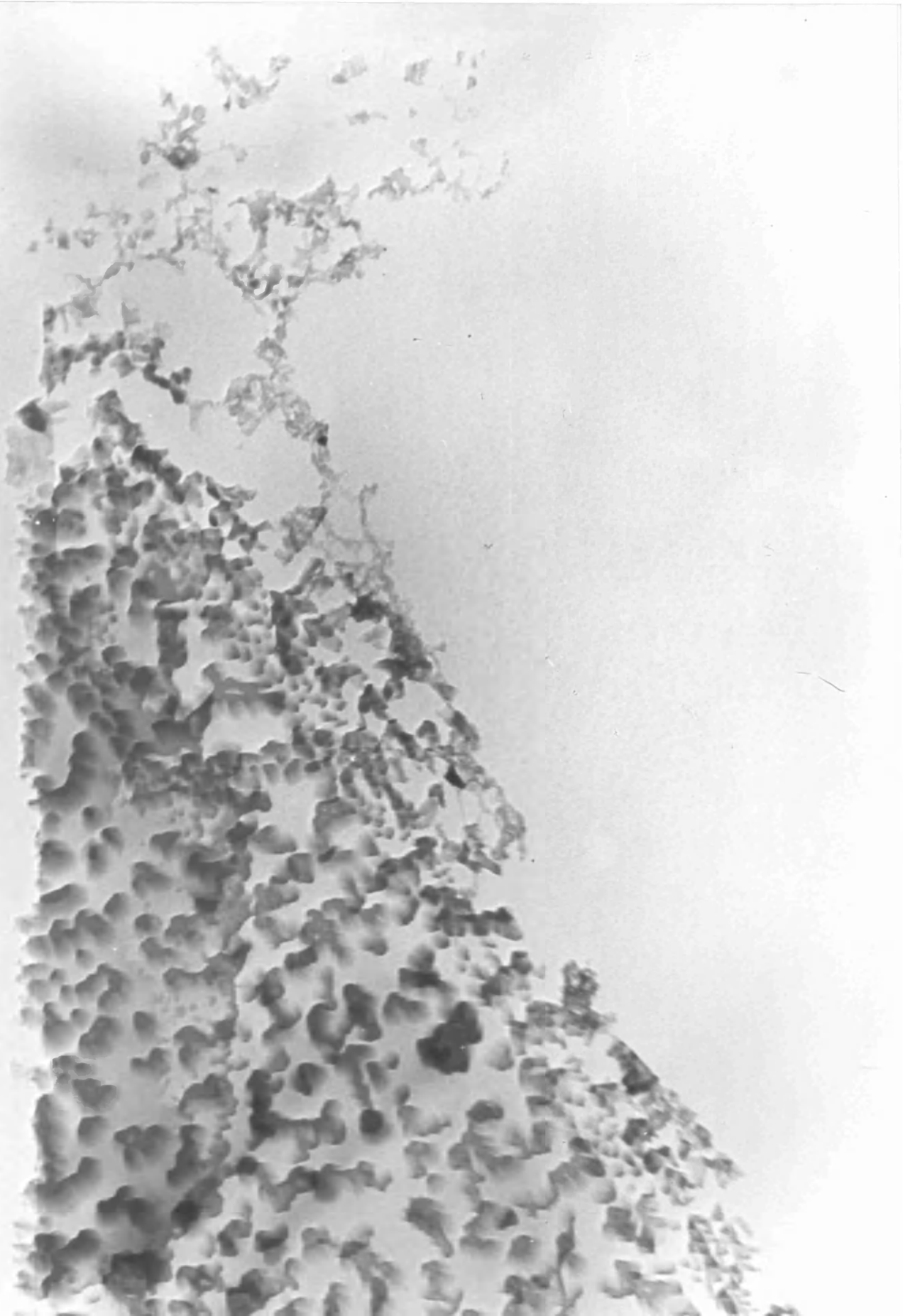

PLATE 37

Area of nuclear grade graphite after 2.3×10^{19} q.u. in the carbon dioxide, carbon monoxide, methane mixture at 350°C. x 120,000

P L A T E S 38 A and B

Area of nuclear grade graphite before and after 2.3 x 10^{19} q.u. in the carbon dioxide, carbon monoxide, methane mixture at 350°C.

x 120,000

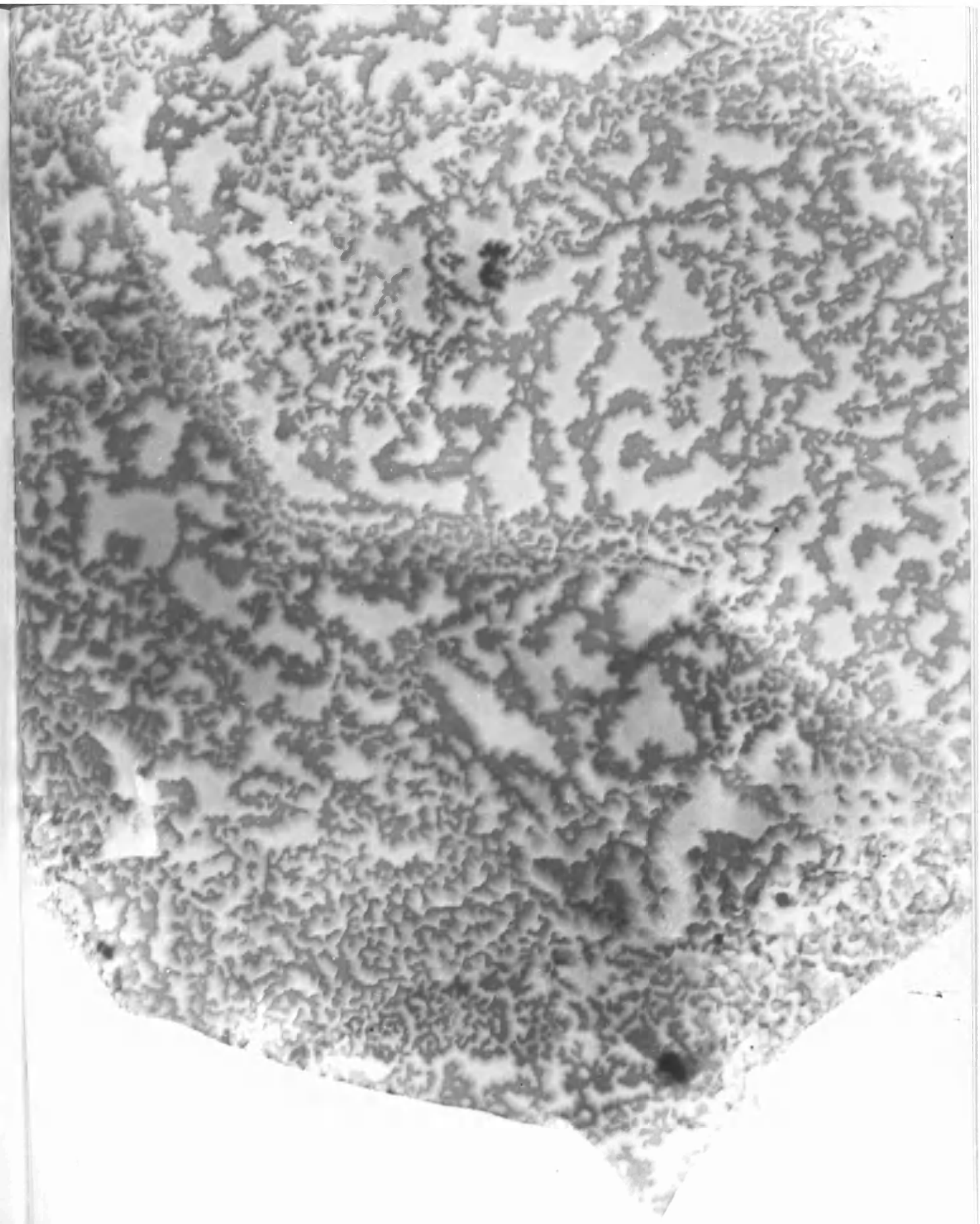

P L A T E S 39 A and B

Area of purified natural graphite before and after 2.3 x 10^{19} q.u. in the carbon dioxide, carbon monoxide, methane mixture at 350°C.

x 120,000

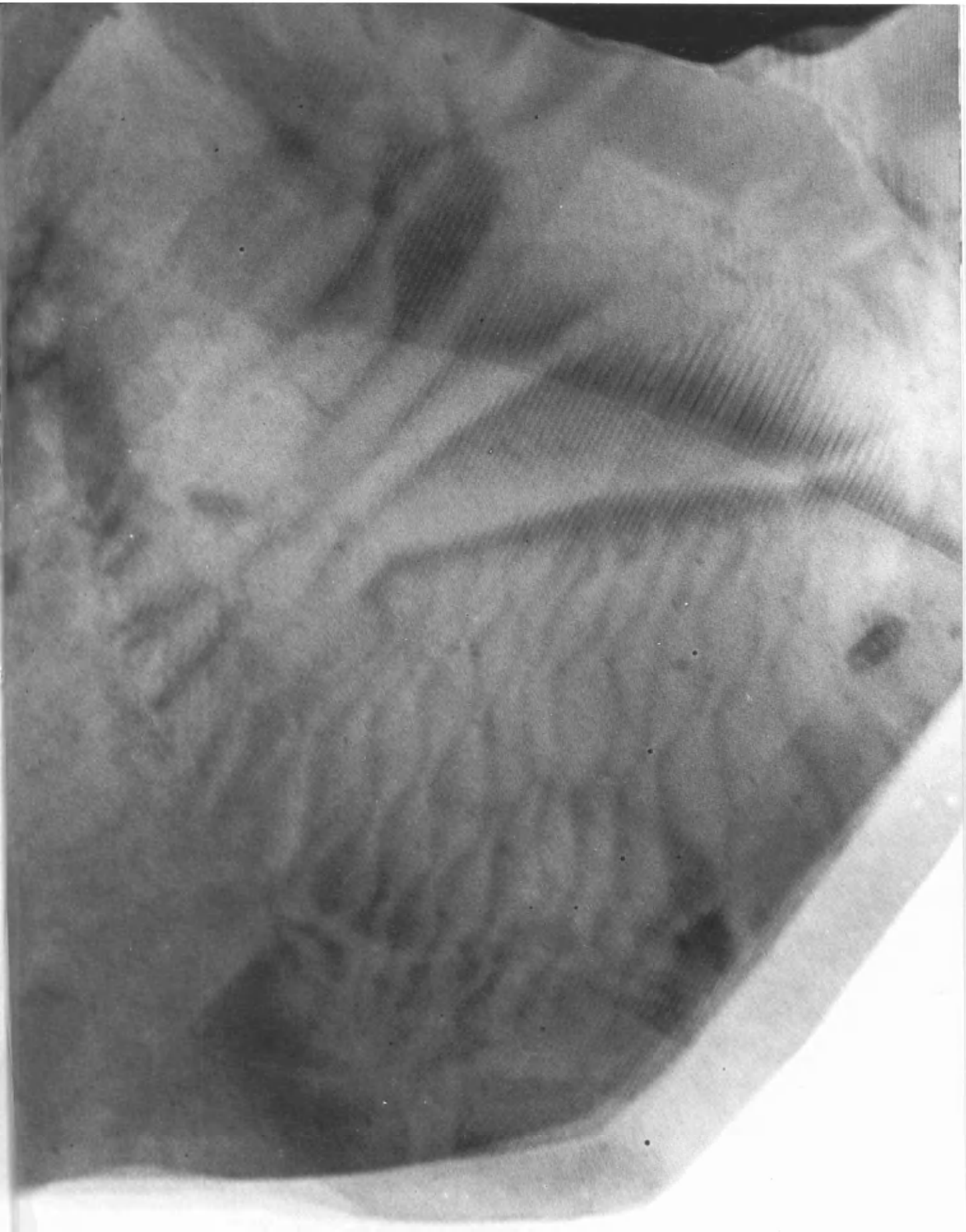

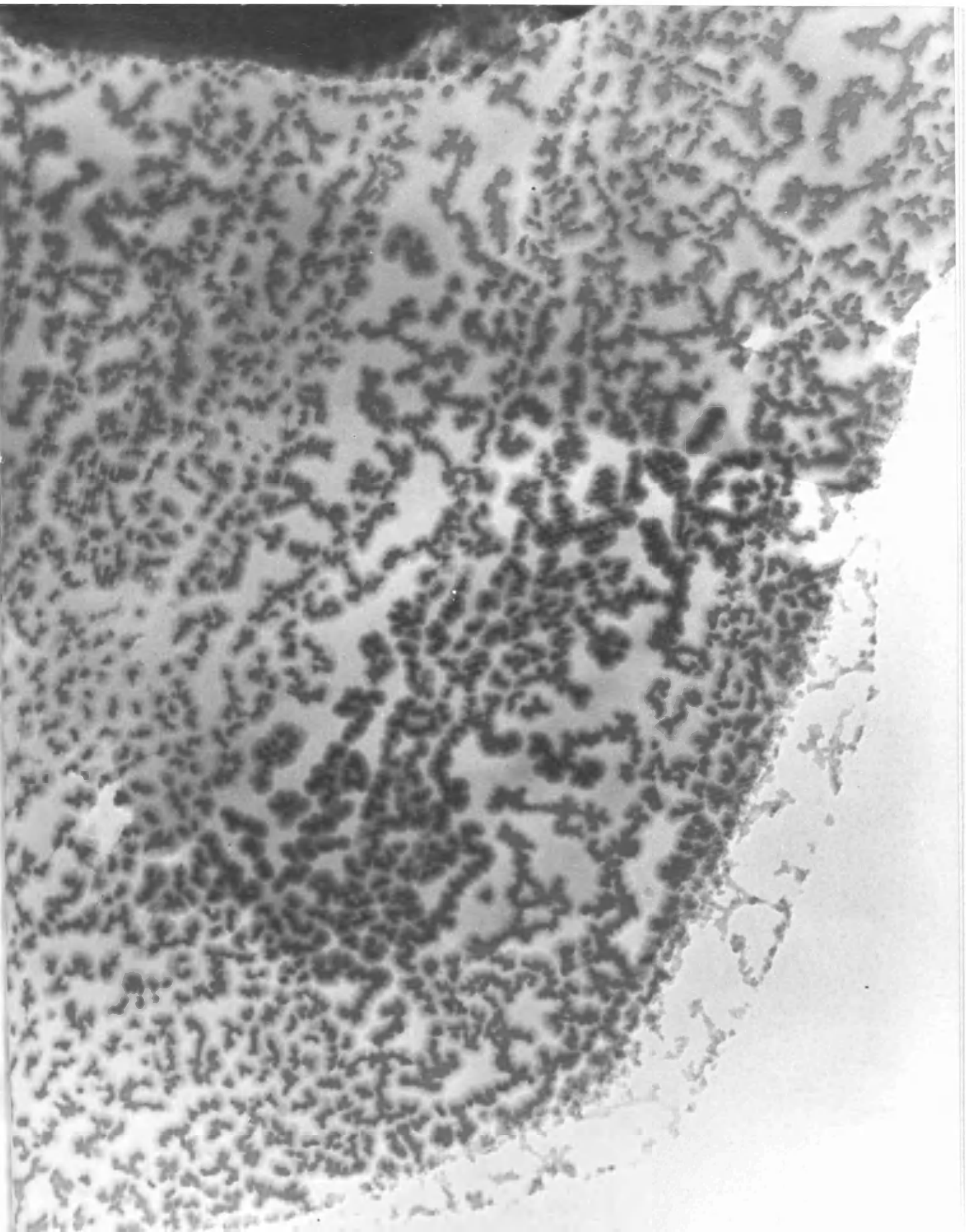

PLATE 40

Same area as Plate 39 after exposure to the atmosphere for one week. x 120,000

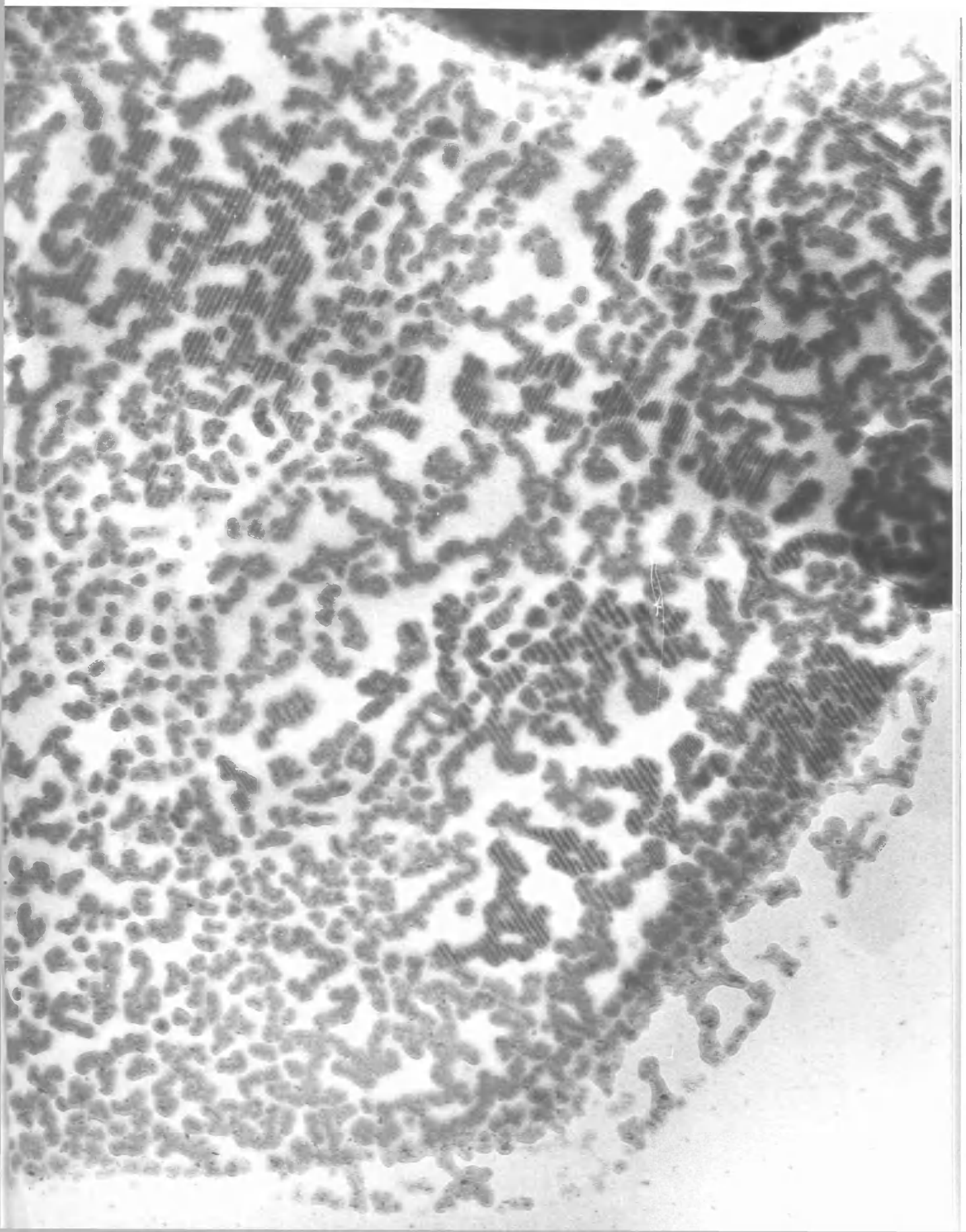

4. Experiments Using Gamma Irradiation

Samples of both graphites were irradiated in a gamma flux of up to 1000 M. Rad at 300°C. in pure carbon dioxide in a static gas system at atmospheric pressure.

Initial exposures of 2 weeks (approximately 350 M. Rad) produced no signs of reaction. After 5 weeks (1000 M. Rad), still no gasification was observed. Since 1 Rad = 6.25×10^{13} ev/gm., this corresponds to 4.6×10^{-9} ev/molecule of carbon dioxide. At 1000 M. Rad, the dose rate is therefore 4.6 ev/mol. This figure is comparable to the dose rate received by the gas in the BEPO reactor irradiation samples where very little attack was found in a static system at that dose, but substantial gasification was obtained using a gas flow system. The results of the gamma flux experiments can therefore also be explained by the build up of carbon monoxide around the sample and this will inhibit reaction either by recombining with any active oxygen present, or else by adsorbing on the surface active sites and blocking them.

In order to confirm the similarity with the BEPO experiments and to initiate reaction, specimens with a higher than usual impurity and defect content were prepared as described for the case of neutron irradiation. Gold particles were again used as impurity on the graphites and two samples of nuclear graphite, pre-irradiated in a neutron flux to produce defects, were also used. The same conditions were applied at a dose of 1000 M. Rad. It was not considered advisable

to increase this dose since the extra time required for reaction would increase the contamination of the specimens, some areas of which were appreciably contaminated after the 5 week experimental run.

When the impurity doped specimens were re-examined, attack had been catalysed and oxidation features were visible under the same conditions where lack of impurity produced no graphite attack. The features of carbon gasification were identical to those observed in the BEPO reactor experiments although attack was slower, due to the difference between the flow and static systems. An area of natural graphite is illustrated by Plate 41. The original small gold particles have undergone some migration to form larger particles which again are only active when they are in contact with active sites. This is illustrated by the fact that the gold particle at the flake edge, which is a normal active site, was found to have catalysed carbon gasification in its path. Also a gold particle on the flake surface, which does not usually provide active sites in natural graphite, showed no activity and no carbon removal associated with it. Nuclear graphite samples were not much different from the natural graphite since most attack occurred at flake edges and little occurred at surface sites, probably due to the limited oxidative attack under the static conditions.

Examination of the samples with increased defect content showed that the nuclear graphite with the higher pre-irradiation dose

(4×10^{20} n/cm^2) showed more of the features of attack. This is illustrated by Plate 42. The pattern of attack again resembles that found after the corresponding BEPO reactor experiment, although the reactivity has been reduced. This illustrates that radiation induced vacancies can act as oxidation centres.

From these results, it can be concluded that the graphite-carbon dioxide reaction will be identical under gamma and neutron irradiation, where the dose rates are approximately equal. Since the dose rate is low compared with the other radiation systems, this is again the likely reason for the absence of deposited material after the gamma irradiations, even although a closed system favours carbon monoxide build up, which would be expected to favour polymerisation.

P L A T E 41

Area of purified natural graphite with gold catalyst after 1000 M. Rad. in carbon dioxide at 300°C. in TIG pond.

x 165,000

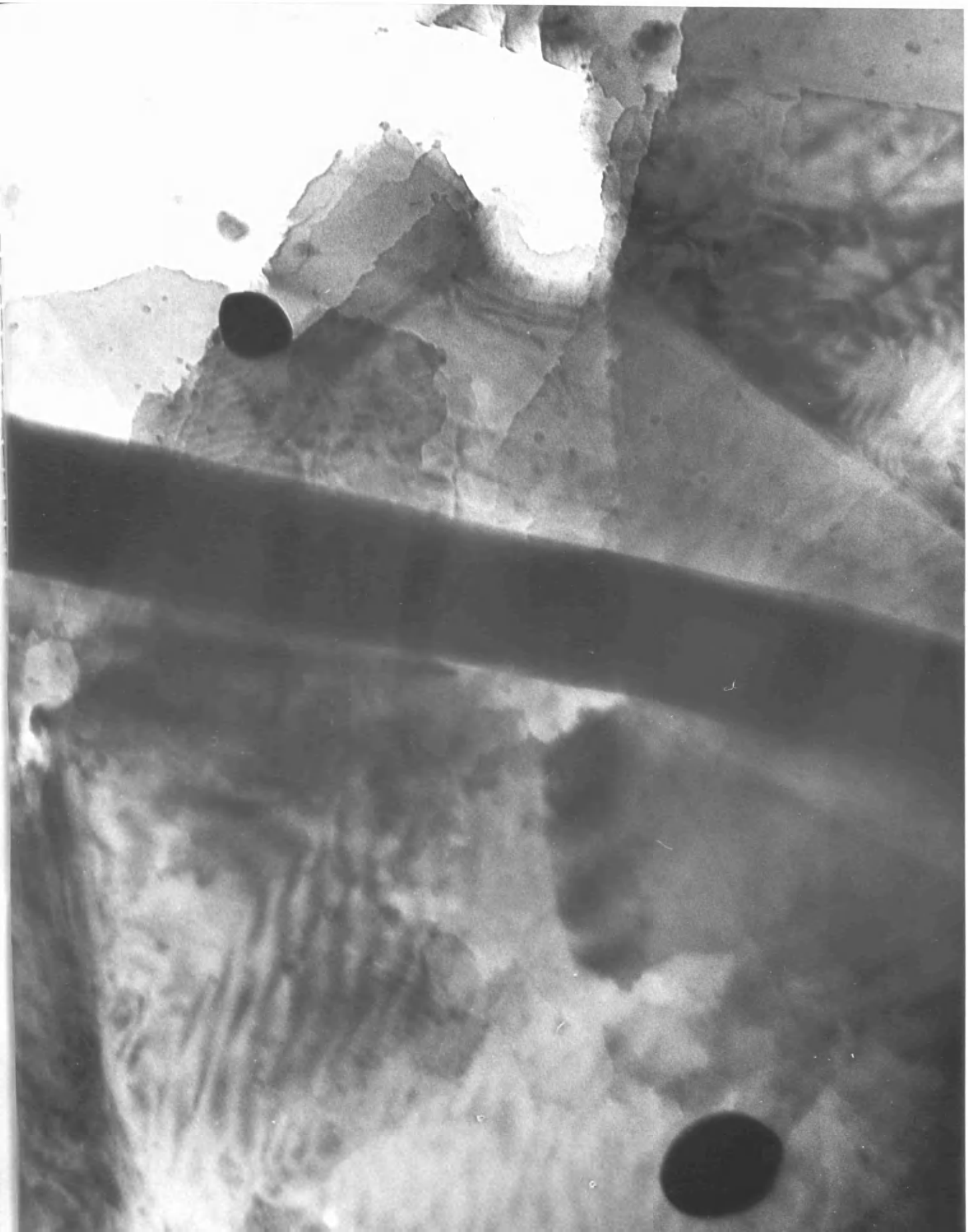

P L A T E 42

Area of nuclear grade graphite, pre-irradiated to 4×10^{20} n/cm^2, after 1000 M. Rad. in carbon dioxide at 300°C. in TIG pond.

x 190,000

5. Decoration Experiments

(a) Untreated Samples

Specimens of both graphites were decorated with silver at 300°C. to give a standard check for later experiments. On all areas migration of the thin metal film to produce small silver particles over the mounts was produced. The background film retained the metal in small closely spaced, evenly distributed particles whereas greated mobility of the metal had taken place on the surface of graphite.

An area of purified natural graphite is illustrated by Plate 43. The graphite area has been decorated at flake edges and other surface sites and many substantial metal-free regions are seen. According to Hennig (1964), metal is likely to be found at surface steps, dislocations, impurity sites and point defects. An important point on this and other micrographs is the size of the surface particles. If migration had taken place and particles were halted by any of the above sites, it would be expected that around any clear graphite area, large particles would be found and in the centre of areas of large particle density, small particles would be seen. This is not observed and from the micrographs examined, there was a reasonable consistency in particle size. This is a good indication that metal must be continually mobile between particles so that those at the centres and perimeters of dense regions appear to be of uniform size. Particle distribution counts were made over this and other areas and the result was that there were

$.95 \times 10^{11}$ particles per sq. cm. on the graphite and 5.05×10^{11} on the background film.

The particle counts were found to vary with the experimental conditions, in particular the weight of metal used, the time and temperature of heating to induce mobility, and the condition of the graphite surface. The first three points could be reasonably controlled by careful experimental work. Since it is known that any substance absorbed on the graphite surface could reduce mobility and thus increase the particle number, most specimens were heated to a higher temperature, usually 350°C., for a few minutes and then cooled to the normal decoration temperature. Counts were also found to vary with the condition of the graphite. The above count figure was for natural graphite powder, but graphite scraped from a pellet of the same substance after compression gave an increased count and therefore must contain more defect centres. By annealing the pellet to 3000°C. in vacuum, these extra defects must have been removed because the particle counts returned to normal. Also specimens after oxidation were found to give increased counts and therefore extra metal collecting sites must have been produced. These were particularly noticeable at step edges.

Samples of nuclear grade material were also examined and a typical area is shown in Plate 44. These samples showed a lesser degree of metal alignment and decoration, and this can be attributed to the greater defect and impurity content of this material. These

P L A T E 43

Standard area of purified natural graphite after normal silver decoration at 300°C. x 120,000

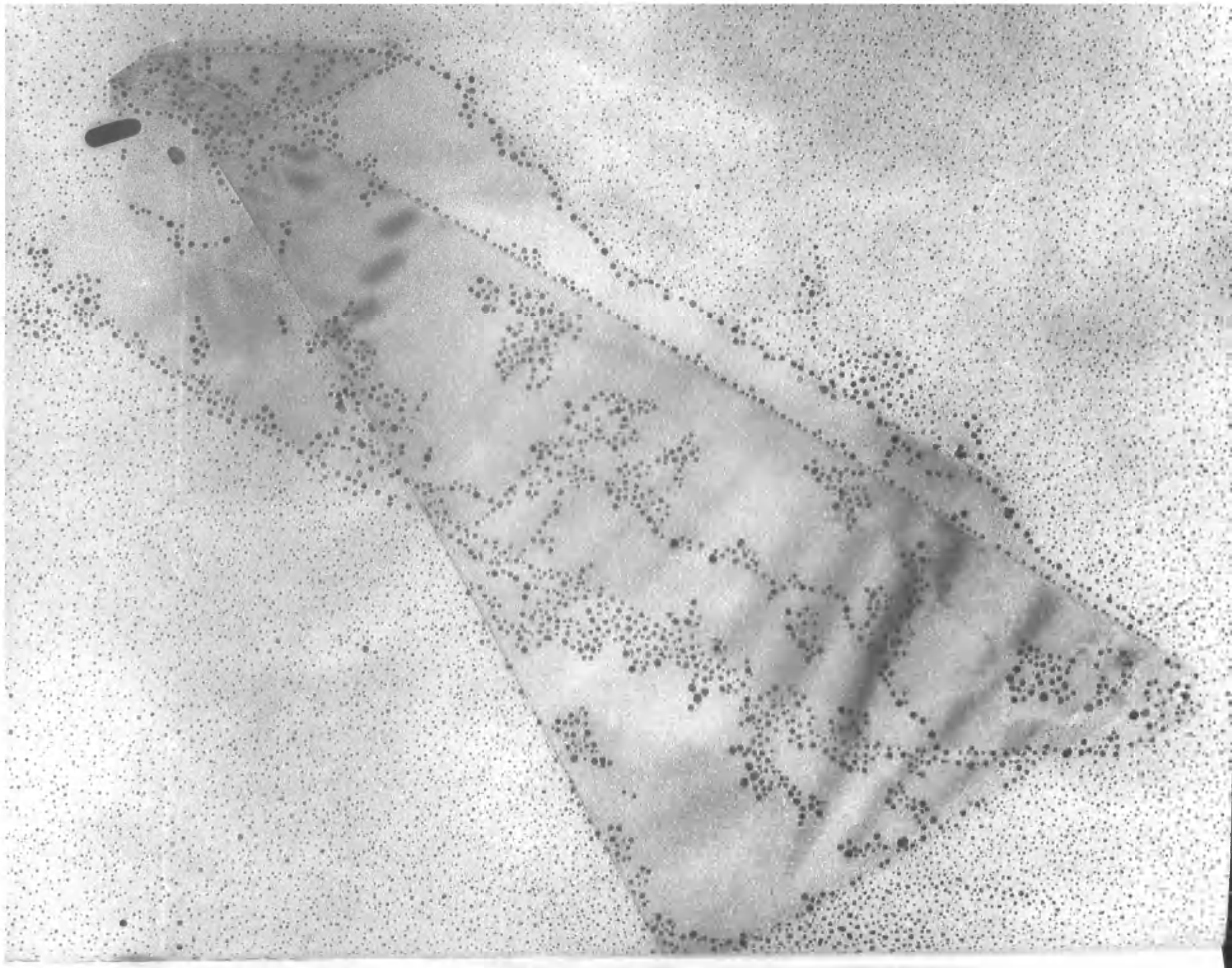

P L A T E 44

Standard area of nuclear grade graphite after normal silver decoration at 300°C. x 120,000

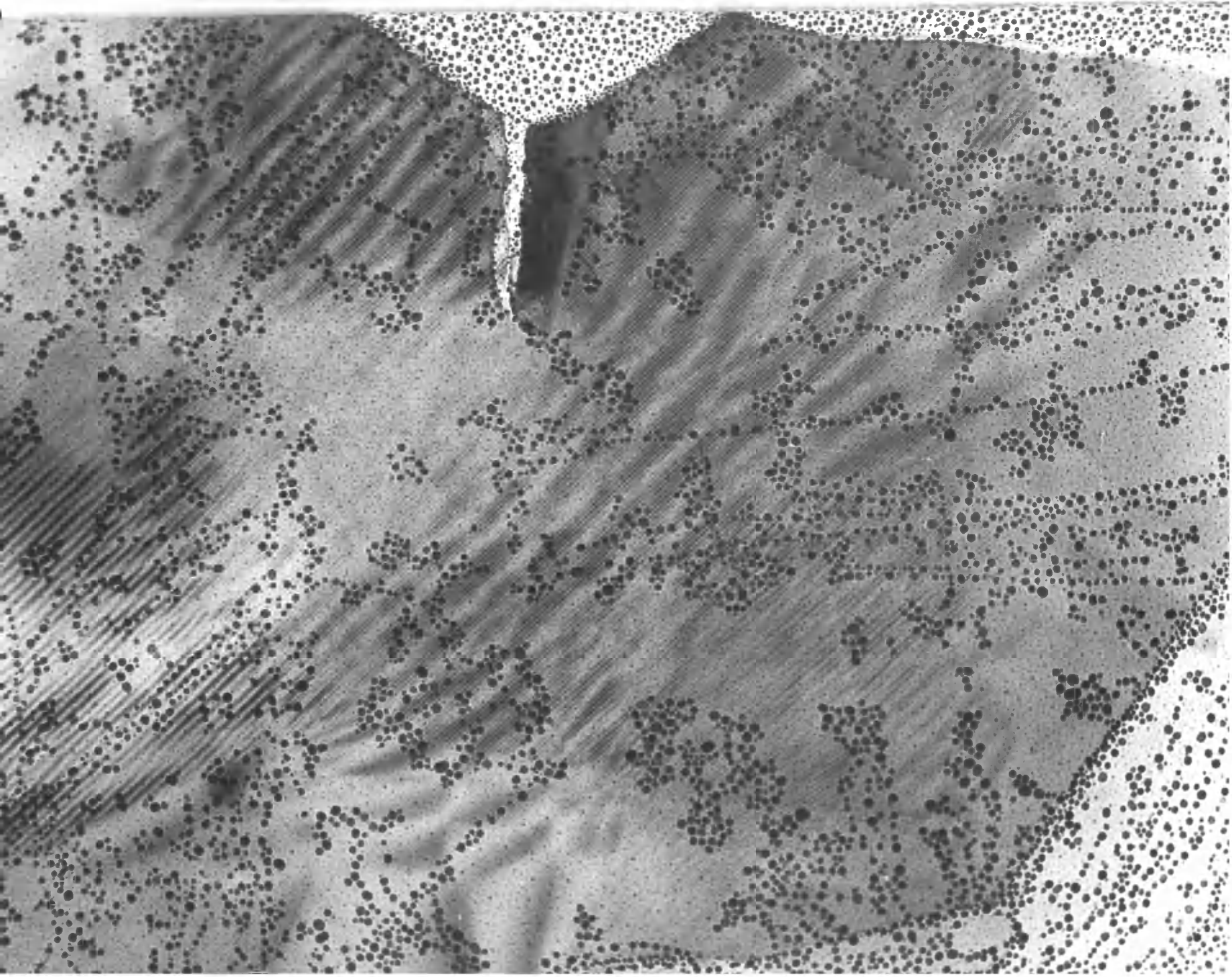

extra sites could provide more collecting points for metal and so increase the count numbers. The mean figures for typical specimens are 1.68×10^{11} particles per sq. cm. on the graphite with 5.1×10^{11} on the background.

At this point it is convenient to introduce a quantity to be referred to as the decoration percentage. This is defined as the number of particles on the graphite, divided by the number on the background, multiplied by 100. Since the background film received the same amount of metal and is under similar conditions to the graphite it can be used in this way as a standard to compare different experimental results. The standard decoration percentage of natural graphite was found to be 18% while that of nuclear graphite was 33%.

(b) Irradiated Samples

In this section, results of decoration experiments will be described where samples had been subjected to radiation conditions without showing attack, and then decorated.

Samples from the proton beam and vacuum ultra violet experiments were usually found to give no decoration due to surface contamination from their treatments but the areas which did show decoration gave pictures similar to the standard graphite samples. Samples after initial gamma irradiation were much cleaner and they also showed pictures similar to those of the standard material. Some specimens in this set were heated before decoration to 650°C. to try and remove any

surface volatiles, and the actual decoration was carried out at a higher temperature than usual. These conditions resulted in a different appearance of the sample. Due to the initial heating, and higher decoration temperature, the surface must have been cleaned and the particles had become more mobile and the count was reduced. Also the higher temperature caused the formation and growth of some silver crystals. The mean counts for natural graphite, an example of which is shown in Plate 45, are 3.12×10^{10} particles per sq. cm. on the graphite and 19.3×10^{10} on the background, giving a decoration percentage of 16.2%. For nuclear graphite, illustrated by Plate 46, there are 7.75×10^{10} particles on the graphite and 19.9×10^{10} on the background, giving a percentage of 38.7%. This shows that no graphite damage, namely extra defect centres, had been produced.

The natural graphite area illustrated shows the effect looked for earlier, namely large particles or crystals surrounding small ones. It would therefore seem likely that the higher temperature had caused particle collection and crystal growth to occur to the exclusion of the exchange mechanism suggested for the mobile liquid particles. Further collision with a crystal forming mass would seem to have the effect of producing larger crystals.

In contrast to these results is the behaviour of graphite under neutron bombardment. As discussed in the introductory section, this treatment can produce interstitial and vacancy defects in the lattice,

and specimens, which showed no attack by carbon dioxide after 1 x 10^{18} n/cm^2, were subsequently decorated. A typical area of natural graphite is shown in Plate 47, while nuclear material is shown in Plate 48. Both graphites show decoration but to a lesser extent than the standard samples or those from the gamma irradiations. The particle counts substantiated this. On natural graphite there are 2.36 x 10^{11} particles per sq. cm. on the graphite and 7.3 x 10^{11} on the background, giving a decoration percentage of 32.3%. On nuclear graphite there are 4.50 x 10^{11} particles per sq. cm. on the graphite and 7.95 x 10^{11} on the background film, giving a decoration percentage of 56.6%.

By comparing these percentages with the previous figures, it can be seen that there has been an increase in particle collection sites which could only be due to the extra vacancy content of the graphite after the reaction attempt in BEPO. It can therefore be concluded that neutrons damage the graphite while specimens under vacuum ultra violet, gamma, and out-of-beam proton irradiation suffer no structure damage. However the attack characteristics found on both graphites after neutron irradiation experiments were independent of the irradiation induced defects which could not have had any effect under the conditions used.

P L A T E 45

Area of purified natural graphite after 350 M. Rad. at 300°C.
then decorated by silver at 450°C. x 120,000

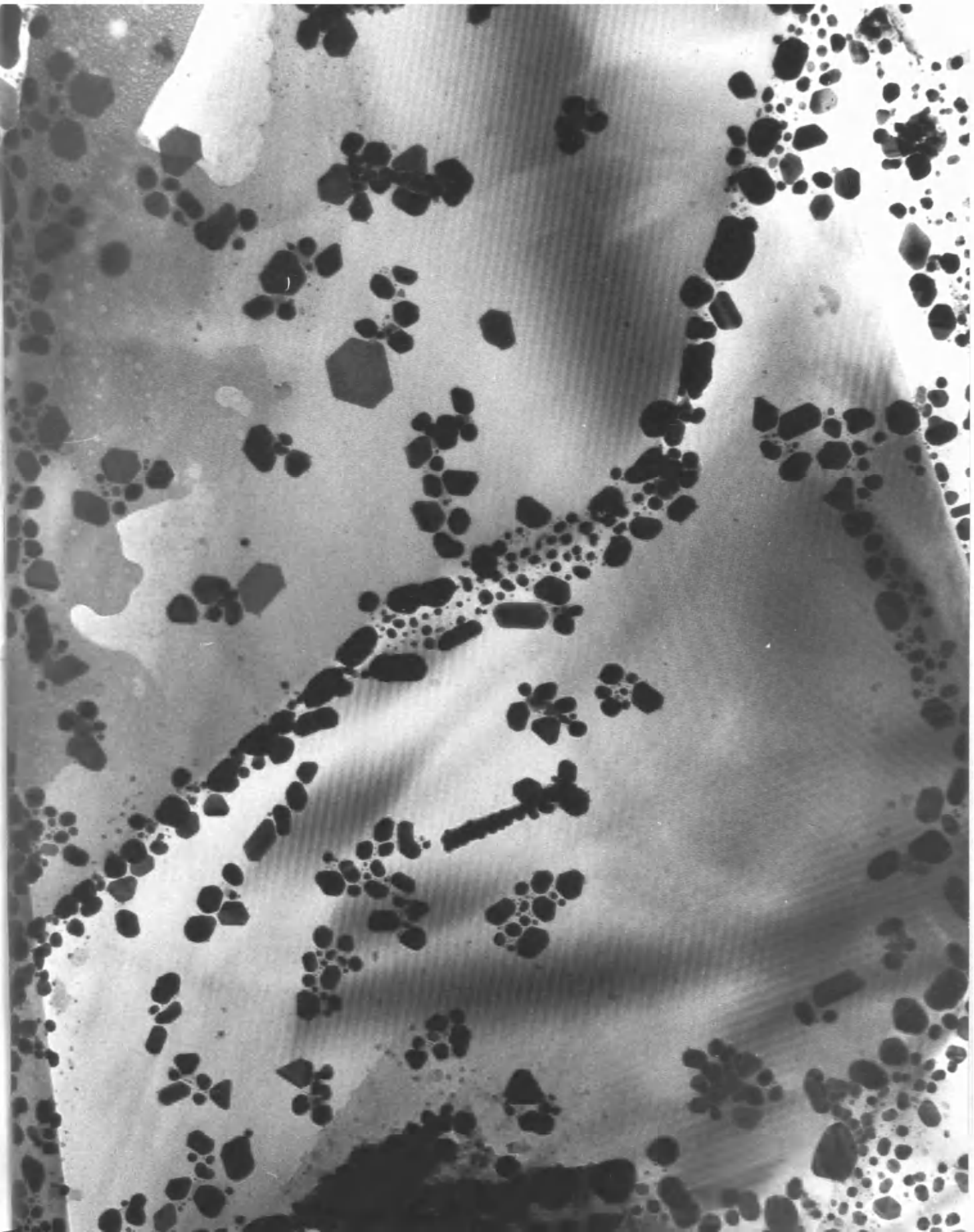

P L A T E 46

Area of nuclear grade graphite after 350 M. Rad. at 300°C. then decorated by silver at 450°C. x 120,000

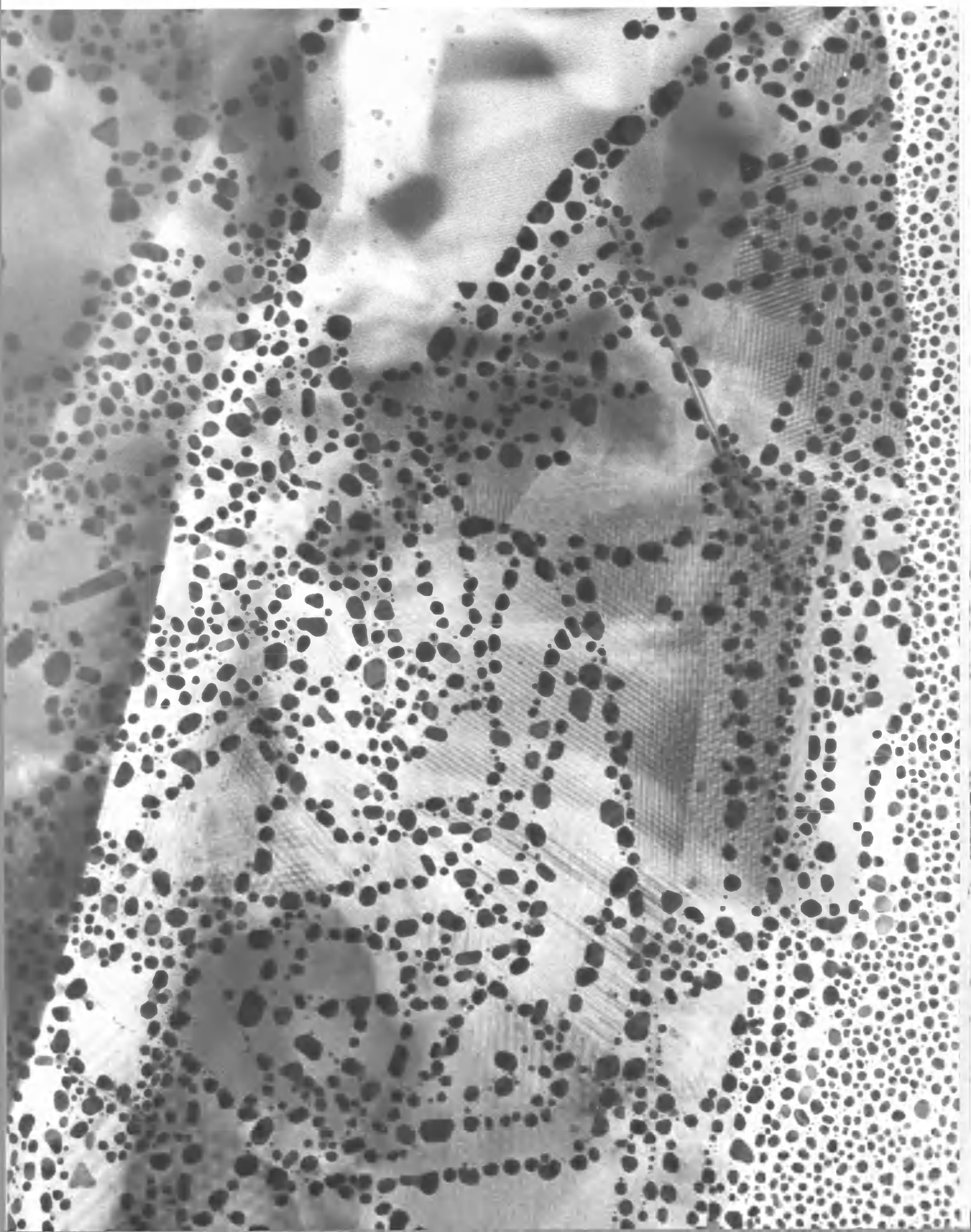

PLATE 47

Area of purified natural graphite after 1.0×10^{18} n/cm^2 then decorated by silver at $300^{\circ}C$. x 120,000

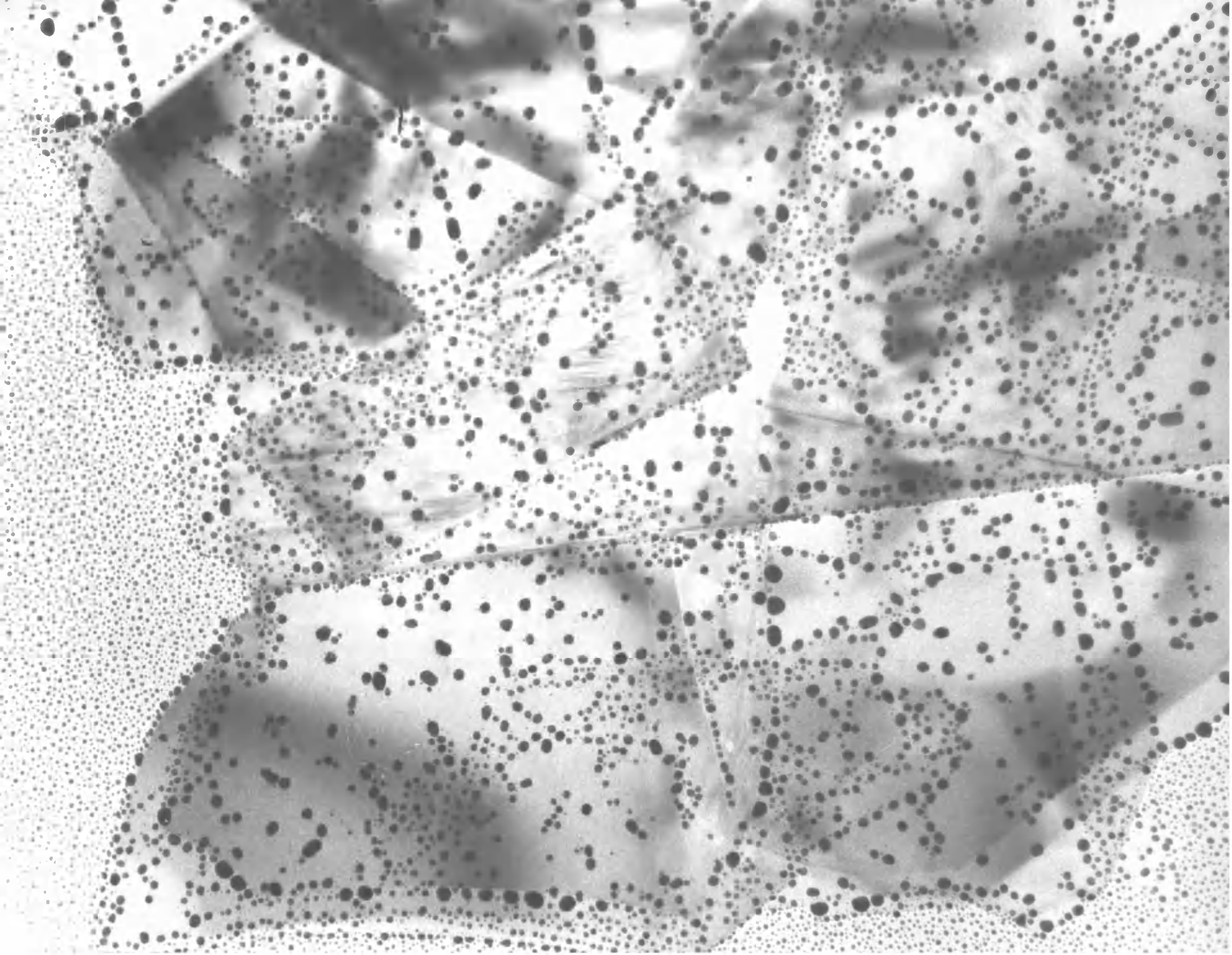

P L A T E 48

Area of nuclear grade graphite after 1.0 x 10^{18} n/cm^2 then decorated by silver at 300°C. x 120,000

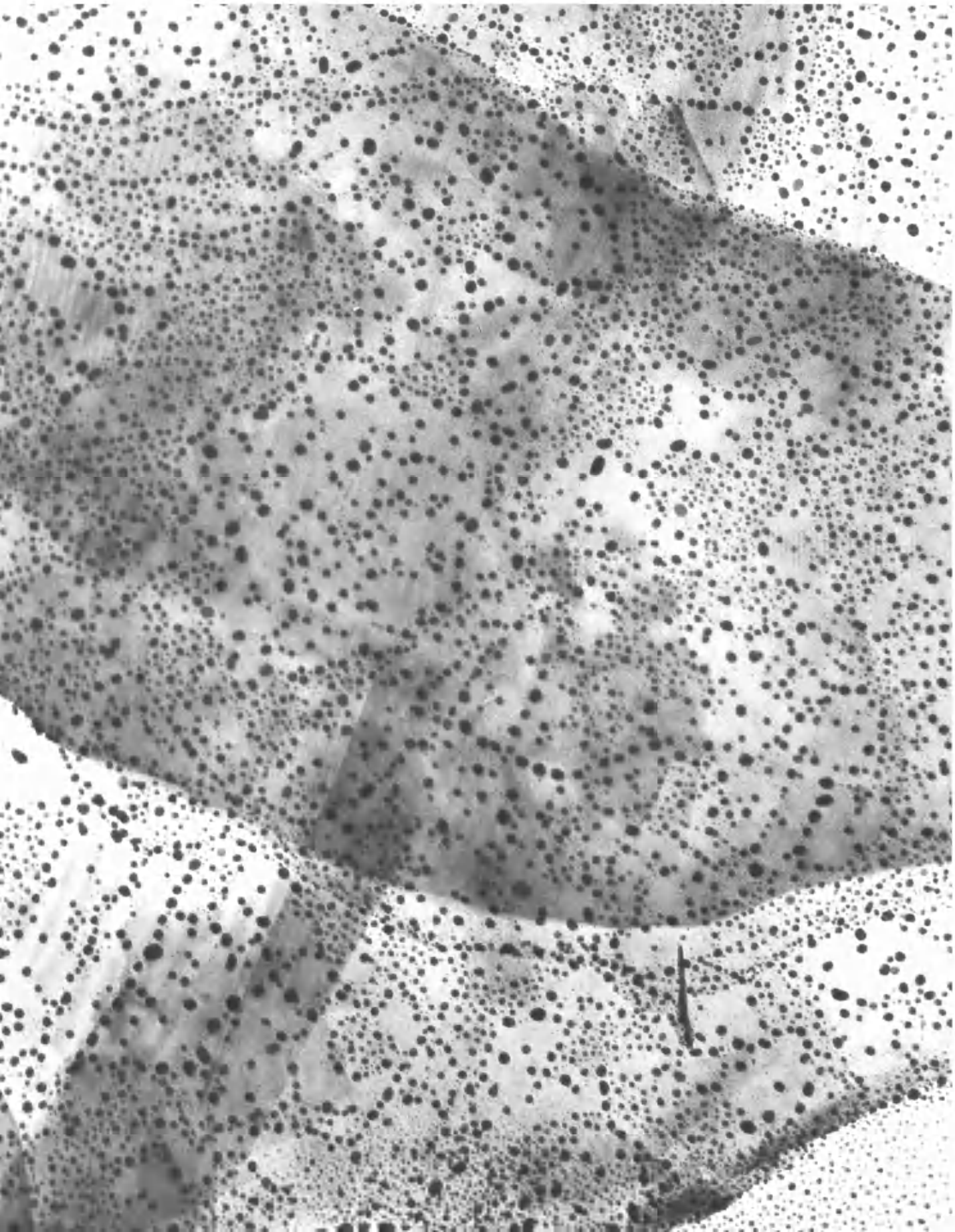

D I S C U S S I O N

Contents

1. Proton Irradiation

The main feature to emerge from these investigations is the difference in reactivity of natural and nuclear grade graphites. Since both materials were reacted under identical conditions, the different results obtained must be due to property differences of the graphites. Natural graphite is known to be the purer, more defect free material and purification must have resulted in a reduced inpurity content. Nuclear graphite manufacture processes have the effect of producing a less pure, more defective graphite.

Both materials show substantial edge gasification and this can be related to the incomplete use of bonding electrons at these sites which then become available for the chemisorption of any attacking gaseous species and therefore subsequent gasification. Carbon atoms in the central lattice plane use all their bonding electrons in the normal structure and so are far less susceptible to an attacking species. In a similar way, sites at grain boundaries are also active, since the boundary is the meeting point of two grain edges which have not been completely linked by bonding and may be separated by a micro-channel or pore, and thus double edge attack can be produced. During crystal growth, any defect and impurity sites tend to migrate to the edges, so these sites will show increased reactivity. Where a grain boundary emerges at the edge of a flake, reaction proceeded faster along that boundary due to its double edge and this has been seen in

both graphite materials and more especially in nuclear graphite which has smaller crystallites and therefore more grain boundaries.

In addition, any graphite which contains surface impurity and defect sites will also have bonding weaknesses at these points and so attack would be expected there. This was found on nuclear graphite where attack perpendicular to the graphite basal plane at some sites produced pits in the graphite. Since this effect was not found on natural graphite, it was attributed to the additional impurity and defect content of the nuclear material. These pits would be produced at suitable surface sites of any crystallite and also at isolated points along grain boundaries where there could be a localised high impurity density.

Another reaction feature was the appearance of particulate material after reaction. Since the deposit only occurred on the graphite surface, it can be concluded that it is a product of the reaction. A reasonable explanation is that this deposit is a solid polymer of the type described as carbon suboxide polymer in the literature, which was produced by the radiolysis of the carbon monoxide formed by the carbon gasification reaction. The location of the deposit is significant. In natural graphite, it occurred predominately near the flake edges while in nuclear grade material it also occurred over the bulk of the material. It is therefore likely that the deposit was formed near reaction sites which are at edges in the natural graphite but also

at surface defect and impurity sites in nuclear material. The gasification at a particular site must produce a carbon monoxide molecule which can be bonded nearby. After a sufficient number of these have gathered round a particular site of attack and polymerisation has occurred, the deposit particle can be found at or near that site of attack. The fact that reaction does not increase greatly with time after deposition has occurred is a good indication that the particles can inhibit further gasification by blocking possible sites of attack and reducing carbon gasification. Resistence to additional attack by re-irradiation experiments could be due to contamination build up, or to the deposit blocking mechanism or possibly both processes.

2. Neutron Irradiation

By comparing the oxidation pattern of the natural and synthetic graphites under identical conditions, it can be inferred that the properties of the graphite, rather than radiation effects, caused the reaction differences. These differences can be explained by the increased defect and impurity content of synthetic nuclear grade material.

Both materials show attack at impurity and defect sites whose exact nature cannot yet be determined. The main graphite defects are line and screw dislocations, point defects and impurity atoms, any of which may act in conjunction with others. The experiments where pre-irradiated graphite showed enhanced surface attack indicate

that vacancy content can influence reactivity and these sites can be active alone. Plates 7B and 9B show the purified natural graphite with isolated areas of surface attack which is not normally found in this material. These areas could be active sites at grain boundaries, or perhaps c-axis screw dislocations which were found by Hughes, Thomas, Marsh and Reed (1964) to stimulate pit formation on natural graphite. Nuclear graphite showed widespread attack perpendicular to the basal plane and this material is known to contain impurity plus many types of defects which are induced by its conditions of manufacture.

The role played by impurity in catalysing gasification is a complicated one. All samples which contained additional impurity showed attack at the same sites as samples without added impurity, and the only attack difference was in the rate of carbon gasification. This shows that impurity particles do not increase reaction by inducing attack at extra sites on the surface, but that catalysis takes place where impurity particles act in conjunction with a lattice site, which would produce attack at a later stage in the normal oxidation cycle. Good evidence to support this can be found in the series of experiments where two irradiation steps were performed. The specimens which were contaminated and showed dark particles on the surface, were only attacked at certain sites where impurity particles had landed over an active site on the surface of nuclear graphite and

only at edge regions in natural graphite. Also, from the micrographs of the specimens to which gold had been added, it can be noticed that reaction again only took place at the identical sites to those normally attacked when gold was absent. The temperature of 350°C. is high enough to promote continual mobility of gold particles and only a very limited number of sites seem capable of trapping the enlarged particles. The facts that both graphites, after reaction, contained gold particles which have little or no signs of reactivity and gasification of carbon near them, and that, on nuclear graphite, pits have been produced at areas where no gold was present, gives a clue to the probable mechanism of this reaction.

This explanation is based on the energy adsorbed by metal impurity from a reactor system. It is well known that metal particles become much more active and have a larger energy content than carbon, due to their higher energy adsorption from the system. Since the reaction conditions produced mobility of gold particles, these can transfer some of their energy to the underlying material as they migrate over the surface. In this way, any energy transferred to normally active sites could produce attack features characteristic of that particular graphite, at a stage before usually enough energy could be built up by the normal processes. Under the reactor conditions, the normal holding sites of an area such as Plate 9A become ineffective, and from subsequent micrographs, it would appear that only

sites where graphite has been removed and a sufficiently deep surface impression has been made, are capable of holding the particle. The extent of pitting or edge attack will therefore depend on the energy transferred to a particular site and on the time of reaction after this transfer has occurred. By this mechanism it is possible for a pit to be formed without being finally associated with a gold particle and conversely for a particle to be found with no pitting associated with it. This can occur where the migration has been stopped by the reduction in temperature as the experiment was concluded before the particle had found an effective holding site.

Under certain conditions, the trapped gold particles can instigate attack of the type given by a mobile catalyst, whose most characteristic feature is the formation of channels with a particle at each head. Catalytic attack of this kind has been found by Presland and Hedley (1962), who examined attack on graphite containing a platinum catalyst. In this case, the gold particle becomes trapped at a flake edge and as gasification proceeds, it can act in conjunction with freshly exposed sites, which can be considered as edge atoms, and thus also be favourable sites for attack. The gold particles may take up any bonding electrons of these edge sites and so weaken the neighbouring bonds and facilitate attack at these points. The metal particles can therefore induce attack along any preferred crystallographic direction, and because of their mobility, they can recede

with any attack front. In creating a channel in the graphite, any particle will effectively expose fresh edge sites which are then subject to edge attack, and thus the channel can widen. The channelling procedure is more likely to take place on natural graphite with its larger, more defect-free crystals than on nuclear grade material where channels are likely to merge with surface pits shortly after initiation. The channel widening process was not found by Presland and Hedley (1963) after the thermal attack of graphite by carbon dioxide.

The argument has already been set out to show the similarity between the features of attack on impurity enhanced graphite and those on untreated graphite. The conclusion is drawn that the normal mode of attack on graphite can largely be attributed to a combined impurity-defect mechanism, particularly for the case of pit production on nuclear graphite. As above, the impurity originally present at defect sites in nuclear graphite can perturb the neighbouring carbon-carbon bonds, and so aid the reactant species in its carbon attack process. The impurity plus defect mechanism is similar to that reported for thermal oxidation.

The difference between the catalytically induced pits above and those produced by contamination impurity particles, can be accounted for by mobility of the catalyst. When a particle is mobile and can proceed along definite crystallographic directions with the attack

front, definite linear contours can be seen at the pit edges and, when seen in cross-section, these can be represented by any typical sketch such as Figure 7 (a) or (b).

When attack has been initiated by a non-mobile catalyst, the only motion of the particle will be straight down through the graphite lattice as the carbon around it is gasified. Such a catalyst is the zirconium impurity or the unknown non-diffracting contaminant seen on some specimens after two irradiation cycles. From the study of the contrast around the pits, it can be deduced that these pits have been etched out symmetrically from a central point to produce the rounded edges. This suggests that attack started at a point in the contamination layer where an impurity particle was acting in conjunction with an active surface site. As the carbon around the particle was removed, it could drop to the layer below and so could 'burn' vertically through the graphite layers. In this way, at any given time the features of attack would be greatest at the surface and lessen on descending through the lattice, since each successive layer would be slightly behind the one above in gasification. The initial and final stages of this type of pit formation are represented by Figures 7 (c) and (d). The non-crystalline impurity would probably be more easily removed by 'burn-off' than would the zirconium crystals, although some of them were also removed. The reason for particle mobility or non-mobility over a surface is not fully understood and different effects have been found

F I G U R E 7 (a) and (b)

Cross-sections of two possible pits produced by a mobile catalyst.

F I G U R E 7 (c) and (d)

Cross-sections of the initial and final stages of pitting produced by a non-mobile catalyst.

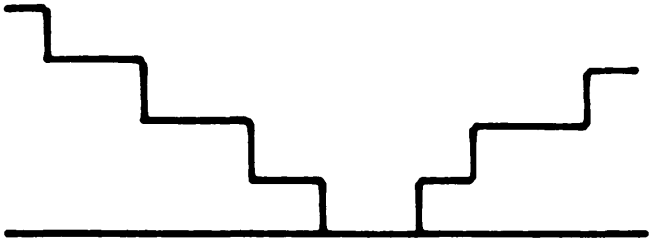

(a)

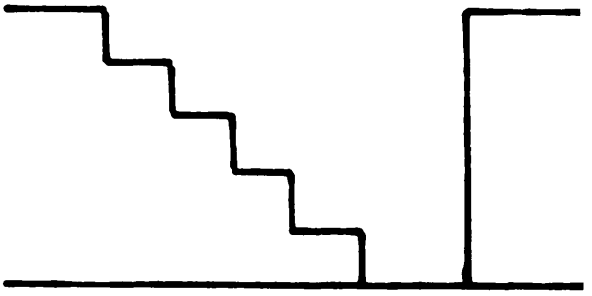

(b)

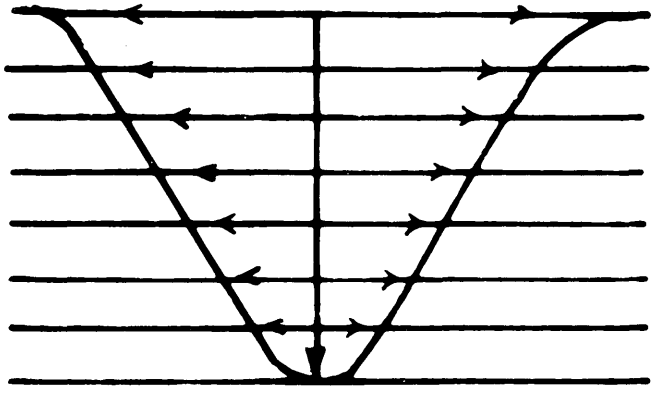

(c)

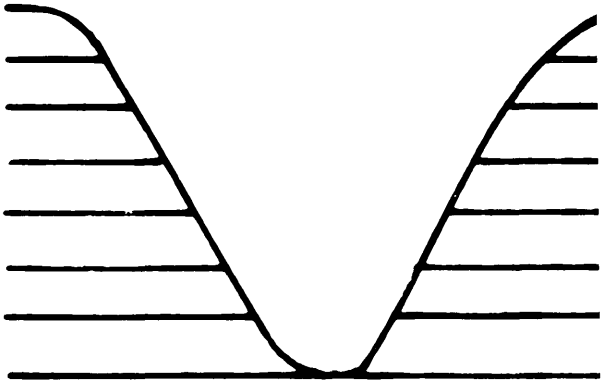

(d)

for different metals by different authors, among them Thomas and Walker (1965).

Another set of results to be explained were obtained from irradiation at 1.06 x 10^{18} n/cm^2 in carbon dioxide followed by 2.14 x 10^{18} n/cm^2 in the methane, carbon monoxide, carbon dioxide mixture. Reaction in this series shows two distinct patterns. Firstly, samples containing visible impurity particles show features of attack similar to those found after identical doses in pure carbon dioxide, while samples containing clean areas show attack of the type seen in the uninterrupted carbon dioxide experiments discussed earlier. Thus it can be seen that gasification has not been completely inhibited in these experiments, although it has been reduced. Since both treatments separately gave inhibition, this reactivity must be explained. The possible explanation that increase in dose is the reason cannot be upheld since similar experiments in pure carbon dioxide did not give as much attack as a lower dose continuous cycle. A second theory is based on the fact that samples, pre-irradiated to 1 x 10^{18} n/cm^2 and then subjected to microscopy and irradiation, gave enhanced reactivity (Plate 10) and therefore this sample could show the initial stages of attack at irradiation defect regions. Against this is the observation that attack takes place particularly along grain boundaries where pits appear and etch out the crystallite shapes, as seen in Plate 19. This attack is typical of that seen in specimens where damage is not

significant and gasification occurs at inherent defect and impurity sites. Also samples irradiated in a gas will not receive the full dose due to energy absorption by the gas during excitation, so the pre-irradiated samples must contain more defects than those which received a similar dose in carbon dioxide. The most likely explanation of the reactivity of this set of samples is based on reaction mechanism. The fact that attack similar to that obtained in pure carbon dioxide was obtained after a subsequent exposure to the inhibition mixture, is strong evidence in favour of an adsorbed species from the original irradiated gas (carbon dioxide) being held on the active surface sites during the interruption. In the re-irradiation cycle, when the energy of the system had built up again, the normal oxidation pattern could be produced at those sites where the original gas species were retained. These sites would be the only ones unprotected by the inhibiting species from the mixture. The original dose of 1.06×10^{18} n/cm^2 has been shown to be inadequate for carbon gasification but presumably it was high enough for the production and adsorption of an active gas species on suitable surface sites. The subsequent dose of 2.14×10^{18} n/cm^2 was high enough to produce the attack features of carbon dioxide attack before the inhibiting species could protect the freshly exposed sites.

An interesting point is the comparison of the widespread graphite attack obtained from neutron irradiation experiments and the much

reduced attack but extensive deposition which was found in proton beam experiments. One difference between these two systems is the temperature, since BEPO irradiations were carried out at 350°C. while the Van de Graaff experiments were performed at 25°C. Gow and Marsh (1960) showed that there was only a factor of two involved in the difference in reaction rate in going from 0°C. to 350°C. in a BEPO system. It is therefore unlikely that the difference in carbon gasification can be explained by the increase in temperature.

A more likely cause is the presence of deposit. In the proton beam experiments, an exaggerated dose rate of 10^3 ev/mol was produced, while in BEPO the dose rate was 4.7 ev/mol. This great difference is likely to be the reason why deposit was produced in the Van de Graaff experiments, and not in the BEPO experiments. It has been proposed that the deposit is a carbon suboxide polymer which has a blocking effect on the gasification of the carbon atoms below it. If this is correct, it is probable that the reactivity found in the BEPO experiments is due to the normal scheme of gasification at defect and impurity sites where there is no species present to block these sites and inhibit gasification as could be the case in the proton irradiation experiments.

3. Vacuum Ultra Violet Irradiation

(a) Carbon Dioxide Experiments

Again, it has been established that there are great differences

between natural and nuclear graphites in their behaviour to oxidation by carbon dioxide under irradiation at room temperature. Both samples show a marked edge attack coupled with deposition at these edges which suggests that the particulate material has been deposited at or near reactive sites. Since nuclear graphite shows a much greater tendency to surface attack and deposition, it can be concluded that reactivity and deposition occur at defect and impurity sites on the graphite surface, which contains more imperfections than purified natural material.

In common with the proton irradiation experiments, micrographs from this series also show that stepped layer edges exhibit rapid attack compared with some thick 'cliff' edges sometimes seen on the same flake, e.g. Plates 23A and B. This observation is strongly in support of attack by an adsorbed active species which can migrate freely over both the substrate film and the graphite surface. The results give the impression that the extent of attack varies directly with the area of the collecting surface (0001) below the step, and inversely with the step height. This is confirmed by the observations which show that the thinner the edge, the greater the graphite gasification. This suggests that the active species is adsorbed on the (0001) planes and migrates over the surface till it finds a reaction site. This may be a point defect, an impurity atom or a step edge, otherwise the adsorbed active species could return to the gas phase

spontaneously or by migration off the 'cliff' edge.

When a temperature of 350°C. was used, the behaviour of both graphites on oxidation was identical and there was no anisotropy of attack. This substantiates the results of other workers on graphite attack by atomic oxygen, and therefore is a good indication that gasification of carbon was caused by an atomic oxygen species which is a radiolysis product of carbon dioxide. This has caused carbon gasification around the deposit masses by random basal plane attack.

(b) Inhibition Experiments

The mixture of methane, carbon monoxide and carbon dioxide has been shown to be most effective in inhibiting gasification at low temperatures, but above a certain dose rate, the production of a large amount of deposited material resulted.

Although doses up to 2.2×10^{19} quanta produced no reaction or deposition where both would be found after exposure to the same dose in carbon dioxide, the increase in dose to 4×10^{19} quanta produced both effects. Under these conditions, attack was reduced but deposit cover was increased. This can be established from the fact that the deposit particle count was approximately the same for both gas systems but the use of methane produced a particle around 90Å in diameter compared with a size of 55Å for pure carbon dioxide experiments.

After the exposure to the inhibition mixture at 350°C. at a dose of 2.3×10^{19} quanta, which produced no reaction effects at room

temperature, the extensive gasification and deposit masses show that the reaction has some temperature dependence as was found using pure carbon dioxide. Another similarity found was that enlarged but fewer particle areas were formed and this suggests that the species forming the deposit must have been mobile over the surface under these conditions, and by comparison with the high dose, low temperature experiments, it is apparent that mobility is a temperature effect. A likely explanation for the observed effects can be proposed. If originally the photolysis of methane produced a species which was adsorbed randomly on the graphite surface, then as the surface content built up, polymerisation of this gaseous adsorbed species could lead to a liquid polymer and then at a more advanced stage, a solid could be produced. Low temperature and high dose rate would produce this effect and polymer solidification at central regions is seen on Plate 29B. At higher temperatures, it appears that the gaseous adsorbant can migrate over the surface and polymerise at a lower dose due to the heating effects. This could produce deposit clusters at some points, and deposit-free graphite regions at others. These graphite areas could then be attacked by the non-anisotropic atomic oxygen species and carbon would be gasified between the deposit centres. In this case the increase in oxidation with temperature can therefore be explained by a migration and collection mechanism of the polymer producing species, which at low doses and temperatures covered a

large number of surface sites and prevented attack. A similar process for polymer production and migration probably occurred in the pure carbon dioxide experiments at high temperature.

The experiments using ketene produced no attack or visible deposition at doses where the methane mixture and pure carbon dioxide showed both effects. This must again be a surface effect where a product of the ketene photolysis was adsorbed on the surface and blocked the sites from attack. This is most likely to be ethylene.

(c) Origin of Deposits

In reactions using pure carbon dioxide, or with 1% carbon monoxide added, the deposits are believed to be produced by radiolysis of carbon monoxide, which must be bonded to the surface. The likely result of this is the production of a carbon suboxide polymer. Radiolysis products have been mainly studied by workers using α radiation and the proposed products were C, C_2O, C_3O_2 and C_4O_3, etc. Since it is unlikely that the single carbon could survive attack in the oxidation conditions used, the polymer products are more feasible. Presumably, the more carbon monoxide present, the greater will be the chance of polymerisation and the above systems were found to give particles around 56Å in diameter, which could be the stable individual particle size in this system.

When methane was introduced, the evidence points to the deposit being a product of methane photolysis. Even though only .1% is used,

this product must be formed fast and be preferentially adsorbed rather than the carbon monoxide which is present in the initial stages. Since the photolysis of methane is known to give a CH_2 (methylene radical) and hydrogen, and this radical can produce long chain compounds by an insertion process, it is likely that this process could occur at the surface. Magee (1963) proposed that reactions took place through excited molecules rather than ions and so if any excited methane molecules came into contact with a methylene radical bonded to the surface, the insertion process could continue at that site. Polymer products have been found in methane radiolysis by many authors and great variety was found in the proposed structures which include saturated and unsaturated hydrocarbons.

The question then arises as to why ketene produces no visible deposit when its photolysis products are methylene radicals and carbon monoxide. A possible explanation is that, in this case, the radical insertion process leads to compounds of the general formula $(CH_2)_nCO$, whose only photolysis product is ethylene. No higher polymers and no evidence of direct radical combination have been found by Strachan and Noyes (1954). It is therefore possible that ethylene molecules could be firmly bonded across two lattice carbon atoms without producing a large polymer but still giving a blocking effect.

4. Gamma Irradiation

The behaviour of graphite under this type of irradiation has been

shown to resemble the results of BEPO reactor experiments and so the same mechanisms can be assumed to apply. The only difference in the two systems is the fact that neutrons can inflict damage to the graphite while gamma irradiation does not. This was illustrated by decoration studies. However, it has been mentioned that the neutron damage has no effect on the reaction under the conditions used in a normal irradiation cycle and so this will account for the similarity between the systems at these low doses. But, it has also been shown that pre-irradiation can increase reactivity, so it is likely that damage would be a more significant factor at higher doses.

5. A Possible Reaction Mechanism

The first two steps in the reaction scheme could be

$$CO_2 \xrightarrow{h\nu} CO_2^* \qquad ----(1)$$

$$C_f + CO_2^* \longrightarrow CO + C(O) \qquad ----(2)$$

Three further possible reactions could account for the adsorbed species.

$$C(O) \xrightarrow{(O)} \begin{cases} CO \text{ (gas)} & ----(3a) \\ CO_2 \text{ (gas)} & ----(3b) \\ C(CO) \longrightarrow \text{Polymer} & ----(3c) \end{cases}$$

Results suggest that any polymer produced must be retained at or near the site of carbon gasification. In a flow system of the kind used for vacuum ultra violet experiments, it is unlikely that gaseous carbon monoxide would be radiolytically decomposed to give a localised deposit,

but when 1% carbon monoxide was added to the pure carbon dioxide, deposition was increased. The particle appearance and size were similar to those obtained in experiments using pure carbon dioxide and so both deposits are probably radiolysis products of carbon monoxide decomposition. Since no deposit appeared on the background film, this gas must have been adsorbed on the graphite surface before deposit polymerisation occurred.

Since the high temperature results of this experimental series can be explained by the attack of atomic oxygen, the only other possible active species present is the activated carbon dioxide molecule. This is produced as the first stage product in all systems, but it is later decomposed. Low temperature experiments under vacuum ultra violet radiation and proton beam irradiation gave similar results and probably so would the neutron irradiated series if a protecting deposit had been produced. Due to its absence, gasification took place at the defect and impurity centres but definitely not at random sites, as seen in vacuum ultra violet experiments at the same high temperature.

Activated carbon dioxide attack cannot therefore be the simple reaction $CO_2^* + C = 2\ CO$ since the surface plays an important role. The intermediate step could be as before:

$$CO_2^* + C_f = CO + C(O)$$

This gives the same surface intermediate C(O) but presumably at low temperatures, reaction (3c) is favoured if the dose is high enough,

and at high temperature reaction (3a) also becomes important with the decomposition of the surface oxide.

It can therefore be concluded that at 350°C. in neutron and gamma irradiations, reaction (3c) is eliminated due to the low dose rate and reaction (3a) proceeds preferentially at active sites in the lattice. Low temperature proton beam and vacuum ultra violet experiments have a sufficient dose rate to produce polymer by (3c) at active sites which are then blocked from reaction. The temperature cannot be high enough for reaction (3a) to be appreciable, except at the most reactive sites. Only the very high dose rate of the proton irradiations produces pits at the most reactive surface sites of nuclear graphite. At the higher temperature, the deposit still blocks the normal attack sites but reaction (3a) proceeds rapidly at all other sites where no protection is available. It can therefore be concluded that the species of attack is atomic oxygen in all cases and only the different unprotected sites available for attack result in the differences in attack features.

6. Decoration

By this method, defects in the graphite surface which are normally invisible, can be made visible by decorating them with silver particles and so some estimation of the graphite defect content could be made.

The decoration pattern of the standard graphite samples shows the normal decoration pattern of linear arrays, mostly at edges, and

irregular interior groupings. Some samples show areas where edges are preferred collecting areas only when surface retentive sites are absent. Although the decoration pattern of both graphites is similar, their oxidation behaviour is not. Natural graphite shows predominately edge attack while nuclear graphite in addition exhibits surface attack. It is therefore concluded that the sites decorated cannot be the oxidation centres which give rise to etch pits. However, since nuclear graphite gives a greater decoration count than natural graphite, it is possible that this difference is made up by the sites which would be oxidised in a suitable system.

The decoration sites must however be significant in structural studies since the pattern of decoration by metal is very similar to the decoration produced by the reaction products of the vacuum ultra violet photolysis of the methane, carbon monoxide, carbon dioxide mixture as illustrated by Plate 39B. In that case, migration of a polymer species had occurred and deposit formation and subsequent graphite protection occurred at the same pattern of sites as in the silver decorations.

Examination of samples which showed no reaction in any system used and which were then decorated, showed that vacuum ultra violet and gamma radiation produced no graphite damage. Proton irradiation produced the same effect after out-of-beam experiments, although it is probable that in-beam experiments would produce great damage.

The nuclear reactor system is known to produce vacancies and interstitials by collision processes and this is borne out by the low dose irradiation and decoration results. This damage has already been shown to be unimportant in reactions under the low dose conditions used.

REFERENCES

Amelinckx S.,(1956), Phil.Mag. 1, 269.

" (1963), Interaction of Radiation with Solids, Mol, 68.

Amelinckx S., Delavignette P.,(1960a), Phil.Mag. 5, 533.

" " (1960b), Nature 185, 603.

" " (1960c), Phys.Rev.Lett. 5, 50.

" " (1961), Direct Observations of Imperfections in Crystals, 295.

" " (1963), El. Mic. and Strength of Crystals, 441.

Anderson A.R., Best J.V., Dominey D.A.,(1962), J.Chem.Soc. 3, 3498.

Anderson A.R., Davidson H.W., Lind R., Stranks D.R., Tyzack C., Wright J., 2nd Conf. Peaceful Uses of At. En., 335.

Ashton B.W., Labaton V.Y., Wilson P.D.,(1965), 2nd Conf. Ind. Carbon and Graphite.

Ashton B.W., Winton J.,(1961), T.R.G. Report 128(c).

Bacon G.E.,(1950), Acta Cryst. 3, 137.

" (1951), Acta Cryst. 4, 558.

" (1952), Acta Cryst. 5, 392.

" (1958a), Ind. Carbon and Graphite, 183.

" (1958b), AERE R-2702.

Bacon G.E., Sprague R.,(1961), Proc. 5th Conf. Carbon, 466.

Baker C.,(1962), 5th Inter. Cong. El. Mic., Philadelphia, I - 11.

Baker C., Gillin L.M., Kelly A.,(1965), 2nd Conf. Ind. Carbon and Graphite.

Baker C., Kelly A.,(1962), 5th Int. Cong. El. Mic., Philadelphia, F - 8.

Bassett G.A.,(1958), Phil.Mag. 33, 1040.

" (1960), Proc. Eur. Conf. El. Mic., Delft, 1, 270.

Bassett G.A., Menter J.W., Pashley D.W.,(1958), Proc.Roy.Soc.A 246, 345.

" " (1959), Disc.Far.Soc. 28, 7.

Bernal J.D.,(1924), Proc.Roy, Soc.A 106, 749.

Blackwood J.D.,(1954), Rev.Pure and Applied Chem. 4, 251.

Board J.A., (1965), 2nd Conf. Ind. Carbon and Graphite.

Board J.A., Squires R.L.,(1965), 2nd Conf. Ind. Carbon and Graphite.

Bollmann W.,(1960), Phil.Mag. 5, 621.

" (1961a), Proc. 5th Conf. Carbon, 2,303.

" (1961b), Proc. Eur. Conf. El. Mic., Delft, 330.

" (1961c), Proc. Int. Conf. Props. of Reactor Materials, Berkeley, 132.

" (1962), Phil.Mag. 7, 1513.

Bollmann W., Hennig G.R.,(1964), Carbon 1, 525.

Bonner F., Turkevich J.,(1951), J.Am.Chem.Soc. 73, 561.

Boudouard O.,(1901), Ann.Chem.Phys. 7, 245.

Bradley D.E.,(1954), Brit.J.Appl.Phys. 5, 65.

Broom W.E.J., Travers M.,(1932), Proc.Roy.Soc.A 135, 512.

Brown F.,(1952), Trans.Far.Soc. 48, 1005.

Butcher J., Grove D.M.,(1961), Proc. 5th Conf. Carbon, 205.

Cameron A.T., Ramsay W.,(1908), J.Chem.Soc. 93, 965.

Carr K.E.,(1965), Ph.D. Thesis, Glasgow.

Claxton K.T.,(1962), Report G.C.M./U.K./40.

Cluley H.J., Corney N.S.,(1962), Report G.C.M./U.K./42.

Copestake T.B., Davidson H.W., Tonge B.L.,(1959), J.Appl.Chem. 9, 74.

Copestake T.B., Feates F.S.,(1962), Conf. on Corrosion of Reactor Materials, Vienna, 2, 319.

Cosslett V.E., (1951), Practical Electron Microscopy.

Coulson C.A.,(1947), Nature, 159, 265.

Coulson C.A., Taylor R.,(1952), Proc. Phys.Soc.A 65, 815.

Davidge P.C., Marsh W.R.,(1955), AERE R - 1374.

Dawson I.M., Follett E.A.C.,(1959), Proc.Roy.Soc.A253, 390.

" " (1963), Proc.Roy.Soc.A274, 386.

Delavignette P., Amelinckx S.,(1960), Phil.Mag. 5, 729.

" " (1961), Proc. Eur. Conf. El. Mic., Delft, 404.

Dienes G.J., Vineyard G.H.,(1957), Radiation Effects in Solids.

Dominey D.A.,(1961a), AERE R-3725.

" (1961b), AERE R-3481.

Dominey D.A., Morley H.,(1964), AERE R-4817.

Dominey D.A., Palmer T.F.,(1963), Disc.Far.Soc. 36, 35.

Dowell W.C.T., Farrant J.L., Rees A.L.G.,(1958), 4th Int. Conf. El. Mic., Berlin, 367.

Dresel E.M., Roberts L.E.J.,(1953), Nature 171, 170.

Duval X.,(1961), J.Chim.Phys. 58, 3.

Earp F.K., Hill M.W.,(1958), Ind. Carbon and Graphite, 326.

Ergun S.,(1956), J.Phys.Chem. 60, 480.

Ewald P.P.,(1914), Sitzungsber Munch. Akad. 4, 7.

Feates F.S., Parry J.R.,(1964), AERE R-4819.

Feates F.S., Sach R.S.,(1965), 2nd Conf. Ind. Carbon and Graphite.

Feates F.S., Sach R.S., Walker F.A.,(1964), AERE R-4658.

Feates F.S., Walker F.A.,(1964), AERE R-4659.

Finch G.I., Wilman H.,(1936), Proc.Roy.Soc. A155, 345.

Follett E.A.C.,(1964), Carbon 1, 329.

Franklin R.E.,(1951a), Proc.Roy.Soc. A209, 196.

" (1951b), Acta Cryst. 4, 253.

Gadsby J., Long F.J., Sleightholm P., Sykes K.W.,(1948), Proc.Roy. Soc. A193, 357.

Gallagher J.T., Harker H.,(1964), Carbon 2, 163.

Goland A.N.,(1962), 5th Int. Cong. El. Mic., Philadelphia, F-1.

Gow H.B.F., Marsh W.R.,(1958), AERE R-381.

" " (1960), AERE R-3194.

Greer E.N., Topley B.,(1932), Nature 129, 904.

Grenall A.,(1958), Nature 182, 448.

Grenall A., Sosin A.,(1960), Proc. 4th Conf. Carbon, 371.

Grisdale R.D.,(1953), J. Appl.Phys. 24, 1288.

Groth W.,(1937), Z. Physik Chem. Leipsig, B37, 307.

Groth W., Passara W., Rommel H.J.,(1962), Z. Physik Chem. 32, 192.

Gulbransen E.A., Andrew K.F.,(1952), Ind.Eng.Chem. 44, 1048.

Hall C.E.,(1953), Introduction to Electron Microscopy.

Harker H., Marsh H., Wynne-Jones W.E.K.,(1958), Ind. Carbon and Graphite, 291.

Harteck P., Dondes S.,(1955), J.Chem.Phys. 23, 902.

" (1957), J.Chem.Phys. 26, 1727.

Hashimoto H., Uyeda R.,(1957), Acta Cryst. 10, 143.

Hennig G.R.,(1959), Proc. 3rd Conf. Carbon, 265.

" (1960), Proc. 4th Conf. Carbon, 145.

" (1961a), J. Chim.Phys. 58, 12.

" (1961b), Proc. 5th Conf. Carbon, 143.

" (1962a), J. Inorg.Nucl.Chem. 24, 1129.

" (1962b), Z. Electrochem. 66, 629.

" (1964), Appl.Phys. Letters 4, 52.

" (1965), 2nd Ind. Conf. Carbon and Graphite.

Hennig G.R., Dienes G.J., Kosiba W.,(1958), 2nd Conf. Peaceful Uses of At. En., Geneva, 301.

Hennig G.R., Kanter M.A.,(1960), Proc. 4th Conf. Carbon, 141.

Hillier J.,(1954), Nat.Bur.Stand.Circ. 527, 413.

Hirsch P.B., Horne R.W., Whelan M.J.,(1956), Phil.Mag. 1, 677.

Hirschfelder J.O., Taylor H.S.(1938), J.Chem.Phys. 6, 783.

Horn F.H.,(1952), Nature 170, 581.

Howie H.,(1961), 'Direct Observations of Imperfections in Crystals', 269.

Howie H., Whelan M.J.,(1961), Proc.Eur.Conf.El.Mic., Delft, 194.

Hucher M., Oberlin A.,(1961), Comptes Rendus, 252, 3081.

Hughes E.E.G., Thomas J.M.,(1962), Nature 193, 838.

" " (1964), Carbon 1, 209.

Hughes E.E.G., Thomas J.M., Marsh H., Reed R.,(1964), Carbon 1, 339.

Hughes E.E.G., Williams B.R., Thomas J.M.,(1962), Trans.Far.Soc. 58, 2011.

Hummel R.W.,(1963), Disc.Far.Soc. 36, 75.

" (1965), AERE R-4838.

Hurst R., Wright J.,(1955), Proc. Conf. Peaceful Uses of At.En., Geneva, 9, 373.

Hutcheon J.M., Cowen H.C., Godwin N.F.,(1962), T.R.G. Report 235C.

Inn E.C.Y., Watanabe K., Zelikoff M.,(1953), J.Chem.Phys. 21, 1648.

Jacquet M., Guerin H.,(1962), Bull.Soc.Chim., France, 55, 411.

Jucker H., Rideal E.K.,(1957), J.Chem.Soc. 1, 1058.

Kay D.,(1965), Techniques for Electron Microscopy.

Kelly B.T.,(1964), Phil.Mag. 9, 721.

" (1965), 2nd Conf. Ind. Carbon and Graphite.

Kistiakowski G.B., Rosenberg N.W.,(1950), J.Am.Chem.Soc. 72, 321.

Kosiba W.L., Dienes G.J.,(1957), Adv.Cat. 9, 398.

Labaton V.Y.,(1965), Private Communication.

Laidler D., Taylor A.,(1940), Nature 146, 130.

Laine N.R., Vastola F.J., Walker P.L.,(1963), 67, 2030.

Lampe F.W.,(1957), J.Am.Chem.Soc. 79, 1055.

Lang F.M., Magnier P.,(1961), Proc. 5th Conf. Carbon, 453.

" " (1963), J.Chim.Phys. 60, 251.

Lang F.M., Magnier P., Sella C., Trillat J.J.,(1962), Comptes Rendus 254, 4114.

Langmuir I.,(1915), J.Am.Chem.Soc. 37, 1139.

Leighton P.A., Steiner A.B.,(1936), J.Am.Chem.Soc. 58, 1823.

Lind S.C., Bardwell D.C.,(1925), J.Am.Chem.Soc. 47, 2675.

Lind R., Wright J.,(1963), J.Brit.Nucl.En.Soc. 2, 287.

Lipson R., Stokes A.R.,(1942a), Nature 149, 328.

" " (1942b), Proc.Roy.Soc. A181, 101.

Loch L.D., Austin A.E.,(1956), Proc. 1st and 2nd Conf. Carbon, 65.

Loch L.D., Austin A.E., Harrison R.J., Duckworth W.H.,(1958), U.S. A.E.A. Report.

Long F.J., Sykes E.W.,(1948), Proc.Roy.Soc. A193, 377.

" " (1950), J.Chim.Phys. 47, 361.

Magee E.M.,(1963), J.Chem.Phys. 39, 855.

Mahan B.H.,(1960), J.Chem.Phys. 33, 959.

Mahan B.H., Mandal R.,(1963), J.Chem.Phys. 37, 207.

Mains G.H., Newton A.S.,(1961), J.Chem.Phys. 65, 212.

Marsh H., O'Hair T.E., Reed R.,(1965), Trans.Far.Soc. 61, 285.

Mitsuishi T., Nagasaki H., Uyeda R.,(1951), Proc.Imp.Acad., Japan 27, 86.

Mrozowski S.,(1950a), Phys. Rev. 77, 838.

" (1950b), Phys. Rev. 78, 644.

Mrozowski S.,(1952a), Phys. Rev. 85, 609.

" (1952b), Phys. Rev. 86, 822.

Munson M.S.B., Field F.H., Franklin J.L.,(1965), J.Chem.Phys. 42, 442.

Nightingale R.E.,(1962), 'Nuclear Graphite'.

Okabe H., McNesby J.R.,(1961), J.Chem.Phys. 34, 668.

Pinsker Z.G.,(1953), Electron Diffraction.

Presland A.E.B., Hedley J.A.,(1962), 5th Int.Cong.El.Mic., Philadelphia, I - 10.

Presland A.E.B., Hedley J.A.,(1963), AERE/EMR/PR/1538/2.

Ragone D.V., Zumwalt L.R.,(1961), Proc.Int.Conf. Props. of Reactor Materials, Berkeley, 388.

Rakszawski, J.F., Rusinko F., Walker P.L.,(1961), Proc. 5th Conf. Carbon, 243.

Reif A.E.,(1952), J.Phys. Chem. 56, 785.

Reynolds W.N., Simmons J.H.W.,(1961), Proc. 5th Conf. Carbon, 255.

Reynolds W.N., Thrower P.A.,(1962), IAEA Symposium on Radiation Damage, Venice, 4, 553.

" " (1963), AERE R-4316.

" " (1964), Carbon 1, 185.

Reynolds W.N., Thrower P.A., Sheldon B.E.,(1961), Nature 189, 824.

Reynolds W.N., Thrower P.A., Simmons J.H.W.,(1965), 2nd Conf. Ind. Carbon and Graphite.

Roberts L.E., Harper E.A., Small C.T.,(1958), AERE R-882.

Roscoe C., Thomas J.M.,(1966), Report GCM/UK/A16.

Sach R.S.,(1961), AERE R-3721.

Sauer M.C., Dorfman L.M.,(1961), J.Chem.Phys. 35, 497.

Sears G.W., Hudson J.B.,(1963), J.Chem.Phys. 29, 2380.

Sella C., Conjeaud P., Trillat J.J.,(1959),Comptes Rendus, 249, 1987.

Sieck L.W.,(1963), Diss.Abs. 24, 98.

Siems R., Delavignette P., Amelinckx S.,(1962), 5th Int.Cong.El.Mic., Philadelphia, B - 2.

Smith W.R., Polley M.H.,(1956), J.Phys.Chem. 60, 689.

Smyth H.D.,(1931), Rev.Mod.Phys. 3, 347.

Standring J., Ashton B.W.,(1965), Carbon 3, 157.

Strachan A.N., Noyes W.A.,(1954), J.Am.Chem.Soc. 76, 3258.

Strickland - Constable R.F.,(1947), Proc.Roy.Soc. A189, 1.

" (1950), J.Chim.Phys. 47, 356.

Sykes K.W., Thomas J.M.,(1961), J.Chim.Phys. 58, 70.

Thomas J.M., Hughes E.E.G., Williams B.R.,(1963), Phil.Mag. 85, 8_2, 1513.

Thomas J.M., Walker P.L.,(1964), J.Chem.Phys. 41, 587.

" " (1965), Carbon 2, 434.

Thomson G.P., Cochrane W.,(1939), Theory and Practice of Electron Diffraction.

Tomlinson M., Walker F.A.,(1961), AERE R-3669.

Tomlinson M., Wright J.,(1965), AERE R-4201.

Trezbiatowski W.,(1937), Roczniki.Chem. 17, 73.

Trillat J.J., Solla C., Miloche M.,(1962), 5th Int.Cong.El.Mic., Philadelphia, I - 7.

Ubbelohde A.R.,(1957), Nature 180, 380.

Ubbelohde A.R., Lewis F.A.,(1960), 'Graphite and its Crystal Compounds'.

Vanpee M., Grard F.,(1951), Bull.Soc.Chim.Belg. 60, 208.

Vastola P.J., Walker P.L.,(1961), J.Chim.Phys. 58, 20.

Walker P.L., Rusinko F.,(1958) Proc. 3rd Conf. Carbon, 633.

Walker P.L., Rusinko F., Austin L.G.,(1959), Adv.Cat. 11, 133.

Walker P.L., Rusinko F., Rakszawski J.F., Liggett L.M.,(1959), Proc. 3rd Conf. Carbon, 623.

Wallace P.R.,(1947), Phys.Rev. 71, 622.

Warneck P.,(1964a), Disc.Far.Soc. 37, 57.

" (1964b), J.Chem.Phys. 41, 3435.

Warren B.E.,(1934), J.Chem.Phys. 2, 551.

Watt J.D., Franklin R.E.,(1957), Nature 180, 1190.

" " (1958), Ind. Carbon and Graphite, 321.

Weber C.E.,(1956), Proc. Sym. High Temp. Berkeley, 136.

Wexler S., Jesse N.,(1962), J.Am.Chem.Soc. 84, 3425.

Williamson G.K.,(1961), Int. Conf. Props of Reactor Materials, 144.

Williamson G.K., Baker C.,(1958), Proc.Roy.Soc. A249, 114.

" " (1960a), Proc.Roy.Soc. A257, 457.

" " (1960b), Proc.Eur.Conf.El.Mic., Delft, 326.

Williamson G.K., Baker C.,(1961a), Phil.Mag. 6, 313.

" " (1961b), Proc. 5th Conf. Carbon, 2, 521.

Woodley R.E.,(1954), H.W. - 3199.

Woods W.K., Bupp L.P., Fletcher J.F.,(1956), Proc. Conf. Peaceful Uses of At.En. 7, 455.

Wourtzel E.E.,(1919), Le Radium 11, 346.